Antimicrobial Nitric Oxide Releasing Creams/Devices Based on a Novel Reaction Between *S*-Nitrosoglutathione and Zinc Oxide Nanoparticles

by

Joshua C. Doverspike

A dissertation submitted in partial fulfillment
of the requirements for the degree of
Doctor of Philosophy
(Chemistry)
in the University of Michigan
2020

Doctoral Committee:

Professor Mark E. Meyerhoff, Chair
Professor Zhan Chen
Professor Kristina Håkansson
Professor Chuanwu Xi

Joshua C. Doverspike

joshdov@umich.edu

ORCID iD: 0000-0002-6062-9607

DEDICATION

To my family and loved ones.

Thank you for all your love and support!

ACKNOWLEDGEMENTS

During my graduate studies and research at the University of Michigan, I've had the privilege of working with fabulous individuals. First and foremost, I would like to thank my advisor Dr. Mark Meyerhoff for being such an amazing mentor, friend, and father-figure. He always provides me with endless encouragement and motivation. His guidance and teachings have made me the scientist I am today. He has truly impacted my life in many positive ways. I am forever grateful for all of the time and dedication he has given me throughout my graduate school journey. Again, thank you from the bottom of my heart.

I would also like to thank my dissertation committee members: Dr. Kristina Håkansson, Dr. Zhan Chen, and Dr. Chuanwu Xi. I greatly appreciate all of your recommendations and suggestions for my research projects, and for taking your valuable time to be on my committee.

A lot of my research projects have been in collaboration with Dr. Chuanwu Xi and his laboratory in the U of M School of Public Health. I would like to extend a special thanks to Dr. Jianfeng Wu for his countless hours of hard work and dedication to every antimicrobial experiment. Also, thank you to Hellen (Dr. Xiaojuan Tan) for her assistance in several antimicrobial studies.

I've had the great privilege of collaborating with nephrologist, Dr. Alexander Yevzlin. He has significantly impacted my dissertation work by his helpful recommendations for various studies and by always being available and willing chat about anything and everything.

I would also like to thank Dr. Robert H. Bartlett and the entire research and surgery team in the Extracorporeal Membrane Oxygenation (ECMO) laboratory: Hayley Lindsay, Candace Walls, Joseph Hill, Shelby Reno, Caroline Foster and Dr. Lise Tchouta. A special thanks to both Marie Cornell and Dr. Alvaro Rojas for their hard work and dedication.

I've been fortunate to have such a great group of lab mates and friends surrounding me each day during my graduate career. I want to especially thank Joe (Dr. Yang Zhou) for his assistance and guidance with numerous experiments. Thank you to all of my other lab mates: Dr. Stephen Ferguson, Dr. Alexander Wolfe, Dr. Andrew Hunt, Dr. Joanna Zajda, Dr. Kamila Katarzyna, Dr. Alex Ketchum, Dr. Orsola Lautner-Csorba, Dr. Gergely Lautner, Dr. Qi Zhang, Griffin Murray, Dr. Xuewei Wang, Dr. Yu Qin, Dr. Yaqi Wo, Dr. Elizabeth Brisbois, Dr. Kyoung Ha Cha, Dr. Zheng Zheng, Dr. Hang Ren, and Dr. Jennifer Reeves. I would also like to thank the undergraduate students I've had the privilege of mentoring: Shale Mack, Amy Luo, Blake Stringer, Undraa Bayasgalan, and James Phan. Thank you all so much for your hard work and dedication to our projects. I would like to thank a few other undergraduates that I did not directly mentor: Nicholas Schmidt, Roopa Gorur, Joshua Wolfe, Aaron Jolliffe, and Jeong Hwang. A few colleagues I would like to thank for their support and assistance from outside of my laboratory are Dr. Sofiya Hlynchuk, Dr. Molly MacInnes, Quintin Cheek, Nathanael Downes, Robert Vasquez, Maria Kim, and Dr. Ricardo Vazquez.

Thank you to all of my family and friends for your continuous love and support throughout my journey as a graduate student. I would especially like to thank my brother Kyle, sister-in-law Macy, and my Unka Dave.

Lastly, I would like to thank my parents Ronald and Marcell Doverspike. Their endless love and support has always been a great blessing. No matter the time of day or circumstance, they have always been there for me. I could never thank them enough for all that they have done and continue to do for me. Thank you so much for everything!

TABLE OF CONTENTS

DEDICATION ii

ACKNOWLEDGEMENTS iii

LIST OF FIGURES xi

LIST OF TABLES xvi

ABSTRACT xvii

Chapter 1 Introduction 1

1.1 Antiseptic Agents 1

1.1.1 Purpose and function of antiseptics 1
1.1.2 Antiseptics used for topical treatments 2
1.1.3 Limitations and downfalls of antiseptics 3

1.2 Antibiotics 4

1.2.1 Purpose and function of antibiotics 4
1.2.2 Antibiotics in ointments, creams, and hydrogels 5
1.2.3 Limitations and downfalls of antibiotics for topical treatments 8

1.3 Nitric Oxide 9

1.3.1 Purpose, function, and properties of nitric oxide 9
1.3.2 NO releasing agents for topical treatments 11

1.4 Summary 15

1.5 Statement of Thesis Research 16

1.6 References 19

Chapter 2 Development and Characterization of Nitric Oxide Releasing Two-Part Creams..... 24

2.1 Introduction 24

2.2 Materials and Methods 27

2.2.1 Materials 27
2.2.2 S-Nitrosoglutathione (GSNO) synthesis 27
2.2.3 Preparation of various wt% GSNO in Vaseline 29
2.2.4 Preparation of various wt% of GSNO in Vaseline for long-term stability studies..... 29
2.2.5 Evaluating stability of GSNO in Vaseline using UV-Vis spectroscopy 29
2.2.6 Preparation of matrices for NO release measurements 30
2.2.7 Measuring NO release from matrices 31

2.3 Results and Discussion 32

2.3.1 Preliminary stability study of 10 wt% and 33 wt% GSNO in Vaseline 32
2.3.2 Initiating NO release using various secondary matrices 34
2.3.3 NO release characteristics and kinetics from GSNO using zinc oxide cream..... 37

2.4 Conclusion..... 40

2.5 References 42

Chapter 3 Antimicrobial Effects of NO Releasing Cream Formulations 46

3.1 Introduction 46

3.2 Materials and Methods 48

3.2.1 Materials 48
3.2.2 S-Nitrosoglutathione (GSNO) synthesis 49
3.2.3 Preparation of various wt% GSNO in Vaseline 49
3.2.4 Preparation of NO releasing and other matrices..... 49
3.2.5 Indirect application antimicrobial studies..... 50
3.2.6 Pig skin treatment 51
3.2.7 Direct application antimicrobial studies on pig skin model 52
3.2.8 Direct application anti-biofilm studies on pig skin model 53
3.2.9 Measuring relative pH of various cream formulations 53
3.2.10 Measuring wt% water within the creams 53
3.2.11 Preparation of matrices for NO release measurements 54

3.2.12 Measuring NO release from matrices 54

3.3 Results and Discussion 55

3.3.1 Indirect application antimicrobial studies 55
3.3.2 Direct application antimicrobial studies on pig skin model 57
3.3.3 Evaluate synergy of combining NO and antibiotics to kill biofilm 59
3.3.4 Evaluate pH of NO releasing creams 61
3.3.5 NO release kinetics from neutral pH cream containing GSNO and ZnO 65
3.3.6 Direct application bacteria studies of neutral pH NO releasing cream on pig skin 67

3.4 Conclusion 69

3.5 References 71

Chapter 4 Investigation of Enhanced NO Release from GSNO in the Presence of ZnO 74

4.1 Introduction 74

4.2 Materials and Methods 76

4.2.1 Materials 76
4.2.2 S-Nitrosoglutathione (GSNO) synthesis 76
4.2.3 Measuring NO release from GSNO in the presence of Zn^{2+} ions 76
4.2.4 Measuring NO release from GSNO for component studies 77
4.2.5 NO release kinetics from GSNO using 30, 50, and 200 nm ZnO nanoparticles 78
4.2.6 NO release from GSNO in the presence 30 nm ZnO in Tris–HCL or $–H_3PO_4$ buffer. 78
4.2.7 ZnO nanoparticle preparation for surface analysis via XPS 79
4.2.8 X-ray photoelectron spectroscopy (XPS) 80

4.3 Results and Discussion 80

4.3.1 Investigation of NO release from GSNO in the presence of Zn^{2+} ions 80
4.3.2 Component study of Desitin® Rapid Relief Cream: Zinc Oxide Diaper Rash Cream 82
4.3.3 NO release kinetics from GSNO using 30, 50, and 200 nm ZnO nanoparticles 84
4.3.4 Comparing NO release from GSNO using ZnO under Tris–HCl and $–H_3PO_4$ 86
4.3.5 Surface analysis of ZnO nanoparticles via X-ray photoelectron spectroscopy 87

4.4 Conclusion 89

4.5 References 91

Chapter 5 Hub Region Disinfecting NO Releasing Insert for Tunnel Dialysis Catheters 93

5.1 Introduction 93

5.2 Materials and Methods 96

5.2.1 Materials 96
5.2.2 S-Nitrosoglutathione (GSNO) synthesis 96
5.2.3 Fabrication of NO releasing inserts 96
5.2.4 Measuring real-time NO release from inserts 97
5.2.5 In vitro simulated catheter hub antimicrobial assay 98
5.2.6 Sterilization studies: Ethylene oxide (EO) vs. hydrogen peroxide (H_2O_2) 98
5.2.7 Stability Study 99
5.2.8 In vitro catheter hub antimicrobial assay 100
5.2.9 Sheep studies - general procedure 100
5.2.10 Sheep Study #1 102
5.2.11 Sheep Study #2 103

5.3 Results and Discussion 103

5.3.1 Design of NO releasing inserts 103
5.3.2 Characterizing real-time NO release of NO releasing insert formulations 104
5.3.3 Antimicrobial effects of NO releasing formulations (a-c) inserts in simulated catheter hubs 106
5.3.4 Sterilization and Stability Testing 109
5.3.5 Antimicrobial effects of NO releasing formulation (a) inserts in hemodialysis catheter hubs 111
5.3.6 Sheep Study #1 112
5.3.7 Sheep Study #2 115

5.4 Conclusion 118

5.5 References 120

Chapter 6 Conclusions and Future Directions 122

6.1 Conclusions 122

6.2 Future Directions 126

6.2.1 Goals for future directions 126

6.2.2 Cytotoxicity study of NO releasing two-part cream via live pig models 126
6.2.3 Determination of mechanism between GSNO and ZnO nanoparticles 128
6.2.4 Leaching study for NO releasing insert 131

LIST OF FIGURES

Figure 1.1. Antibacterial efficacy of 0.2% w/v ciprofloxacin (CIP) tripeptide gel and controls of only tripeptide gel against S. aureus, E. coli, and K. pneumoniae agar layer cultures. Images taken after 20 h of incubation at 37°C.[49] 7

Figure 1.2. Mechanisms by which NO acts as an antibacterial agent.[61] 10

Figure 1.3. Structures of various RSNOs. 12

Figure 1.4. Real-time NO release from GSNO incorporated into (a) hydrogel-dark, (b) H_2O-dark, (c) hydrogel-irradiated, (d) H_2O-irradiated; irradiated with $\lambda > 480$ nm.[79] 13

Figure 1.5. MRSA bacteria counts after being untreated, being treated with just the vehicle hydrogel, and being treated with 2, 6, or 12% concentration of Novan's product on various days (graph taken from novan.com). 15

Figure 2.1. ^{1}H NMR Spectrum of synthesized GSNO in D_2O.[44] 28

Figure 2.2. Schematic of side and top view for a matrix with a defined sample size on a glass slide. 31

Figure 2.3. Schematic of the set-up for measuring NO release from matrices. The reaction cell is amber glass, submerged in a 34°C water bath, and wrapped in aluminum foil. 32

Figure 2.4. GSNO decomposition reactions that can occur in the presence of water, where (1) is a transnitrosation reaction, (2) is a decomposition reaction with GSH, and (3) is a reaction between copper ions and GSNO.[34, 46-48] 33

Figure 2.5. Absorbance (ABS) vs. wavelength plots for (a) 10 wt% GSNO and (b) 33 wt% GSNO mixed in Vaseline on day 583 and day 313, respectively. The crossed circle represents the theoretical ABS value at 334 nm for 100% recovery of GSNO. The percent recovery of GSNO was calculated to be (a) 89.8 ± 3.4% and (b) 87.6 ± 3.5 based on ABS at 334 nm. Samples were stored in a dark, dry environment under N_2 gas at 24°C. Data represents the mean ± SD (n = 3). 34

Figure 2.6. %NO released from 33 wt% GSNO/Vaseline primary matrix mixed with several secondary matrices: (a) Neosporin cream; (b) vitamin C cream; (c) copper cream; and (d) zinc oxide cream at a 27/73 ratio to yield a final 9 wt% GSNO matrix. NO release was measured in the dark over a 6 h period at both 24°C and 34°C. Data represents the mean ± SD (n = 3). 35

Figure 2.7. (a) Real-time NO release of 3, 6, and 9 wt% GSNO matrices in the dark at 34°C. (b) Cumulative NO release vs. time for 3, 6, and 9 wt% GSNO matrices in the dark at 34°C.

GSNO/Vaseline primary matrices were mixed with commercial Desitin zinc oxide cream at a 27/73 ratio to achieve 3, 6, and 9 wt% GSNO final matrices. Data represents mean (n = 3)..... 38

Figure 2.8. Fit of the cumulative NO release versus time of (a) 3 wt% (b) 6 wt%, and (c) 9 wt% GSNO matrices to a first-order rate equation, giving (a) k_{obs} = 0.58 ± 0.01 h^{-1} ($t_{1/2}$ ~ 1.18 h), (b) k_{obs} = 0.63 ± 0.01 h^{-1} ($t_{1/2}$ ~ 1.10 h), (c) k_{obs} = 0.64 ± 0.01 h^{-1} ($t_{1/2}$ ~ 1.08 h). Data represents mean (n = 3)..... 39

Figure 2.9. Real-time NO release of 9 wt% GSNO matrices in the dark and in ambient room light at 34°C over (a) 6 h and (b) 60 min. (c) Fit of the cumulative NO release versus time of 9 wt% GSNO matrices in ambient room light to a first-order rate equation, giving k_{obs} = 0.63 ± 0.01 h^{-1} ($t_{1/2}$ ~ 1.10 h). GSNO/Vaseline primary matrices were mixed with commercial Desitin zinc oxide cream at a 27/73 ratio to achieve 9 wt% GSNO final matrices. Data represents mean (n = 3).... 40

Figure 3.1. Side view schematic of the indirect application antimicrobial study configuration where (1) represents a matrix (NO releasing cream or other), (2) represents a thin silicone membrane/sheet, and (3) represents a LB agar square with bacterial growth cut from a petri dish. 51

Figure 3.2. (a-c) Antimicrobial study results for Control and 0, 3, 6, and 9 wt% GSNO final matrices indirectly applied (with silicone sheet between) to (b) *S. aureus*, (c) *S. epidermidis*, and (d) *P. aeruginosa* inoculated LB agar plates in the dark at 34°C for 6 h. Control means nothing was applied to the surface of the inoculated LB agar. GSNO/Vaseline primary matrices were mixed with Desitin zinc oxide cream at a 27/73 ratio to achieve 0, 3, 6, and 9 wt% GSNO final matrices. Viable cells were determined via plate counting. Horizontal dashed line represents the LOD (7.96×10^2 CFU/cm^2). No error bar means the LOD was reached for each trial. Data represents the mean ± SD (n = 3). * $p < 0.05$, ** $p < 0.025$, *** $p < 0.01$, 0 wt% GSNO vs. 3, 6, and 9 wt% GSNO..... 56

Figure 3.3. (a-c) Antimicrobial study results for No Cream, Neosporin, and 0, 3, 6, and 9 wt% GSNO final matrices directly applied to (a) *S. aureus*, (b) *S. epidermidis*, and (c) *P. aeruginosa* inoculated pig skin pieces in the dark at 34°C for 6 h. No Cream means nothing was applied to the surface of the inoculated pig skin. GSNO/Vaseline primary matrices were mixed with Desitin zinc oxide cream at a 27/73 ratio to achieve 0, 3, 6, and 9 wt% GSNO final matrices. Viable cells were determined via plate counting. Data represents the mean ± SD (n = 3). * $p < 0.05$, ** $p < 0.025$, *** $p < 0.01$, 0 wt% GSNO vs. 3, 6, and 9 wt% GSNO. 58

Figure 3.4. (a-c) Anti-biofilm study results for No Cream, Moisturizer, Neosporin, formulation (**a**), and formulation (**b**) matrices directly applied to 24 h (a) *S. aureus*, (b) *S. epidermidis*, and (c) *P. aeruginosa* biofilms on pig skin pieces in the dark at 34°C for 6 h. No Cream means nothing was applied to the surface of biofilms. Formulations (**a**) = 9 wt% GSNO + ZnO Cream: GSNO-Vaseline/13% ZnO cream mixed at 27/73 ratio. Formulation (**b**) = 9 wt% GSNO + ZnO Cream + Neosporin: Neosporin cream/40% ZnO cream, 67.5/32.5; GSNO-Vaseline/Neosporin-ZnO cream mixed at 27/73 ratio. Viable cells were determined via plate counting. Data represents the mean ± SD (n = 3). * $p < 0.05$, ** $p < 0.025$, *** $p < 0.01$, 0 wt% GSNO vs. 3, 6, and 9 wt% GSNO.60

Figure 3.5. Real-time NO release of 9 wt% GSNO (acidic pH) and 9 wt% GSNO + 4.5 wt% $NaHCO_3$ (neutral pH) matrices in the dark at 34°C over (a) 6 h and (b) 60 min.[24] (c) Fit of the cumulative NO release versus time for the 9 wt% GSNO + 4.5 wt% $NaHCO_3$ matrix to a first-order rate equation, giving $k_{obs} = 0.66 \pm 0.01$ h^{-1} ($t_{1/2} \sim 1.05$ h). Data represents mean ($n = 3$).... 66

Figure 3.6. (a) Legend for bar graphs b-d. (b-d) Antimicrobial study results for various matrices (see below for detailed matrix list) directly applied to (b) *S. aureus*, (c) *S. epidermidis*, and (d) *P. aeruginosa* inoculated pig skin pieces at 34°C, absent from light, for 6 h. Values above bars represent log reduction between that sample bar and No Cream sample bar. Data represents the means ± SD ($n = 3$). 68

Figure 4.1. Real-time NO release from 2 mL of 1 mM GSNO after addition of either 100 µL of 1 mM $ZnCl_2$ or 100 µL of the buffer. Completed in the dark at 24°C. All solutions made with the buffer 10 mM Tris-HCl (pH 7.4). At t=10.5 min, 100 uL of 1 mM $CuCl_2$ was added as a positive control (The $ZnCl_2$ black plot is hidden behind the red plot at t=10.5 min). Data represents the mean ± SD ($n = 3$)..... 81

Figure 4.2. Real-time NO release after addition of 100 µL of 10 mM GSNO into 2 mL bulk solutions containing a given component. Experiments were completed in the dark at 34°C. All solutions were made with a 10 mM Tris-HCl buffer (pH 7.4). The final ratio of component to GSNO was 10:1 µmol. Data represents the mean ± SD ($n = 3$). 83

Figure 4.3. Cumulative NO release vs. time for no ZnO, 30, 50, and 200 nm size ZnO nanoparticles in the dark, at 24°C, in 100 mM Tris-HCL, pH 7.4 (buffer). At t=0 min, 100 µL of 50 mM GSNO was introduced to 2.0 mL of buffer containing 4.1 mg of 30, 50, or 200 nm size ZnO nanoparticles. No ZnO means no ZnO was present and NO release was caused by natural GSNO decomposition in the dark, at 24°C, in 100 mM Tris-HCL buffer, pH 7.4. The first hour of NO release was removed due to inconsistent initial NO release rates. Error bars were omitted for clarity. Data represents mean ($n = 3$). 85

Figure 4.4. Real-time NO release after addition of 100 µL of 50 mM GSNO (t=1 min) into 2 mL of (a) 100 mM Tris-HCL or (b) 100 mM Tris-H_3PO_4 buffer (pH 7.4) containing no ZnO or 4.1 mg of 30 nm size ZnO nanoparticles. Completed in the dark at 24°C. Data represents the mean ± SD ($n = 3$)..... 87

Figure 4.5. High-resolution (a) S 2p, (b) Zn 2p, (c) O1s, and (d) N 1s XP spectra of 30 nm size ZnO nanoparticles exposed and not exposed to GSNO in 100 mM Tris-HCl buffer (pH 7.4) in the dark at 24°C for 5 h..... 88

Figure 5.1. (a) (top) NO releasing insert cap used in Sheep Study #1 and #2 and (bottom) the silicone tubing filled partially with adhesive glue prior to gluing it to cap (pre-glued section is inside of cap). (b) Regions of catheter studied in Sheep Study #1 and #2. 102

Figure 5.2. Design of NO releasing insert. 104

Figure 5.3. Real-time NO flux of inserts prepared with different formulations a-d in the dark at 24°C over a 72 h period. Data represents the mean ± SD ($n = 3$)..... 105

Figure 5.4. Viable cell counts of *S. aureus* from the liquid broth of simulated catheter hubs after 72 h of exposure to control (no insert) and NO release inserts with formulations (a), (b), and (c), in the dark at 24°C. The horizontal dashed line represents the LOD (100 CFU/mL) for the assay. Data represents the mean ± SD (n = 3). 107

Figure 5.5. Fluorescent microscopic images of *S. aureus* bacteria/biofilm adhered to the inner lumen wall of the simulated hub after exposure to no insert (control) or NO releasing inserts with formulations (a-c) for 72 h in the dark at 24°C. Live/Dead dye stain was used where green = alive cells and red = dead cells. 108

Figure 5.6. %Recovery of GSNO measured on Day 1, 7, and 56 from NO releasing inserts using formulation (a), stored in the dark at 24°C after hydrogen peroxide (H_2O_2) sterilization. Control (no sterilization) NO releasing inserts using formulation (a) were measure for %recovery of GSNO on Day 0. Data represents the mean ± SD (n = 3). 111

Figure 5.7. Sheep Study #1 bacteria counts from the hub solution on days 2, 4, 7, 9, 11, and 14 using normal catheter caps (Control) and NO releasing insert caps (Experimental). Dashed line is the limit of detection (200 CFU/mL). Log reduction values are given for Experimental vs. Control. The number of samples (n = X) is specified for each day. Data with an error bar represents the mean ± SD. 113

Figure 5.8. Sheep Study #1 bacteria/biofilm adhered to the inner lumen wall of the hub region, tunneled region, distal intravascular region, and proximal tip of catheters using normal catheter caps (Control) and NO releasing insert caps (Experimental). Dashed line is the limit of detection (400 CFU/segment). Log reduction values are given for Experimental vs. Control. The number of samples (n = X) are specified for each section of catheter. Data with an error bar represents the mean ± SD. 114

Figure 5.9. Sheep Study #1 fluorescent microscopic images of bacteria/biofilm adhered to the inner lumen wall of the (1) hub region, (2) tunneled region, (3) distal intravascular region, and (4) proximal tip of catheters using normal catheter caps (Control) and NO releasing insert caps (Experimental). Live/Dead dye stain was used where green = alive cells and red = dead cells. 115

Figure 5.10. Sheep Study #2 bacteria/biofilm adhered to the inner lumen wall of the hub region, tunneled region, distal intravascular region, and proximal tip of catheters using normal catheter caps (Control) and NO releasing insert caps (Experimental). Dashed line is the limit of detection (400 CFU/segment). Log reduction values are given for Experimental vs. Control. The number of samples (n = X) are specified for each section of catheter. Data with an error bar represents the mean ± SD. 117

Figure 5.11. Sheep Study #2 fluorescent microscopic images of bacteria/biofilm adhered to the inner lumen wall of the (1) hub region, (2) tunneled region, (3) distal intravascular region, and (4) proximal tip of catheters using chlorhexidine caps (Chlorhexidine) and NO releasing insert caps (Experimental). Live/Dead dye stain was used where green = alive cells and red = dead cells. 118

Figure 6.1. Proposed scheme for the mechanism by which ZnO nanoparticles react with GSNO to enhance NO release. Blue dots represent electrons trapped in oxygen vacancies on the surface of ZnO. The red positive sign represents a net positive area that remains in the oxygen vacancy after the trapped electron facilitates a reduction reaction with GSNO. 128

Figure 6.2. Image depicting the production of superoxide radicals via atmospheric oxygen reacting with an electron from the surface of ZnO (oxygen vacancy).[19] 129

Figure 6.3. Preliminary leaching study from the NO releasing inserts using ICP-MS. (a) Concentration of Zn (ppb) detected for Control (only silicone tubing and glue, no GSNO and no ZnO present), NO insert under the condition defined as "entire insert soaked", and NO insert under the condition defined as "partial insert soaked" after 24 h soaking increments in purified deionized water for a total of 72 h. Data represents the mean ± SD (n = 3). (b) Conditions defined for the leaching test, defined as entire insert soaked or partial insert soaked. 132

LIST OF TABLES

Table 2.1. Summary of %NO release in 6 h, first order rate constant (k_{obs}), and half-life ($t_{1/2}$) for 3, 6, and 9 wt% GSNO final matrices measured in the dark at 34°C. GSNO/Vaseline primary matrices were mixed with commercial Desitin zinc oxide cream at a 27/73 ratio. (n = 3 separate preparations). 38

Table 3.1. Average pH of 1 mM GSNO, GSH, and SNAP solutions. Data represents the mean ± SD (n = 3)..... 62

Table 3.2. Average pH of formulations diluted 1:10 in purified water. Data represents the mean ± SD (n = 3)..... 64

Table 3.3. Summary of wt% water content for various creams/emulsions and their corresponding classifications of water-in-oil (w/o) or oil-in-water (o/w) emulsions. Data represents the mean ± SD (n = 3)..... 65

Table 3.4. Comparison summary of %NO release in 6 h, first order rate constant (k_{obs}), and half-life ($t_{1/2}$) for 9 wt% GSNO and 9 wt% GSNO + 4.5 wt% $NaHCO_3$ matrices measured in the dark at 34°C.[24] Data represents the mean ± SD (n = 3 separate preparations). 66

Table 4.1. Summary of rate constant (k_{obs}) measured and the available surface area of ZnO present for trials containing no ZnO, 30, 50, and 200 nm size ZnO nanoparticles; where at t=0 min, 100 µL of 50 mM GSNO was introduced to 2.0 mL of 100 mM Tris-HCL buffer, pH 7.4, containing 4.1 mg of 30, 50, or 200 nm size ZnO nanoparticles. Trials were completed in the dark at 24°C. No ZnO means no ZnO was present. Data represents the mean ± SD (n = 3). 85

Table 5.1. %Recovery of GSNO after no sterilization (control), hydrogen peroxide (H_2O_2) sterilization, or ethylene oxide (EO) sterilization processes. Values are normalized to the highest amount of GSNO recovered from the control (no sterilization) trials. Data represents the mean ± SD (n = 3)..... 110

ABSTRACT

In recent years, a small diatomic free radical gas molecule known as nitric oxide (NO) has gained much attention by the biomedical community due to its potential use as a therapeutic agent. In this dissertation, a NO donor (*S*-Nitrosoglutathione (GSNO)) is incorporated into newly devised NO releasing topical creams to potentially treat wound or skin infections, and within novel NO releasing insert devices for disinfecting the hub region of tunnel dialysis catheters (TDCs). GSNO is used throughout this research because it is an endogenous carrier of NO in the human body and is therefore likely to be non-toxic for potential biomedical applications.

In Chapter 2, GSNO is shown to be stabilized when mixed in Vaseline and stored under dry conditions for 300+ days. Also, it is demonstrated that a commercial ZnO-containing cream, when combined with the GSNO in Vaseline mixture, enhances the NO release rate from GSNO. In Chapter 3, the antimicrobial effects of the NO releasing creams are shown to exhibit significant antimicrobial activity versus *S. aureus*, *S. epidermidis*, and *P. aeruginosa*. A NO releasing cream modified by the addition of $NaHCO_3$ to achieve a neutral pH cream also exhibits similar antimicrobial effects.

In Chapter 4, solution phase studies reveal that ZnO is the primary component responsible in the commercial ZnO cream for the enhanced NO release rate from GSNO. Further studies show that 30 nm size ZnO nanoparticles increase NO release rate by a factor of 2.78 compared to no ZnO present. Surface analysis of ZnO suggests no evidence of Zn-S bond formation or thiol attachment after interaction with GSNO.

In Chapter 5, a NO releasing insert device is introduced as an innovative method to disinfect the hub region of TDCs. A short-term shelf-life stability study shows minimal GSNO degradation within the insert device after 56 d of dry/dark storage after H_2O_2 sterilization. Once wetted up by soaking in saline solution, the NO releasing insert device exhibits significant antimicrobial effects against *S. aureus* and *P. aeruginosa* present in the liquid of catheter hubs. Two 14 d long sheep studies demonstrate that the NO releasing insert device is exceptionally potent at preventing bacteria/biofilm growth on the inner lumen walls of the catheters compared normal caps and a chlorhexidine cap.

Significant achievements showcased in this thesis include creation of potent antimicrobial NO releasing creams, discovery of increased NO release from GSNO using ZnO nanoparticles, and creation of NO releasing insert devices capable of preventing bacteria and biofilm growth in catheters. The NO releasing creams provide an attractive alternative method to antibiotic creams to treat dermal infections. The NO releasing insert devices have the potential to significantly lower the number of infections caused by TDCs and other intravascular catheters.

Chapter 1 Introduction

1.1 Antiseptic Agents

1.1.1 Purpose and function of antiseptics

Throughout history, dermal wound infections have been quite prevalent. Primitive treatments include substances from animals, plants, and minerals.[1] Some of these earliest primitive treatments would now be classified as antiseptic agents. The first recorded use of an antiseptic agent was by Dr. Joseph Lister in 1867.[2] Using carbolic acid to sterilize his surgery tools, instruments, and wound bandages, significantly lowered the number of deaths after surgery due to infection. Since that time, several other antiseptic agents have been utilized for their antimicrobial properties. Some antiseptics that have been widely utilized include chlorhexidine, silver compounds (silver nitrate or silver nanoparticles), iodine compounds (cadexomer or povidone-iodine), and honey to name a few. Their antimicrobial functions vary immensely. For instance, chlorhexidine decreases cell wall integrity by binding to the negatively charged groups located on the outside of bacteria cells.[3, 4] Silver ions can also bind to the negatively charged groups present on the cell membrane causing denaturation of the cell membrane.[5] Silver nanoparticles can readily penetrate cell walls and produce intracellular reactive oxygen species (ROSs). These ROSs can damage DNA, RNA, lipids, and proteins leading to apoptosis.[6] Iodine-containing compounds such as cadexomer and povidone-iodine function by delivering iodine to the cell surface. Iodine can easily penetrate cell walls and bind to proteins, nucleotides, and fatty acids present in the cell wall or cytoplasm.[7] Lastly

honey, arguably one of the oldest traditional medicines, inhibits bacteria growth by its inherent low pH, high osmolarity (high sugar content), and production of hydrogen peroxide.[8] Hence, as described by the selected examples above, antiseptics can demonstrate various functions/mechanisms by which killing or inhibition of bacteria growth is carried out.

1.1.2 Antiseptics used for topical treatments

An antiseptic that has remained the dominant biocide in the prevention of infections is chlorhexidine.[7] The most common form of chlorhexidine used in clinical settings is chlorhexidine gluconate (water-soluble).[4, 9] Chlorhexidine has been incorporated into many products such as shampoos, eye creams, hand creams, and sunblocks.[9] Chlorhexidine is a broad-spectrum antimicrobial agent, but it is most effective against gram-positive bacteria.[10-13] As stated above, chlorhexidine's mechanism of action against bacteria involves binding to negatively charged moieties present on bacteria cell walls/membranes, which leads to instability and cell death.[3, 4] Kramer *et al.* demonstrated the antimicrobial effects of a commercially available cream containing chlorhexidine against *Enterococcus hirae* and *Candida albicans*.[14] After 10 min of exposure to the chlorhexidine cream during a standard quantitative suspension test with simulated wound bio-burden, >3 log unit reduction was observed in the number of live *E. hirae* and *C. albicans* cell counts.[14] To date numerous reports have been published on the impressive, fast killing capabilities of chlorhexidine in preventing and fighting infections.

Another antiseptic agent that is commonly used is iodine. The antiseptic properties of iodine were discovered in the early 1800s and have been utilized ever since.[15] The most common form of iodine is called povidone-iodine, which consists of complexed iodine and poly(vinylpyrrolidone).[7, 15] Povidone-iodine arguably has the broadest spectrum of activity of any antiseptic, with reports

of activity against a vast range of fungi and bacteria, including *Pseudomonas*, *Staphylococcus*, *Mycobacterium*, *Candida*, and *Trichophyton* species.[3, 16] Hill *et al.* showed the antimicrobial capabilities of a 5% povidone-iodine cream at killing methicillin-resistant *Staphylococcus aureus* (MRSA).[17] Upon direct inoculation of the 5% povidone-iodine cream with various strains including three MRSA types (separately), all strains were killed after 30 s of exposure, leading to a killing rate of ~10^4 CFU/s.[17] This report clearly demonstrated the potent antimicrobial nature of povidone-iodine.

1.1.3 Limitations and downfalls of antiseptics

In general, antiseptics are effective at killing both gram-positive and gram-negative bacteria strains. The degree to which the antiseptic is effective is typically concentration dependent. However, increasing the concentration of an antiseptic can have cytotoxic effects. For example, there have been cases of chlorhexidine causing anaphylaxis to occur.[18, 19] Additionally, chlorhexidine has trouble dispersing and killing bacteria within biofilms, and this is a concern for treating tissues/areas that are already infected.[20] One mechanism of resistance that has been reported for chlorhexidine is the presence of efflux pumps. Efflux pumps are protein complexes capable of removing chlorhexidine from the cell.[21] Efflux pumps are usually found in gram-positive *Staphylococci* bacteria.[22] Prag *et al.* observed a chlorhexidine tolerance of 37.5% towards 143 Staphylococcus epidermidis isolates, collected from a hospital.[23] Overall, however, chlorhexidine has many positive benefits with only minor/few downfalls or limitations.

Povidone-iodine has been used for a wide variety of clinical applications, with no reports of fungi or bacteria resistance or increased tolerance to this agent.[7, 24] However, in several clinical applications, povidone-iodine has been replaced with chlorhexidine because of chlorhexidine's

more prolonged/lingering activity.[25] There are some reports of contact dermatitis and skin irritation after prolonged contact with povidone-iodine but these are considered to be rare.[26-28] Overall, povidone-iodine has withstood the test of time and has proven itself as an effective broad-spectrum antimicrobial agent with few downfalls or limitations.

1.2 Antibiotics

1.2.1 Purpose and function of antibiotics

When it became generally accepted that micro-organisms were the cause of infection, the door for scientists to develop chemicals/medicine with specific targeting capabilities was opened. This led to the rapid development of a class of antimicrobials known as antibiotics. During the 19th and 20th centuries, hundreds of antibiotics were developed with the purpose to destroy or inhibit the growth of vulnerable bacteria by various means.[29] In general, antibiotics are nontoxic, making them ideal for human use.[30] Most antibiotics can be classified into 6 groups: penicillins, cephalosporins, aminoglycosides, tetracyclines, macrolides, and fluoroquinolones. The function by which these types of antibiotics kill or inhibit bacteria growth varies depending the antibiotic itself and upon bacteria type (gram-positive or negative, aerobic or anaerobic). For example, penicillin-based antibiotics function by affecting the structural integrity of the bacteria's cell wall. Specifically, they block protein struts that cross-link peptidoglycans, which are essential for building a protective layer around the plasma membrane of bacteria cells.[31] Inhibition of peptidoglycans indirectly causes the rupture of the cell wall by allowing foreign material/fluid to enter the cell through tiny holes causing the cell to burst from the excess pressure.[32] Gram-positive bacteria contain higher levels of peptidoglycan compared to gram-negative organisms.[31, 32] Therefore, penicillin-based antibiotics are most effective against gram-positive bacteria strains.

Another general antibiotic group called the aminoglycosides function in a different manner to kill and inhibit bacterial growth. Aminoglycoside-based antibiotics are known to inhibit bacteria protein synthesis by binding to specific ribosomal subunits present in the intercellular fluid.[31] This causes misreading of mRNA and synthesis of atypical peptides, which leads to errors in protein synthesis and cause cell death.[33] Reports demonstrate that aminoglycosides are mostly effective against aerobic, gram-negative bacteria because their crossing of the bacteria cell membrane depends on the aerobic metabolism.[31, 33] The above examples demonstrate how certain antibiotics function. In general, antibiotics are highly selective towards specific strains and types of bacteria due to their inherent bactericidal function.

1.2.2 Antibiotics in ointments, creams, and hydrogels

One use of antibiotics is within ointments, creams, and hydrogels for topical antimicrobial applications due to their efficacy and low toxicity. Utilized since 1956 and approved by the U.S. Food and Drug Administration (FDA) in 1971, the most common nonprescription triple-antibiotic ointment (TAO) (<20% water content) contains a combination of neomycin, polymyxin B, and bacitracin.[34-36] The triple antibiotic combination is utilized because of the limited spectrum each has individually. Neomycin is an aminoglycoside antibiotic effective mainly against aerobic gram-negative organisms while excluding most *Pseudomonas* species.[31, 34] Polymycin B is effective against some gram-negative strains, including *Pseudomonas* species.[31, 34] Bacitracin is most effective against gram-positive strains.[31, 34] This TAO has been evaluated and studied extensively over many decades and has become the standard antimicrobial topical ointment. A clinical study performed from 1989-1990 demonstrated how effective TAO can be at preventing infections of soft-tissue wounds repaired in a hospital emergency department.[37] This study compared TAO,

bacitracin zinc ointment (BAC), silver sulfadiazine cream (SIL), and petrolatum (PTR) (control) applied three times a day to the wound site. Upon study completion, use of TAO resulted in significantly lower infection rates compared to the PTR control: 4.5% and 17.6%, respectively (BAC=5.5%, SIL=12.1%) (*n*=106.5 patients each treatment). TAO had the lowest infection percentage of all evaluated treatments, labeling it as a safe way to prevent infection of wounds that require closure. This is just one of many studies involving the antimicrobial efficacy of TAO.

For a topical treatment to be considered a cream, the amount of water must be >50%. One example of a commonly used antibiotic-containing cream is 0.1% gentamicin cream.[30] Gentamicin is a broad spectrum antibiotic, effective against a number of gram-positive and gram-negative strains.[30, 38] Several studies report using 0.1% gentamicin cream to treat/prevent exit-site infections (ESIs) from peritoneal dialysis catheters.[38-42] In these reports, the treatment of ESIs using the gentamicin cream was mainly compared to a mupirocin cream/ointment (another common topical treatment for ESIs). Mupirocin is an antibiotic mainly effective against gram-positive bacteria strains and therefore highly effective at reducing ESIs caused by *S.* aureus.[43, 44] Reports that compared these two topical treatments, collectively showed that the gentamicin cream was able to match or exceed the reduction of ESIs compared to the mupirocin cream/ointment. In particular, Bernardini *et al.* showed that ESI rates were 0.23/yr using a gentamicin cream and 0.54/yr using a mupirocin cream.[40] Interestingly, there were no *P. aeruginosa* (gram-negative bacteria strain) ESIs when using the gentamicin cream compared to a 0.11/yr ESI rate using the mupirocin cream because mupirocin is not a broad-spectrum antibiotic.

Hydrogels have also been used in combination with antibiotics for various topical applications. Hydrogels are 3D porous materials synthesized using water-soluble polymers that can turn into a gel under defined conditions (temperature, pH, ultraviolet exposure, enzyme catalyst, etc.).[45-47]

Some advantages to using a hydrogel include protection of the antibiotic(s), controlled release, high surface area to volume ratio, and controlled porosity to increase biocompatibility with natural tissues.[45, 46] Ciprofloxacin is a popular antibiotic incorporated into a hydrogel because of its broad-spectrum antimicrobial activity against gram-positive and gram-negative bacteria strains.[48-55] Zhou *et al.* demonstrated that ciprofloxacin incorporated into a poly(vinyl alcohol) (PVA)/poly(ethylene glycol) (PEG) porous scaffold hydrogel was able to completely inhibit the growth of *E. coli* in solution compared to a PVA/PEG control.[55] Marchesan *et al.* reported the antimicrobial capabilities of a ciprofloxacin self-assembled with a tripeptide (^{D}Leu–Phe–Phe) to yield a hydrogel after a pH trigger.[49] A qualitative micro gel well diffusion assay was performed against *S. aureus* (gram-positive), *E. coli* (gram-negative), and *K. pneumoniae* (gram-negative) (Fig. 1.1). An inhibition zone was seen for all ciprofloxacin-loaded hydrogels, demonstrating the broad-spectrum antimicrobial effects of ciprofloxacin.

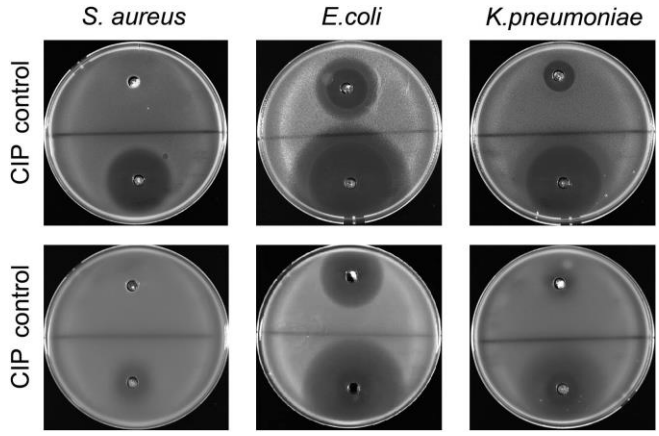

Figure 1.1. Antibacterial efficacy of 0.2% w/v ciprofloxacin (CIP) tripeptide gel and controls of only tripeptide gel against S. aureus, E. coli, and K. pneumoniae agar layer cultures. Images taken after 20 h of incubation at 37°C.[49]

1.2.3 Limitations and downfalls of antibiotics for topical treatments

One user-convenience that the triple-antibiotic ointment (TAO) lacks is spreadability, especially over large areas of skin, because it is inherently an ointment (<20% water). To increase spreadability, manufacturers increased the water percentage to >50%, classifying it as a cream. Unfortunately, bacitracin is not stable over long periods of time in an aqueous environment.[36] Therefore, bacitracin was removed from the cream formulation, leaving only neomycin and polymyxin B. Removal of bacitracin lowers the effectiveness of the new cream with only neomycin and polymyxin B against gram-positive strains. This is an example that demonstrates how a major limitation of using antibiotics is their specificity towards specific bacteria types/strains.

As mentioned previously, gentamicin- or mupirocin-containing creams are commonly used for treating/preventing exit-site infections (ESI) from peritoneal dialysis catheters.[38-44] However, a limitation of using the mupirocin cream/ointment is its lack of broad-spectrum activity, especially towards gram-negative bacteria such as *P. aeruginosa*.[40] Even though gentamicin is a broad-spectrum antibiotic, occurrence of ESIs when using a gentamicin cream have been linked to its lengthy broad-spectrum suppression of indigenous skin flora, causing atypical organisms to grow.[39] Another study aimed to avoid this prolonged broad-spectrum suppression by interchanging applications of gentamicin cream and mupirocin cream. However, there was no change in ESI rate compared to just using the gentamicin cream.[38] Instead, the alternating application regimen caused a higher incidence of antibiotic-related fungal peritonitis.[38] These examples demonstrate how even broad-spectrum antibiotics have downfalls.

In general, antibiotics are nontoxic to humans. However, some antibiotics display toxic behavior depending upon their concentration. For example, ciprofloxacin-loaded hydrogels (mentioned

earlier) have a history of toxicity related to dosage/concentration of ciprofloxacin.[46] Du *et al.* demonstrated the cytotoxicity of ciprofloxacin-loaded nano-in-micro hydrogel particles on RAW macrophage cells.[56] Versus a control of ciprofloxacin-free hydrogel particles, the viability of the RAW macrophage cells was reduced by 38.4% after 24 h of exposure at 37°C for the lowest concentration of ciprofloxacin tested (320 μg/mL).[56] This example demonstrates how some antimicrobials have cytotoxic effects even though the vast majority of antibiotics are deemed nontoxic.

1.3 Nitric Oxide

1.3.1 Purpose, function, and properties of nitric oxide

Over the past three decades, a small gaseous molecule, nitric oxide (NO), has gained much attention due to its potential as a therapeutic agent. In the 1980s, NO was discovered to be the endothelium-derived relaxing factor (EDRF) that causes relaxation of smooth muscle cells located in blood vessel walls.[57] This effect causes vasodilation, increasing blood flow to body tissues, and lowers blood pressure. NO is synthesized from L-arginine *in vivo* via three nitric oxide synthase (NOS) enzymes.[57] In the presence of molecular oxygen, L-arginine is oxidized to NO and L-citrulline. Two of these NOS enzymes, neuronal NOS (nNOS) and endothelial NOS (eNOS), are permanently active and play key roles in biological functions such as neurotransmission and prevention of platelet activation and aggregation.[57, 58] However, induced NOS (iNOS) is active only when the body undergoes an immune response to foreign species (proteins, bacteria, viruses, etc.).[57, 59] The half-life of NO in blood is short, 0.5-1.0 s, because it is highly reactive and is quickly scavenged by oxyhemoglobin (to form methemoglobin).[57, 58] NO also reacts with thiols

(RSHs) to form S-nitrosothiols (RSNOs), and can thereby be stored and transported to target locations within the body.[60]

Nitric oxide is highly reactive because it is a diatomic free radical molecule. Therefore, NO is a potent broad-spectrum antimicrobial agent because it can cause multiple reactions that lead to bacteria cell death.[58, 61] The two main mechanisms by which NO can cause cell death are via nitrosative and oxidative stress (Fig 1.2).[61] Nitrosative stress occurs by NO reacting with molecular oxygen to yield NO_2 radical. This species reacts with another NO to yield the reactive product N_2O_3. N_2O_3 then reacts with thiol groups (RSH) present on the surface proteins of bacteria, causing the cell wall to denature and break apart, killing the bacteria cell. Oxidative stress occurs when NO is present in the intracellular fluid of the bacteria cell. NO is highly lipophilic and therefore can readily pass through bacteria cell walls/membranes.[62] Once inside, NO reacts with superoxide (derived from cellular respiration) to form peroxynitrite ($ONOO^-$). Peroxynitrite triggers lipid peroxidation reactions to occur, which causes cell membrane destruction.

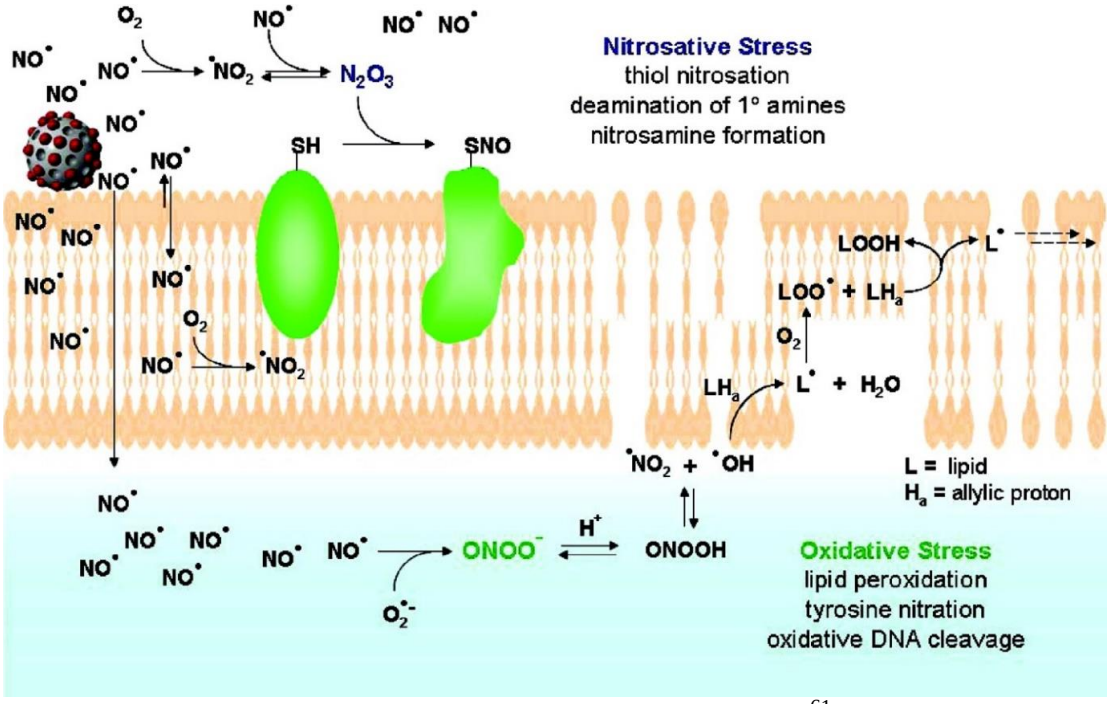

Figure 1.2. Mechanisms by which NO acts as an antibacterial agent.[61]

NO not only displays antimicrobial effects against a broad range of bacteria, it is also effective against viruses, fungi, and yeast.[63, 64] NO also displays great dispersal/displacing activity against microbial biofilms.[65-68] One example of NO's anti-biofilm effects was demonstrated by Wo *et al.*, where the authors achieved a 5 log unit reduction in *S. aureus* cell counts between a NO releasing catheters versus a control catheters when placed within a 7 d drip-flow bioreactor under physiological conditions.[68] Overall, NO's many unique properties make it an attractive and potent antimicrobial/anti-biofilm agent.

1.3.2 NO releasing agents for topical treatments

NO is synthesized in skin tissue by fibroblasts, keratinocytes, melanocytes, and Langerhans cells.[57, 69] On the skin surface, NO is produced via chemical and bacterial reduction of sweat nitrate.[69] In recent years, the application of NO for the treatment of dermal conditions has been explored as it has several attractive properties, such as being a potent antimicrobial and anti-inflammatory agent, as well as increasing angiogenesis, i.e. proliferation of new blood vessels (for potential wound healing applications). Various NO donor platforms and methods have been investigated with the goal to develop systems capable of delivering/releasing NO in a controlled and efficient manner.

S-Nitrosothiols (RSNOs) are a class of NO donor molecules that have immense therapeutic potential because of their inherent low toxicity and ability to store and release NO (Fig. 1.3).[70] However, RSNOs are fairly reactive and can release NO in the presence of reducing agents, metal ions (e.g. Cu(I/II)), as well as by thermal degradation and photolysis.[71-78] Therefore, incorporating RSNOs into various topical matrices may increase their stability.

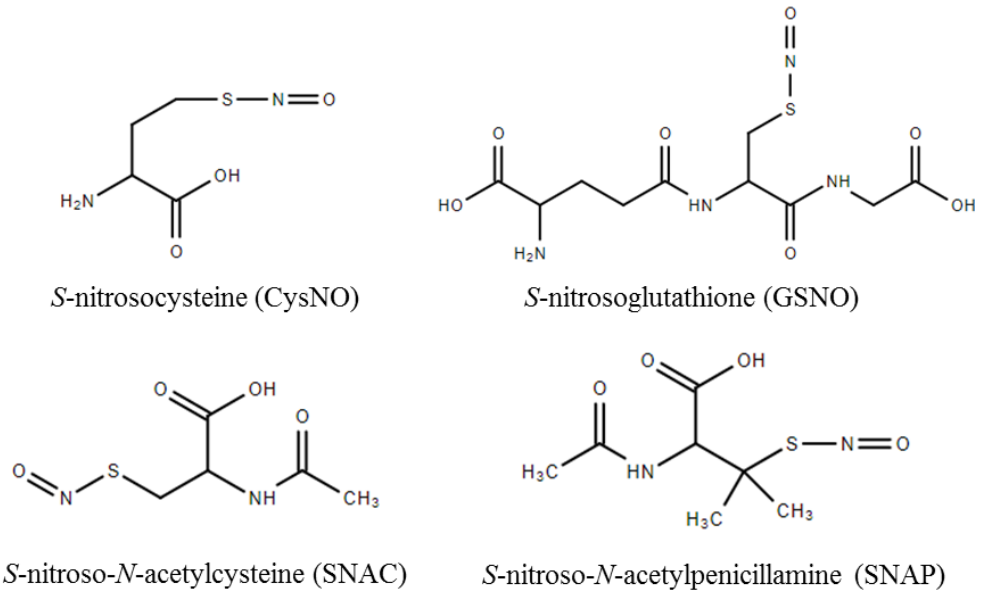

Figure 1.3. Structures of various RSNOs.

Oliviera *et al.* studied the effect of incorporating GSNO and SNAC into a hydrogel comprised of Pluronic F127, a triblock copolymer of poly(ethylene oxide)—poly(propylene oxide)—poly(ethylene oxide).[79] Thermal and photochemical NO-release rates from *S*-nitrosoglutathione (GSNO) and *S*-nitroso-*N*-acetylcysteine (SNAC) in water and the hydrogel were determined. Comparing GSNO incorporated within the hydrogel to GSNO incorporated within water, the NO-release rate decreased 2.0-fold at 37°C and 1.5-fold when irradiated at >480 nm (Fig. 1.4).[79] The Pluronic F127 hydrogel has the unique property of reverse thermal gelation, and this stabilizes the RSNO by a cage recombination effect. The geminate radical pair that forms from the hemolytic cleavage of the S—N bond is more likely to undergo radical pair recombination in the solvent cage, thus reducing the decomposition of RSNOs and prolonging the NO-release to approximately 2 h.[79]

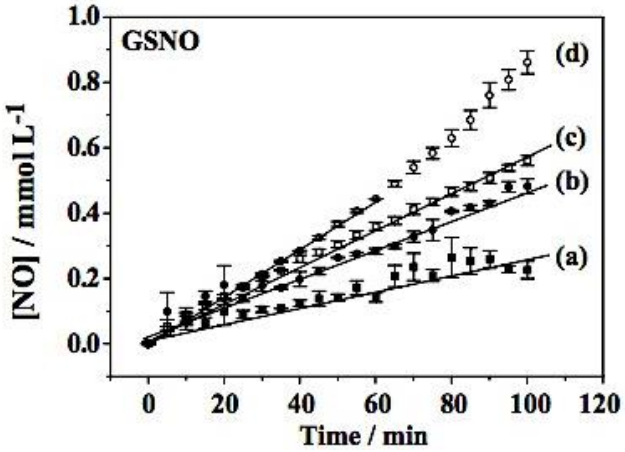

Figure 1.4. Real-time NO release from GSNO incorporated into (a) hydrogel-dark, (b) H_2O-dark, (c) hydrogel-irradiated, (d) H_2O-irradiated; irradiated with $\lambda > 480$ nm.[79]

Other literature reports have demonstrated how incorporating GSNO into a hydrogel increased blood flow when applied to human skin and improved and accelerated the wound healing process of rat models.[80-85] For example, Georgii *et al.* showed that application of a hydrogel containing GSNO to an ischemic wound versus a control hydrogel, increased the wound closure rate. The faster wound closure was attributed to NO's antimicrobial, anti-inflammatory, and pro-angiogenesis properties.

Another class of NO-donor molecules that have been extensively studied are diazeniumdiolates. One advantageous property of diazeniumdiolates is that they release two moles of NO per mole of NO donor via acid catalyzed spontaneous decomposition.[86] A potential issue with using diazeniumdiolates as a NO-donor is the possibility of N-nitrosamine formation, and most nitrosamines are carcinogenic.[87, 88] Nonetheless, various NO releasing diazeniumdiolate scaffolds have been studied for their potential therapeutic purposes because they can store and release large payloads of NO. For example, *N*-diazeniumdiolate-functionalized dendrimers have been examined thoroughly and the NO release rates can be tuned based on the number of terminated

primary amines. Stasko *et al.* determined that the NO release half-lives under physiological conditions of dendrimer polypropylenimine with 16 or 64 terminated primary amines were 12 and 29 min, respectively.[89] The slowed decomposition rate of the larger dendrimer was attributed to the abundance of neighboring amine sites. The neighboring amines sites provide alternative sites of protonation, which slows the proton driven dissociation of diazeniumdiolates.[90] Similar diazeniumdiolate-modified dendrimers were tested on *Streptococcus mutans* for biofilm disruption.[91] The bactericidal and anti-biofilm activity was increased for the NO-releasing dendrimers with greater exterior hydrophobicity. Also, the faster NO-release kinetics yielded greater bactericidal activity compared to slow NO-release dendrimers. However, higher concentrations of diazeniumdiolate-modified dendrimer lead to greater toxicity to mammalian cells, reducing cell viability by up to 70%. The authors attributed the inherent toxicity to the large dose of NO.[91]

NO-releasing silica nanoparticles modified with diazeniumdiolate NO donors have also been investigated. Instead of functionalizing just the outside of the silica nanoparticles like for the modified dendrimers, Hetrick *et al.* developed a synthetic scheme that allowed NO moieties to be present on the surface as well as within the pores of the silica nanoparticles.[61] This new method involves forming the diazeniumdiolate on the silane's secondary amine before performing a condensation reaction with tetraalkoxysilane to synthesize the NO-releasing silica nanoparticle. This unique structure allowed for the storage of larger NO payloads. When tested against *P. aeruginosa*, the NO releasing silica nanoparticle provide a 3 log unit reduction in cell counts with within 90 mins of exposure under physiological conditions.

A company called Novan Therapeutics Inc. is using a version of these NO releasing silica nanoparticles within a type of hydrogel for topical treatments. The company's product at various

concentrations has shown promising antimicrobial effects against methicillin-resistant *Staphylococcus aureus* (MRSA) (Fig. 1.5).

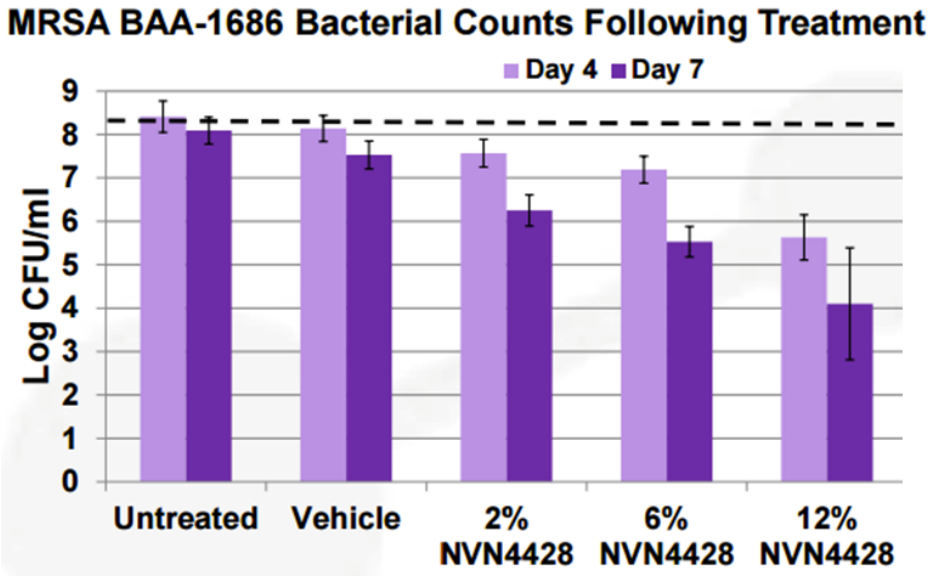

Figure 1.5. MRSA bacteria counts after being untreated, being treated with just the vehicle hydrogel, and being treated with 2, 6, or 12% concentration of Novan's product on various days (graph taken from novan.com).

1.4 Summary

Antiseptic agents have long been utilized by the biomedical field for their broad-spectrum antimicrobial effects. Unfortunately, given antiseptics are not always suitable/safe for all applications. The discovery and development of antibiotics brought the medical community an effective/nontoxic way to target specific bacteria strains/infections. However, the evolution of antibiotic resistant bacteria strains has severely reduced the effectiveness of antibiotics. This phenomenon has made development of new antimicrobial agents/techniques a hot topic in the biomedical field. Overall, NO's potential to be used for various biomedical applications is quite

high. NO's many advantageous properties has driven researchers to utilize NO for several antimicrobial applications including topical treatments.

1.5 Statement of Thesis Research

The purpose of this dissertation is to examine the characteristics and antimicrobial capabilities of newly devised NO releasing creams and devices. Moreover, this research introduces a novel method for releasing NO from *S*-nitrosoglutathione (GSNO) using zinc oxide (ZnO) nanoparticles. There is a heavy focus on using GSNO as the NO donor because it is endogenously produced and therefore relatively non-toxic. Furthermore, the stability of GSNO is a primary topic addressed in several chapters. Each NO releasing project has considerable practical application, with the goal of preventing/treating infections in the biomedical field.

Chapter 2 analyzes the characteristics and capabilities of various NO releasing two-part cream formulations. This includes evaluating the long-term storage capabilities of GSNO within a hydrophobic matrix, namely Vaseline. Also, the NO release kinetics from GSNO stored in Vaseline when combined with a commercial ZnO-containing cream are reported. The NO release properties of this mixture are shown to be promising for potential antimicrobial applications.

Chapter 3 evaluates the antimicrobial effects of the NO releasing two-part creams developed in Chapter 2. Indirect and direct application studies of the NO releasing creams onto different bacteria strains cultured on agar plates and also on pig skins were performed. Very significant antimicrobial activities for all bacteria tested are reported. Experiments to assess the antimicrobial activity of the NO releasing creams with various pH's were also conducted.

Chapter 4 investigates the NO release from GSNO in the presence of ZnO nanoparticles. ZnO was proved to be substance responsible within the commercial ZnO cream that enhances NO release from GSNO. Solution phase studies were performed with GSNO and ZnO nanoparticles of different diameters to gain insight into how enhanced NO release from GSNO occurs in the presence of such particles.

Chapter 5 introduces a NO releasing insert device to disinfect the hub region of tunnel dialysis catheters (TDC). The NO release characteristics of various GSNO/ZnO-containing inserts were evaluated, along with their antimicrobial capabilities. Sheep studies evaluated the performance of the NO releasing insert device against normal TDC caps and a commercially available antimicrobial cap.

Finally, Chapter 6 provides a summary of the major conclusions drawn from the research described in Chapters 2-5. In addition, this chapter details suggestions for future experiments that can expand on the existing knowledge for the new GSNO-ZnO based NO release chemistry discovered via the research described in this dissertation.

The research reported herein consists of studying novel NO releasing creams/devices for various biomedical applications. The NO releasing creams utilizing GSNO, Vaseline, and ZnO cream display significant antimicrobial effects on three bacteria strains associated with dermal or wound infections. These NO releasing creams have the potential to be a better alternative to using existing antibiotic-containing creams for dermal or wound infections. It was discovered that ZnO nanoparticles can enhance the NO release rate from GSNO. This discovery can potentially impact

future research studies to incorporate ZnO nanoparticles to increase NO release from GSNO or other RSNO species. The NO releasing insert device is shown to exhibit significant antimicrobial/anti-biofilm effects when used with tunneled dialysis catheters. This NO releasing insert device could significantly lower the number of catheter related infections for hemodialysis patients.

1.6 References

(1) Forrest, R. D. *J R Soc Med* **1982,** *75* (3), 198-205.

(2) Hirsch, T.; Seipp, H. M.; Jacobsen, F.; Goertz, O.; Steinau, H. U.; Steinstraesser, L. *Eplasty.* **2010,** *10* (39), 320-326.

(3) Lim, K. S.; Kam, P. C. A. *Anaesthesia and Intensive Care* **2008,** *36* (4), 502-512.

(4) Russell, A. D.; Path, F. R. C. *Infection* **1986,** *14* (5), 212-215.

(5) Ishida, T. *MOJ Toxicology* **2018,** *4*.

(6) Fu, P. P.; Xia, Q.; Hwang, H.-M.; Ray, P. C.; Yu, H. *Journal of Food and Drug Analysis* **2014,** *22* (1), 64-75.

(7) Williamson, D. A.; Carter, G. P.; Howden, B. P. *Clin. Microbiol. Rev.* **2017,** *30* (3), 827-860.

(8) Mandal, M. D.; Mandal, S. *Asian Pacific Journal of Tropical Biomedicine* **2011,** *1* (2), 154-160.

(9) Silvestri, D. L.; McEnery-Stonelake, M. *Dermatitis* **2013,** *24* (3), 112-118.

(10) Macias, J. H.; Alvarez, M. F.; Arreguin, V.; Muñoz, J. M.; Macias, A. E.; Alvarez, J. A. *American Journal of Infection Control* **2016,** *44* (12), 1530-1534.

(11) Gantait, S.; Bhattacharyya, J.; Das, S.; Biswas, S.; Ghati, A.; Ghosh, S.; Goel, P. *Contemporary Clinical Dentistry* **2016,** *7* (3), 336-342.

(12) Kawana, R.; Kitamura, T.; Nakagomi, O.; Matsumoto, I.; Arita, M.; Yoshihara, N.; Yanagi, K.; Yamada, A.; Morita, O.; Yoshida, Y.; Furuya, Y.; Chiba, S. *Dermatology* **1997,** *195(suppl 2)* (Suppl. 2), 29-35.

(13) Boyce, J. M.; Pittet, D. *MMWR Recomm. Rep.* **2002,** *30*, 1-45.

(14) Kramer, A.; Assadian, O.; Koberger-Janssen, T. *GMS Hyg. Infect. Control* **2016,** *11*.

(15) Durani, P.; Leaper, D. *Int. Wound J.* **2008,** *5* (3), 376-387.

(16) McDonnell, G.; Russell, A. D. *Clin. Microbiol. Rev.* **1999,** *12* (1), 147-179.

(17) Hill, R. L. R.; Casewell, M. W. *Journal of Hospital Infection* **2000,** *45* (3), 198-205.

(18) Parkes, A. W.; Harper, N.; Herwadkar, A.; Pumphrey, R. *British Journal of Anaesthesia* **2009,** *102* (1), 65-68.

(19) Sijbesma, T.; Röckmann, H.; Van Der Weegen, W. *HIP International* **2011,** *21* (5), 630-632.

(20) Bonez, P. C.; dos Santos Alves, C. F.; Dalmolin, T. V.; Agertt, V. A.; Mizdal, C. R.; Flores, V. d. C.; Marques, J. B.; Santos, R. C. V.; Anraku de Campos, M. M. *American Journal of Infection Control* **2013,** *41* (12), e119-e122.

(21) Poole, K. *Journal of Antimicrobial Chemotherapy* **2005,** *56* (1), 20-51.

(22) Wassenaar, T. M.; Ussery, D.; Nielson, L. N.; Ingmer, H. *Eur. J. Microbiol. Immunol. (Bp)* **2015,** *5* (1), 44-61.

(23) Prag, G.; Falk-Brynhildsen, K.; Jacobsson, S.; Hellmark, B.; Unemo, M.; Söderquist, B. *APMIS* **2014,** *122* (10), 961-967.

(24) Bigliardi, P. L.; Alsagoff, S. A. L.; El-Kafrawi, H. Y.; Pyon, J.-K.; Wa, C. T. C.; Villa, M. A. *International Journal of Surgery* **2017,** *44*, 260-268.

(25) Faoagali, J.; Fong, J.; George, N.; Mahoney, P.; O'Rourke, V. *American Journal of Infection Control* **1995,** *23* (6), 337-343.

(26) Reyazulla, M. A.; Gopinath, A. L.; Vaibhav, N.; Raut, R. P. *Eur Ann Allergy Clin Immunol* **2014,** *46* (4), 157-159.

(27) Lachapelle, J.-M. *European Journal of Dermatology* **2014,** *24* (1), 3-9.

(28) Kanagalingam, J.; Feliciano, R.; Hah, J. H.; Labib, H.; Le, T. A.; Lin, J.-C. *International Journal of Clinical Practice* **2015,** *69* (11), 1247-1256.

(29) Powers, J. H. *Clinical Microbiology and Infection* **2004,** *10*, 23-31.

(30) Lipsky, B. A.; Hoey, C. *Clin. Infect. Dis.* **2009,** *49* (10), 1541-1549.

(31) Kapoor, G.; Saigal, S.; Elongavan, A. *J Anaesthesiol Clin Pharmacol* **2017,** *33* (3), 300-305.

(32) Dzidic, S.; Suskovic, J.; Kos, B. *Food Technology and Biotechnology* **2008,** *46*, 11+.

(33) Tolmasky, M. E. *Front. Biosci.* **2000,** *5*, D20-9.

(34) Jones, R. N.; Li, Q.; Kohut, B.; Biedenbach, D. J.; Bell, J.; Turnidge, J. D. *Diagnostic Microbiology and Infectious Disease* **2006,** *54* (1), 63-71.

(35) Hood, R.; Shermock, K. M.; Emerman, C. *The American Journal of Emergency Medicine* **2004,** *22* (1), 1-3.

(36) Bonomo, R. A.; Van Zile, P. S.; Li, Q.; Shermock, K. M.; McCormick, W. G.; Kohut, B. *Expert Review of Anti-infective Therapy* **2007,** *5* (5), 773-782.

(37) Dire, D. J.; Coppola, M.; Dwyer, D. A.; Lorette, J. J.; Karr, J. L. *Academic Emergency Medicine* **1995,** *2* (1), 4-10.

(38) Wong, P.-N.; Tong, G. M. W.; Wong, Y.-Y.; Lo, K.-Y.; Chan, S.-F.; Lo, M.-W.; Lo, K.-C.; Ho, L.-Y.; Tse, C. W. S.; Mak, S.-K.; Wong, A. K. M. *Peritoneal Dialysis International* **2016,** *36* (3), 340-346.

(39) Pierce, D. A.; Williamson, J. C.; Mauck, V. S.; Russell, G. B.; Palavecino, E.; Burkart, J. M. *Peritoneal Dialysis International* **2012,** *32* (5), 525-530.

(40) Bernardini, J.; Bender, F.; Florio, T.; Sloand, J.; PalmMontalbano, L.; Fried, L.; Piraino, B. *Journal of the American Society of Nephrology* **2005,** *16* (2), 539-545.

(41) Chu, K. H.; Choy, W. Y.; Cheung, C. C. W.; Fung, K. S.; Tang, H. L.; Lee, W.; Cheuk, A.; Yim, K. F.; Chan, W. H. H.; Tong, K. L. M. *Peritoneal Dialysis International* **2008,** *28* (5), 505-508.

(42) Tsai, C.-C.; Yang, P.-S.; Liu, C.-L.; Wu, C.-J.; Hsu, Y.-C.; Cheng, S.-P. *The American Journal of Surgery* **2018,** *215* (1), 179-185.

(43) Xu, G.; Tu, W.; Xu, C. *Nephrology Dialysis Transplantation* **2009,** *25* (2), 587-592.

(44) Bernardini, J.; Piraino, B.; Holley, J.; Johnston, J. R.; Lutes, R. *American Journal of Kidney Diseases* **1996,** *27* (5), 695-700.

(45) Yang, K.; Han, Q.; Chen, B.; Zheng, Y.; Zhang, K.; Li, Q.; Wang, J. *Int J Nanomedicine* **2018,** *13*, 2217-2263.

(46) Li, S.; Dong, S.; Xu, W.; Tu, S.; Yan, L.; Zhao, C.; Ding, J.; Chen, X. *Adv Sci (Weinh)* **2018,** *5* (5), 1700527-1700527.

(47) Ng, V. W. L.; Chan, J. M. W.; Sardon, H.; Ono, R. J.; García, J. M.; Yang, Y. Y.; Hedrick, J. L. *Advanced Drug Delivery Reviews* **2014,** *78*, 46-62.

(48) Hosny, K. M. *AAPS PharmSciTech* **2010,** *11* (1), 241-246.

(49) Marchesan, S.; Qu, Y.; Waddington, L. J.; Easton, C. D.; Glattauer, V.; Lithgow, T. J.; McLean, K. M.; Forsythe, J. S.; Hartley, P. G. *Biomaterials* **2013,** *34* (14), 3678-3687.

(50) Lequeux, I.; Ducasse, E.; Jouenne, T.; Thebault, P. *European Polymer Journal* **2014,** *51*, 182-190.

(51) De Giglio, E.; Cometa, S.; Ricci, M. A.; Cafagna, D.; Savino, A. M.; Sabbatini, L.; Orciani, M.; Ceci, E.; Novello, L.; Tantillo, G. M.; Mattioli-Belmonte, M. *Acta Biomater.* **2011,** *7* (2), 882-891.

(52) Manju, S.; Antony, M.; Sreenivasan, K. *Journal of Materials Science* **2010,** *45* (15), 4006-4012.

(53) Das, D.; Ghosh, P.; Dhara, S.; Panda, A. B.; Pal, S. *ACS Appl. Mater. Interfaces* **2015,** *7* (8), 4791-4803.

(54) Das, D.; Pal, S. *International Journal of Biological Macromolecules* **2015,** *72*, 171-178.

(55) Zhou, X.-H.; Wei, D.-X.; Ye, H.-M.; Zhang, X.; Meng, X.; Zhou, Q. *Materials Science and Engineering: C* **2016,** *67*, 326-335.

(56) Du, J.; El-Sherbiny, I. M.; Smyth, H. D. *AAPS PharmSciTech* **2014,** *15* (6), 1535-1544.

(57) Rosselli, M.; Keller, R. J.; Dubey, R. K. *Hum. Reprod. Update* **1998,** *4* (1), 3-24.

(58) Wo, Y.; Brisbois, E. J.; Bartlett, R. H.; Meyerhoff, M. E. *Biomater. Sci.* **2016,** *4* (8), 1161-1183.

(59) Loscalzo, J.; Welch, G. *Prog. Cardiovasc. Dis.* **1995,** *38* (2), 87-104.

(60) Kelm, M. *Biochim. Biophys. Acta Bioenerg.* **1999,** *1411* (2), 273-289.

(61) Hetrick, E. M.; Shin, J. H.; Stasko, N. A.; Johnson, C. B.; Wespe, D. A.; Holmuhamedov, E.; Schoenfisch, M. H. *ACS Nano* **2008,** *2* (2), 235-246.

(62) Fang, F. C. *J. Clin. Invest.* **1997,** *99* (12), 2818-2825.

(63) Ghaffari, A.; Miller, C. C.; McMullin, B.; Ghahary, A. *Nitric Oxide* **2006,** *14* (1), 21-29.

(64) Liew, F. Y.; Cox, F. E. G. *Immunology Today* **1991,** *12* (3), A17-A21.

(65) Barraud, N.; Hassett, D. J.; Hwang, S.-H.; Rice, S. A.; Kjelleberg, S.; Webb, J. S. *J Bacteriol* **2006,** *188* (21), 7344-7353.

(66) Barraud, N.; Storey, M. V.; Moore, Z. P.; Webb, J. S.; Rice, S. A.; Kjelleberg, S. *Microb Biotechnol* **2009,** *2* (3), 370-378.

(67) Xu, L.-C.; Wo, Y.; Meyerhoff, M. E.; Siedlecki, C. A. *Acta Biomater.* **2017,** *51*, 53-65.

(68) Wo, Y.; Li, Z.; Brisbois, E. J.; Colletta, A.; Wu, J.; Major, T. C.; Xi, C.; Bartlett, R. H.; Matzger, A. J.; Meyerhoff, M. E. *ACS Appl. Mater. Interfaces* **2015,** *7* (40), 22218-22227.

(69) Daniela, B.-G.; Thomas, R.; Kolb-Bachofen, V. *Journal of Investigative Dermatology* **1998,** *110* (1), 1-7.

(70) de Oliveira, M. G.; Shishido, S. M.; Seabra, A. B.; Morgon, N. H. *J. Phys. Chem. A* **2002,** *106* (38), 8963-8970.

(71) Broniowska, K. A.; Diers, A. R.; Hogg, N. *Biochim. Biophys. Acta* **2013,** *1830* (5), 3173-3181.

(72) Holmes, A. J.; Williams, D. L. H. *Chem. Commun.* **1998,** (16), 1711-1712.

(73) Dicks, A. P.; Swift, H. R.; Williams, D. L. H.; Butler, A. R.; Al-Sa'doni, H. H.; Cox, B. G. *J. Chem. Soc., Perkin Trans. 2* **1996,** (4), 481-487.

(74) Shishido, S. M.; Oliveira, M. G. *Photochem. Photobiol.* **2000,** *71* (3), 273-280.

(75) Williams, D. L. H. *Acc. Chem. Res.* **1999,** *32* (10), 869-876.

(76) Wood, P. D.; Mutus, B.; Redmond, R. W. *Photochem. Photobiol.* **1996,** *64* (3), 518-524.

(77) de Souza, G. F. P.; Denadai, J. P.; Picheth, G. F.; de Oliveira, M. G. *Nitric Oxide* **2019,** *84*, 30-37.

(78) Lautner, G.; Stringer, B.; Brisbois, E. J.; Meyerhoff, M. E.; Schwendeman, S. P. *Nitric Oxide* **2019,** *86*, 31-37.

(79) Shishido, S. l. M.; Seabra, A. B.; Loh, W.; de Oliveira, M. G. *Biomaterials* **2003,** *24* (20), 3543-3553.

(80) Seabra, A. B.; Fitzpatrick, A.; Paul, J.; De Oliveira, M. G.; Weller, R. *British Journal of Dermatology* **2004,** *151* (5), 977-983.

(81) Amadeu, T.; Seabra, A.; De Oliveira, M.; Costa, A. *Journal of the European Academy of Dermatology and Venereology* **2007,** *21* (5), 629-637.

(82) Seabra, A. B.; Pankotai, E.; Fehér, M.; Somlai, Á.; Kiss, L.; Bíró, L.; Szabó, C.; Kollai, M.; De Oliveira, M. G.; Lacza, Z. *British Journal of Dermatology* **2007,** *156* (5), 814-818.

(83) Georgii, J. L.; Amadeu, T. P.; Seabra, A. B.; de Oliveira, M. G.; Monte-Alto-Costa, A. *Journal of Tissue Engineering and Regenerative Medicine* **2011,** *5* (8), 612-619.

(84) Vercelino, R.; Cunha, T. M.; Ferreira, E. S.; Cunha, F. Q.; Ferreira, S. H.; de Oliveira, M. G. *Journal of Materials Science: Materials in Medicine* **2013,** *24* (9), 2157-2169.

(85) Marcilli, R. H. M.; de Oliveira, M. G. *Colloids Surf. B Biointerfaces* **2014,** *116*, 643-651.

(86) Hrabie, J. A.; Keefer, L. K. *Chemical Reviews* **2002,** *102* (4), 1135-1154.

(87) Wang, P. G.; Xian, M.; Tang, X.; Wu, X.; Wen, Z.; Cai, T.; Janczuk, A. J. *Chemical Reviews* **2002,** *102* (4), 1091-1134.

(88) Lijinsky, W. Cambridge University Press: Cambridge, **1992**.

(89) Stasko, N. A.; Schoenfisch, M. H. *J. Am. Chem. Soc.* **2006,** *128* (25), 8265-8271.

(90) Davies, K. M.; Wink, D. A.; Saavedra, J. E.; Keefer, L. K. *J. Am. Chem. Soc.* **2001,** *123* (23), 5473-5481.

(91) Backlund, C. J.; Worley, B. V.; Schoenfisch, M. H. *Acta Biomater.* **2016,** *29*, 198-205.

Chapter 2 Development and Characterization of Nitric Oxide Releasing Two-Part Creams

Reprinted from Nitric Oxide, Vol. 90, Nitric oxide releasing two-part creams containing *S*-nitrosoglutathione and zinc oxide for potential topical antimicrobial applications, Doverspike, J. C.; Zhou, Y.; Wu, J.; Tan, X.; Xi, C.; Meyerhoff, M. E. Copyright 2019, with permission from Elsevier.

2.1 Introduction

Infected wounds can lead to serious issues such as delayed wound healing, necrosis, limb or life-threatening situations, and spread of infection not only in the patient's body but to others in a hospital setting.[1-3] The most common topical treatments to prevent or treat infections often utilize antibiotics.[4] Consequently, the effects of these treatments over time diminish as multi-drug resistant bacterial strains continue to evolve.[5-7] Over the past decade, the rate of antibiotic resistance has increased rapidly, caused by the misuse of antibacterial agents.[6, 8, 9] Organizations such as the World Health Organization (WHO) and Centers for Disease Control and Prevention (CDC) have declared antibiotic resistance as a global health concern.[8, 9]

When considering topical antimicrobial treatments, either prescription or non-prescription type, the treatment must display several characteristics to be an effective agent. First, active ingredients must be safe and stable. According to U.S. Food and Drug Administration (FDA) standards, new cosmetics with drugs must report an extensive amount of safety data that also demonstrate stability of the ingredients.[10, 11] Topical antimicrobial treatments fall within this category. Second, the active components (e.g., antibacterial agent(s)) should exhibit activity towards a wide range of microbes (non-selective).[6] This will ensure broad application potential of the antimicrobial

treatment. Third, the treatment must be practical and effective over a designated application period. For example, treatments that would require application every 30 minutes would be considered impractical; however topical application once or twice daily would be much more acceptable.

An example of an antimicrobial treatment that is capable of meeting all of the above criteria is one that incorporates nitric oxide (NO) as an active ingredient.[3, 12-18] Nitric oxide (NO) is a simple diatomic free radical that has drawn much attention in the biomedical field due to its potential as a therapeutic agent.[14, 19, 20] NO is naturally synthesized *in vivo* by the enzyme nitric oxide synthase (NOS) and plays a key role in several biological functions such as neurotransmission, prevention of platelet activation and adhesion, and serving as a potent antimicrobial/antiviral agent produced by immune system macrophages to fight infection.[21-24] As a free radical, NO can facilitate a multitude of reactions leading to microbial cell death, making it ideal for therapeutic applications.[14, 19, 25] To date, NO has displayed broad activity, killing many different types of bacteria.[14, 25]

Free radical molecules like NO are highly reactive and therefore NO donor molecules are often utilized to stabilize NO, and then release NO locally upon demand. Some NO donors that have been used for antimicrobial/wound healing applications include nitrite (converted to NO by reduction reaction), *N*-diazeniumdiolates (NONOate), and *S*-nitrosothiols (RSNO).[3, 12-17] A major concern for NO donors is the toxicity of byproducts that are generated upon NO proliferation. NONOates have been shown to form *N*-nitrosamines by back-reaction of some fraction of the NO released, and most nitrosamines are carcinogenic.[26, 27] RSNOs, on the other hand, are NO releasing agents that have the least toxicity-related issues. Most concerns arise from the use of synthetically derived RSNOs and the concentration that humans can be exposed to, which is also an issue with other types of NO donors.[21]

To circumvent any toxicity-related issues, this work utilizes an endogenous RSNO, *S*-nitrosoglutathione (GSNO), that is present in human blood at a concentration between 0.02-0.20 μM, serving as a carrier of NO.[20, 28, 29] Upon liberation of NO, the two most common products are glutathione (GSH) and glutathione disulfide (GSSG), which are also found in human blood at approximately 17 μM and 3 μM, respectively.[29] GSNO is a primary RSNO that can decompose and liberate NO in the presence of certain reducing agents, including trace metal ions (e.g., Cu(I/II)), as well as by thermal degradation and photolysis.[28, 30-38] Hence, maintaining stability of GSNO as well as other RSNOs over long periods of time can be challenging.

Herein, the potential long-term stability issues of GSNO are solved by storage within a highly viscous and hydrophobic matrix, Vaseline. Further, initiating and accelerating the release of NO from GSNO stored within the Vaseline matrix is studied when mixed with various secondary creams containing different NO releasing accelerants/catalysts. The secondary cream that provided the most NO release over a 6 h period contains zinc oxide particles. Zinc oxide (ZnO) particles are widely utilized in pharmaceuticals, cosmetics, textiles, and electronics.[39] For example, ZnO is used in most topical sunscreens because it can absorb UVB (290-320 nm) and UVA (320-400 nm) sunlight radiation.[40] It is also employed within diaper rash creams as a stringent and antimicrobial agent.[41, 42] A method was developed to study the NO release characteristics and kinetics from the GSNO/Vaseline/ZnO cream formulations over a 6 h period in both dark and light settings. Observed first-order rate constants and half-lives are reported for each formulation and scenario studied.

2.2 Materials and Methods

2.2.1 Materials

L-Glutathione reduced (GSH), hydrochloric acid (HCl), and sodium nitrite were purchased from Sigma-Aldrich (St. Louis, MO). Acetone and xylenes were purchased from Fisher Scientific Inc. (Pittsburgh, PA). Vaseline® Jelly, Unilever, Lot 08226JB00 (Vaseline); Neosporin® + Pain Relief Cream, Johnson & Johnson Consumer Inc, Lot 0058LZ (Neosporin cream); Avalon Organics® Intense Defense with Vitamin C Oil-Free Moisturizer, The Hain Celestial Group Inc, Lot 618747 (vitamin C cream); and Desitin® Rapid Relief Cream: Zinc Oxide Diaper Rash Cream, Johnson & Johnson Consumer Inc, Lot 1577LZ/2 (zinc oxide cream) were purchased from a local CVS Pharmacy. Osmotics Cosmeceuticals Blue Copper 5®, Osmotics LLC, Lot 4248D7 (copper cream) were purchased from Amazon.com. All aqueous solutions were prepared with 18.2 M Ω deionized water using a Milli-Q filter (Milli-q purified water) from EMD Millipore (Billerica, MA). *Staphylococcus aureus* ATCC 25923, *Staphylococcus epidermidis* ATCC 12228, and *Pseudomonas aeruginosa* ATCC 27853 were obtained from the American Type Culture Collection (Manassas, VA).

2.2.2 S-Nitrosoglutathione (GSNO) synthesis

An adapted method of the procedure reported initially by Hart *et al.* was used to synthesize GSNO.[43] Synthesis was completed in the absence of light. Reduced glutathione (GSH) (4.59 g) was dissolved in aqueous HCl (0.5 M, 31.5 mL), cooled to 0°C using an ice bath, and continuously purged under nitrogen. An equal molar amount of sodium nitrite (1.035 g) was added directly to

the GSH solution. After stirring for 40 min at 0°C, ice-cold acetone (10 mL) was added into the reaction mixture to precipitate the GSNO. After stirring for another 10 min, the pink precipitate was separated by vacuum filtration. The resulting pink powder was washed by ice-cold water (3 × 10 mL) and acetone (3 × 10 mL), respectively. Finally, the desired GSNO product (3.85 g, 77% yield) was obtained after drying under vacuum at room temperature (24°C) for 24 h. GSNO was stored at freezer temperature (-20°C) in the dark for any further use. The synthesized GSNO was characterized in D_2O at room temperature (24°C) by ^1H NMR spectroscopy (Varian 400 MHz spectrometer) (Fig 2.1). ^1H NMR (400 MHz, D_2O): δ 4.63 (app. t, J = 6.2 Hz, 1 H) , 4.02 (dd, J = 51.2, 12.8 Hz, 2 H), 3.91 (s, 2 H), 3.76 (t, J = 6.4 Hz, 1 H), 2.41 (t, J = 7.6 Hz, 2 H), 2.08 (app. nonet, J = 7.6 Hz, 2 H). The purity of prepared GSNO was > 98% based on the characterization of the ^1H NMR results (Fig. 2.1).

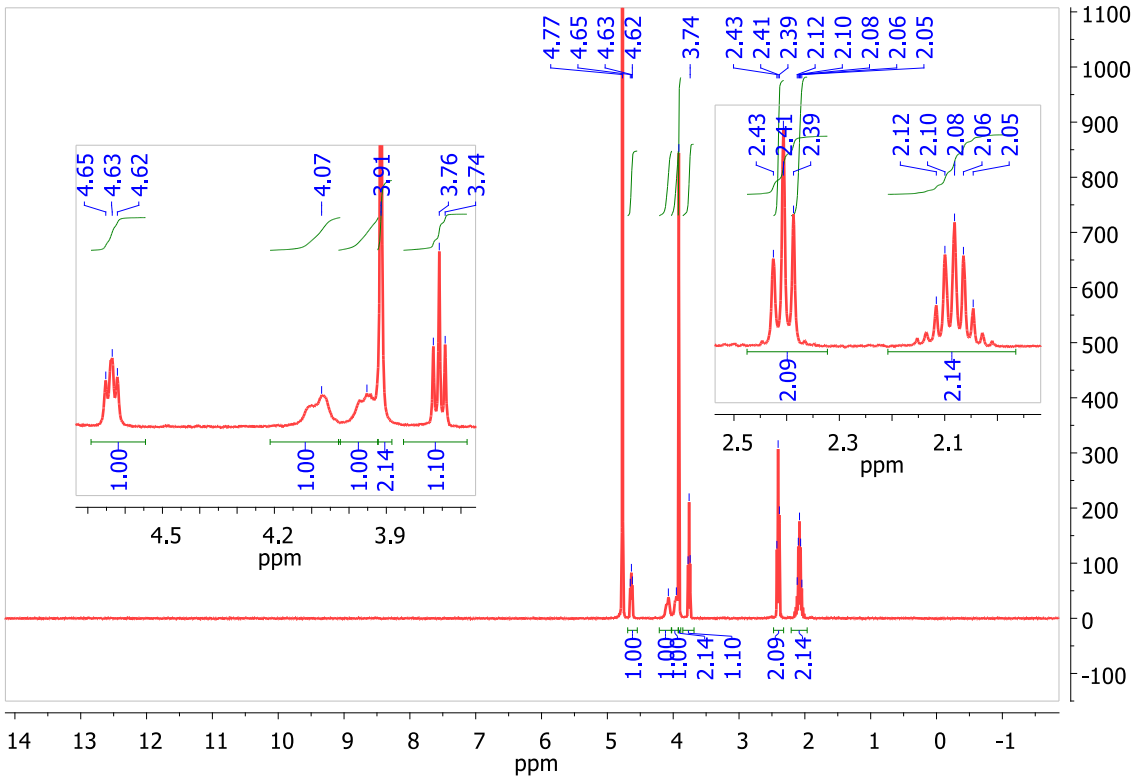

Figure 2.1. ^1H NMR Spectrum of synthesized GSNO in D_2O.[44]

2.2.3 Preparation of various wt% GSNO in Vaseline

The entire preparation of each formulation was completed in the absence of direct light. A mortar and pestle were used to grind GSNO crystals into a fine powder. The desired mass of fine GSNO powder was then weighed out into a mixing vessel. In the same vessel, the desired mass of Vaseline was added. The fine GSNO powder was then mixed thoroughly with the Vaseline using a wooden stirrer for 2.5 min. The resulting mixture was designated as a primary matrix.

2.2.4 Preparation of various wt% of GSNO in Vaseline for long-term stability studies

The desired wt% of the primary GSNO/Vaseline matrix was prepared. The sample was placed into a 20 mL amber glass vial with septum cap and wrapped in aluminum foil. The vial was purged with nitrogen gas via the septum top for 5 h. Samples were then stored in the dark at 24°C for extended time periods.

2.2.5 Evaluating stability of GSNO in Vaseline using UV-Vis spectroscopy

The entire procedure was completed in the absence of direct light. An aliquot of the GSNO/Vaseline primary matrix from the stability study samples was weighed out into a separate 20 mL amber glass vial. Five mL of xylenes was added to the vial. A mixture of xylenes was used to dissolve the Vaseline while not dissolving the GSNO. The vial was shaken on a horizontal shaker (Shaker 30, National Labnet Company, Woodbridge, NJ) at 400 RPM for 10 min. After that time, the contents were transferred into a 60 mL separation funnel. The original sample vial was further washed twice with 1.5 - 2.5 mL of Milli-q purified water and the contents were added

to the separation funnel. The total volume of Milli-q purified water used was noted. The contents in the separation funnel were gently mixed for 1 min. Shaking or agitating the solution too much caused the Vaseline to crash out of the xylenes/organic layer. The bottom aqueous layer that contained dissolved GSNO was then collected. The appropriate volume of aqueous sample was pipetted into a quartz cuvette such that the absorbance measured would be < 1 at 334 nm. Beer's Law ($A = \varepsilon bc$) and an extinction coefficient of $\varepsilon_{334\ nm} = 922\ M^{-1}cm^{-1}$ for the GSNO was used to calculate the theoretical absorbance for each sample.[43] The sample was diluted further if necessary to achieve an absorbance of < 1. UV-Vis spectra were collected using a UV-Vis Spectrophotometer (Lambda 35, Perkin-Elmer, MA). The spectra were obtained by scanning from 300-500 nm at a scanning speed of 240 nm/min. Milli-q purified water was used as the blank to standardize the baseline absorbance. The absorbance at 334 nm was used to calculate the %recovery of GSNO from the stored GSNO/Vaseline primary matrix.[34, 43]

2.2.6 Preparation of matrices for NO release measurements

The entire procedure was completed in the absence of direct light. The GSNO/Vaseline primary matrix was prepared as described above. In the same mixing vessel, the desired mass of a secondary matrix was weighed out such that the ratio of primary to secondary matrix (e.g., commercial ZnO cream, Neosporin cream, copper cream, or vitamin C cream) was 27/73. Both matrices were mixed together using a wooden stirrer for 2.5 min. A small aliquot of the resulting matrix was placed inside of a plastic (polystyrene), circular stencil (diameter 5.85 mm, height 0.33 mm), on top of a glass slide. The excess matrix was scraped away from the top and the stencil was

removed, leaving the matrix at a defined sample size. A schematic of the matrix sample on the glass slide is depicted in Figure 2.2.

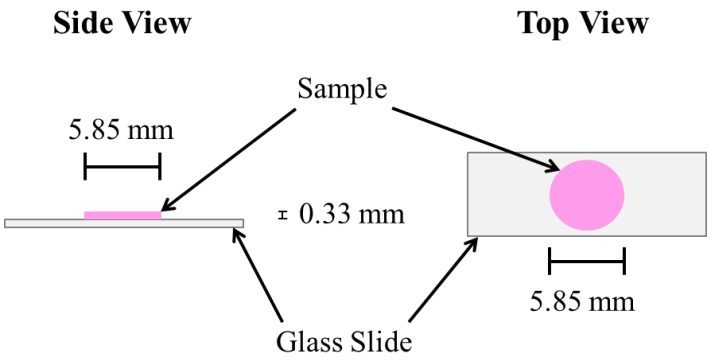

Figure 2.2. Schematic of side and top view for a matrix with a defined sample size on a glass slide.

2.2.7 Measuring NO release from matrices

Nitric oxide release from various mixed matrices was measured using a Sievers Chemiluminescence Nitric Oxide Analyzer (NOA) 280i (Boulder, CO). The NOA was calibrated before via a two-point calibration of N_2 gas passed through a NOA zero air filter and a standard of 44.3 ppm NO in N_2 gas. The test matrix mixture was prepared and put onto a small glass slide as described above. The glass slide was then place into an amber NOA sample cell. The bottom of the amber NOA sample cell was filled with Milli-q purified water and the glass slide was placed on top of a stage above the water line such that the matrix mixture did not come in contact with the water. The water reservoir was bubbled with N_2 gas at a rate of 50 mL/min to humidify the NOA sample cell to prevent the matrix from drying out. The NO generated from the GSNO within the Vaseline/cream mixture was swept into the NOA by N_2 sweep gas. For measuring NO release of samples at 34°C, the amber NOA sample cell was placed in a 34°C water bath. All amber NOA

sample cells were wrapped in aluminum foil to shield the samples from light exposure. A schematic of measuring NO release is depicted in Figure 2.3.

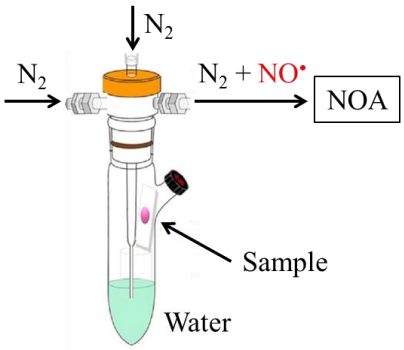

Figure 2.3. Schematic of the set-up for measuring NO release from matrices. The reaction cell is amber glass, submerged in a 34°C water bath, and wrapped in aluminum foil.

2.3 Results and Discussion

2.3.1 Preliminary stability study of 10 wt% and 33 wt% GSNO in Vaseline

Vaseline was chosen as the primary matrix to store and stabilize GSNO. Vaseline is a commercially available matrix consisting of 100% petroleum jelly/petrolatum (white). Petrolatum (white) is insoluble in water because of its extremely hydrophobic nature consisting of saturated hydrocarbons.[45] Having zero water content is a key factor when considering the storage and stability of GSNO. In the presence of water, GSNO can decompose in several manners. A transnitrosation reaction can occur between GSNO and other thiols to yield GSH and the corresponding nitrosated thiol (Fig. 2.4).[46, 47] Singh *et al.* reported that GSNO will decompose in the presence of its parent thiol GSH (and there is always a tiny amount of this species present in the GSNO preparation) and that the decomposition rate is dependent on the concentration of GSH (Fig. 2.4).[34] In aqueous solution, GSNO can also react with other reducing agents such as ascorbate (ascorbic acid) or catalysts such as iron and copper ions (Fig. 2.4).[30-32, 35, 37]

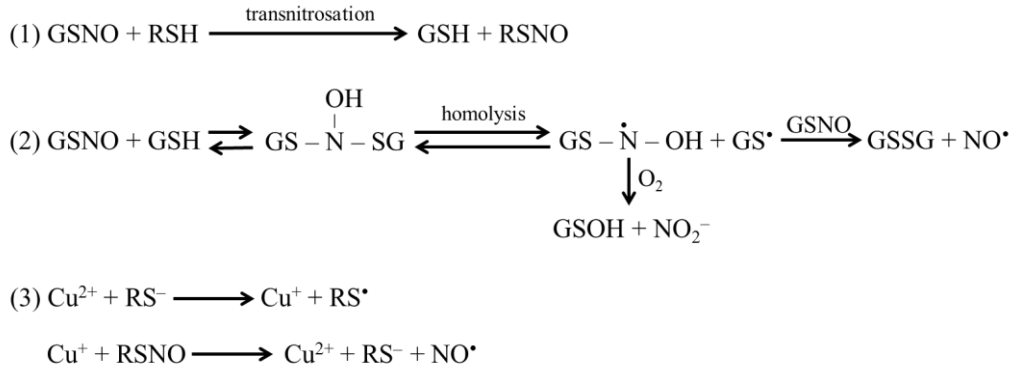

Figure 2.4. GSNO decomposition reactions that can occur in the presence of water, where (1) is a transnitrosation reaction, (2) is a decomposition reaction with GSH, and (3) is a reaction between copper ions and GSNO.[34, 46-48]

Two different concentrations of GSNO in Vaseline, 10 wt% and 33 wt% GSNO, were prepared to evaluate the long-term stability of GSNO in the Vaseline matrix at 24°C, in the dark, and in dry storage. UV-Vis spectroscopy was used to determine the stability of GSNO in Vaseline because GSNO has a strong absorption peak in the UV region at 334 nm.[34, 43] Absorbance (ABS) versus wavelength was measured for both 10 wt% and 33 wt% GSNO in Vaseline stability samples on day 583 and day 313, respectively (Fig. 2.5a,b). The % recovery for the 10 wt% GSNO in Vaseline on day 583 was 89.8 ± 3.4%. The % recovery for the 33 wt% GSNO in Vaseline on day 313 was 87.6 ± 3.5%. The samples were stored in the dark to avoid any photochemical decomposition of GSNO.[36] Traditionally, RSNOs are most stable at colder temperatures. Shishido *et al*. reported increased thermal stability of CysNO in a PEG 400 matrix because a higher viscosity imposes a cage effect on the thiyl and NO radical pair such that geminate recombination occurs more often.[33, 49] Hence, the longevity of GSNO stability at 24°C suggests that the dry GSNO being sequestered within the viscous Vaseline matrix may increase GSNO's thermal stability due to favorable geminate recombination of the thiyl and NO radical pair.

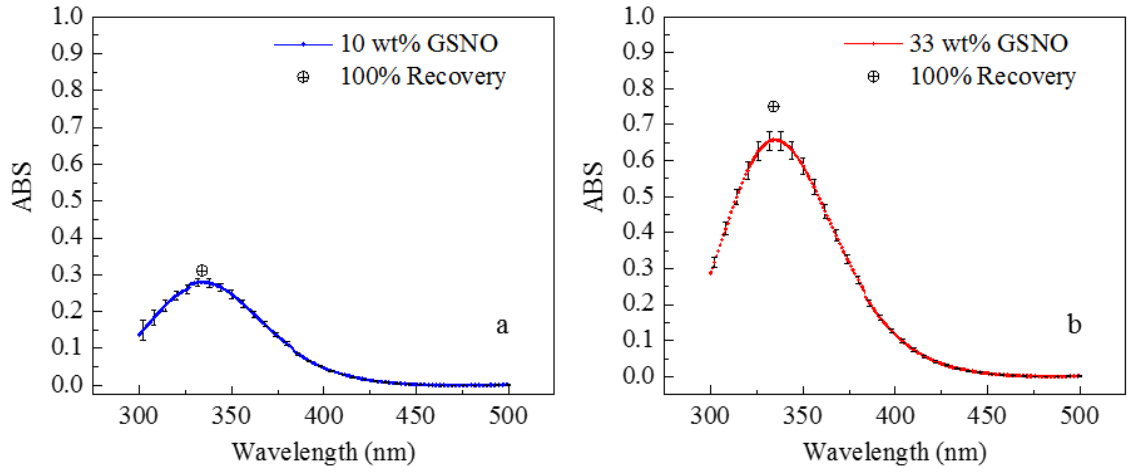

Figure 2.5. Absorbance (ABS) vs. wavelength plots for (a) 10 wt% GSNO and (b) 33 wt% GSNO mixed in Vaseline on day 583 and day 313, respectively. The crossed circle represents the theoretical ABS value at 334 nm for 100% recovery of GSNO. The percent recovery of GSNO was calculated to be (a) 89.8 ± 3.4% and (b) 87.6 ± 3.5 based on ABS at 334 nm. Samples were stored in a dark, dry environment under N_2 gas at 24°C. Data represents the mean ± SD (n = 3).

2.3.2 Initiating NO release using various secondary matrices

Four different commercially available secondary matrices were chosen for testing because they have ingredients that have the potential to assist with NO proliferation from GSNO when mixed with the GSNO/Vaseline primary matrix. The non-prescription matrices selected were Neosporin® + Pain Relief Cream (Neosporin cream), Avalon Organics® Intense Defense with Vitamin C Oil-Free Moisturizer (vitamin C cream), Osmotics Cosmeceuticals Blue Copper 5® (copper cream), and Desitin® Rapid Relief Cream: Zinc Oxide Diaper Rash Cream (zinc oxide cream). The primary matrix (33 wt% GSNO in Vaseline) was mixed with each secondary matrix at a 27/73 ratio. This ratio was chosen primarily based on consistency of the final mixture. NO release for these mixtures at two temperatures was investigated, room temperature (24°C) and a temperature closer to the surface of human skin (34°C).[50] After mixing the primary and secondary matrices, NO release was monitored over a 6 h period using a NOA. Only the first 6 h of NO

release were monitored to simulate a theoretical application period. Figure 2.6 shows the total %NO released from the known amount of GSNO present during the 6 h period for each secondary matrix at 24°C and 34°C. It is clear from the data shown in Figure 2.6 that the zinc oxide cream provides a significantly enhanced rate of NO release when mixed with the GSNO/Vaseline mixture compared to the other three commercial creams tested.

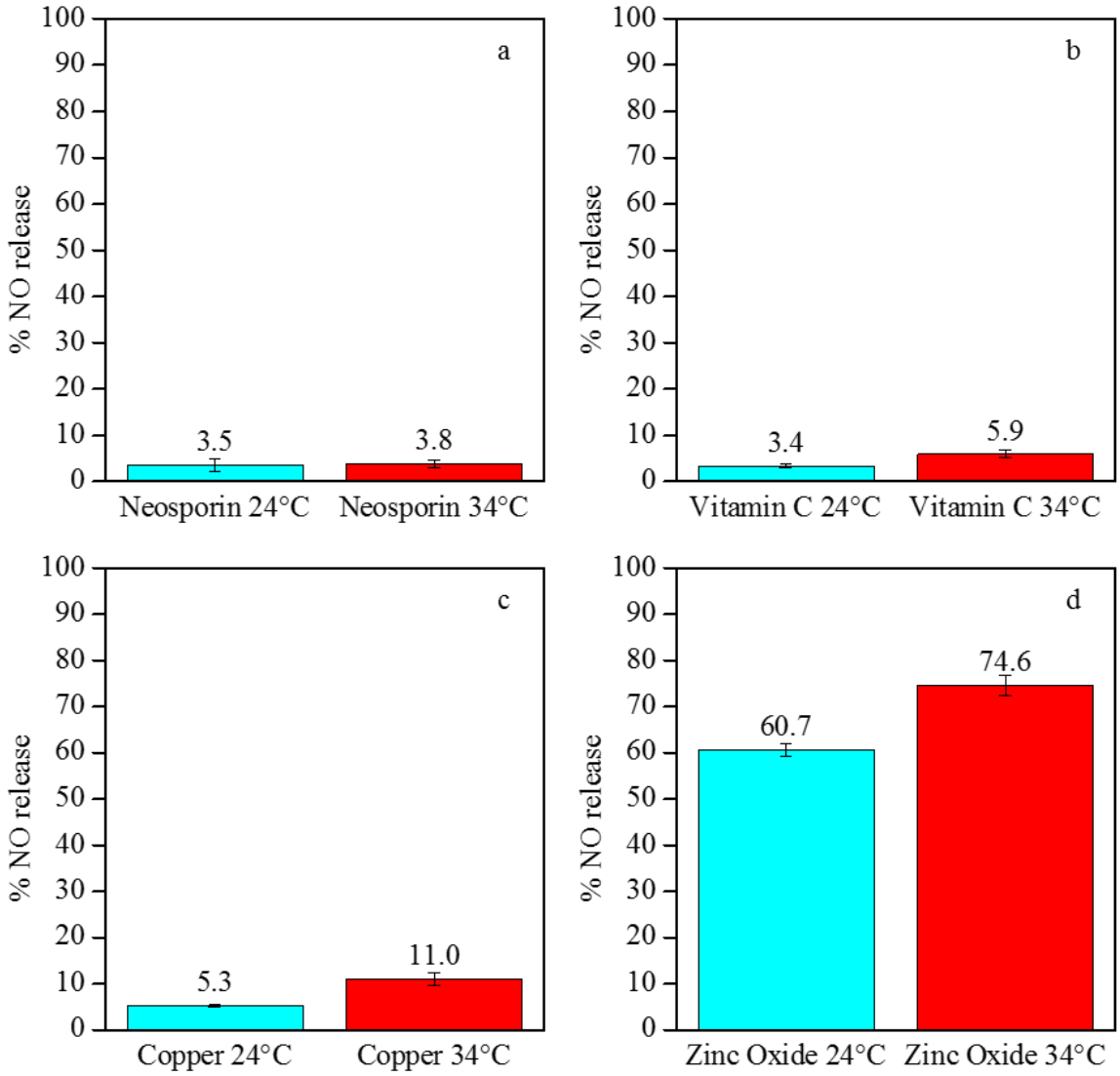

Figure 2.6. %NO released from 33 wt% GSNO/Vaseline primary matrix mixed with several secondary matrices: (a) Neosporin cream; (b) vitamin C cream; (c) copper cream; and (d) zinc oxide cream at a 27/73 ratio to yield a final 9 wt% GSNO matrix. NO release was measured in the dark over a 6 h period at both 24°C and 34°C. Data represents the mean ± SD (n = 3).

In general, for each final matrix mixture there is a minimum of two known mechanisms by which NO is proliferated from GSNO, thermal and via reaction with its parent thiol GSH (a trace amount of GSH is always present in the GSNO preparation).[34, 51] Only these two reactions take place to generate NO in the case where Neosporin is involved. Based on the ingredients present in the Neosporin cream, there are no additional reactions that could likely take place to proliferate NO from GSNO. When Neosporin was mixed with the GSNO/Vaseline mixture, only as small percentage of NO was released after 6 h for both temperatures (Fig. 2.6a). This data shows that Neosporin is not capable of releasing an appreciable amount of NO from GSNO because the NO generation pathways are limited to the two mentioned above.

In the case involving the vitamin C cream, there is an additional reaction that could take place to increase NO release. The active ingredient ascorbic acid/ascorbate (serving as a reducing agent) is known to enhance NO release from GSNO.[30, 32] However, an extremely low %NO release was observed (Fig. 2.6b). The concentration of ascorbic acid in this commercial cream is proprietary and unknown. Therefore, there may not be enough ascorbic acid in the vitamin C cream to release an appreciable amount of NO from GSNO because ascorbic acid is a reactant, not a catalyst for the NO release reaction.[30, 32, 52] Further, the reaction rate between GSNO and ascorbic acid may be hindered by other species present in the Vitamin C cream. It is known that ascorbic acid can be readily oxidized by moisture, light, heat, and metal ions.[53, 54] For this reason, cosmetic formulations use different chemicals or additives to stabilize ascorbic acid such as tocopheryl acetate, citric acid, boric acid, tartic acid, and glycerine.[54]

The %NO released by the copper cream was much lower than expected because copper ions are well-known to be a very good catalyst for NO proliferation from RSNOs (Fig. 2.6c).[31, 35, 55] Similar to the vitamin C cream, there may be a component in the commercial copper cream that inhibits

the reaction between the copper ions and GSNO. One ingredient present in the copper cream is protocatechuic acid (PCA). PCA is known to be a metal ion chelator as well as free radical scavenger.[56, 57] Therefore, the NO produced may be scavenged or the copper ions are likely strongly bound to PCA, not enabling them to serve as a catalyst for NO generation from GSNO.

The zinc oxide cream released significantly more NO from the GSNO/Vaseline mixture than any other secondary matrix tested, at both 24°C and 34°C (Fig. 2.6d). The zinc oxide cream was chosen because McCarthy *et al.* showed that Zn^{2+} ions have the capability of releasing NO from another RSNO (*S*-nitroso-*N*-acetylpenicillamine (SNAP)).[58] However, with no reports on Zn^{2+} ions significantly enhancing the proliferation of NO from GSNO, further experimentation was needed to determine the true source of NO proliferation from GSNO.

2.3.3 NO release characteristics and kinetics from GSNO using zinc oxide cream

The first step to better understand the exact agent in the ZnO cream that accelerates the NO release from GSNO was to investigate the NO release kinetics using three different starting concentrations of GSNO. An aliquot of the appropriate wt% of GSNO in Vaseline was mixed with the zinc oxide cream at a 27/73 ratio such that the final wt% of GSNO in the combined matrix was 3, 6, or 9 wt%. NO release was measured at 34°C for 6 h revealing that the NO release profile for each concentration was fairly similar (Fig. 2.7a). Cumulative NO release plotted versus time reveals a similar NO release trend for all three concentrations of GSNO tested, exhibiting apparent first-order kinetics (Fig. 2.7b). Integration of Figure 2.7a showed that 77.9 ± 3.8%, 75.4 ± 3.8%, and 74.6 ± 2.2% of the total theoretical NO available was released when employing the 3, 6, and 9 wt% GSNO final mixtures over a 6 h test period, respectively (Table 2.1). The observed first order

rate constant for the overall NO release kinetics was determined by the cumulative moles of NO release for 3, 6, and 9 wt% GSNO in the final mixtures versus time, giving k_{obs} = 0.58 ± 0.01 h^{-1} ($t_{1/2}$ ~ 1.18 h), k_{obs} = 0.63 ± 0.01 h^{-1} ($t_{1/2}$ ~ 1.10 h), and k_{obs} = 0.64 ± 0.01 h^{-1} ($t_{1/2}$ ~ 1.08 h), respectively (Fig. 2.8a-c, Table 2.1).

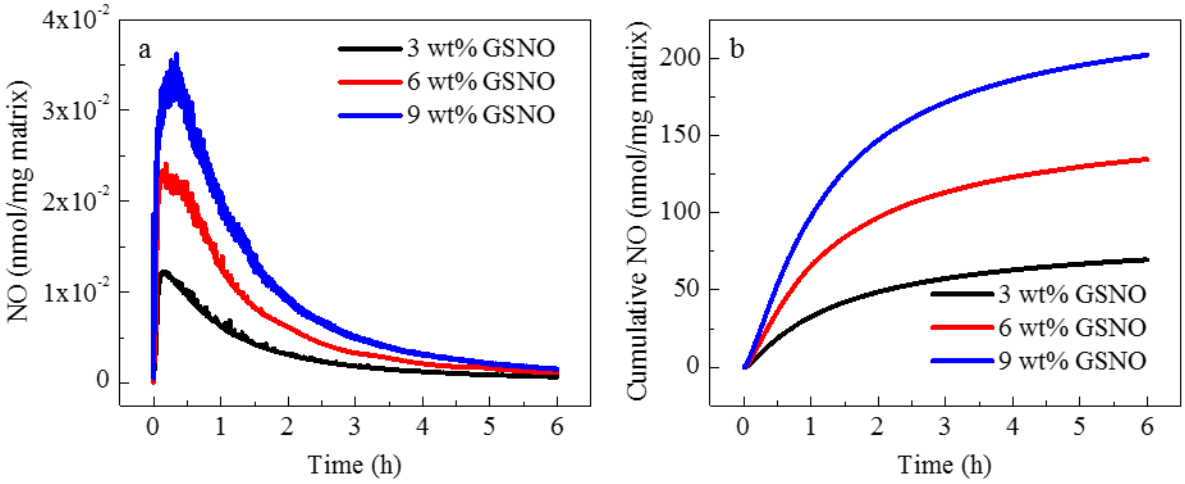

Figure 2.7. (a) Real-time NO release of 3, 6, and 9 wt% GSNO matrices in the dark at 34°C. (b) Cumulative NO release vs. time for 3, 6, and 9 wt% GSNO matrices in the dark at 34°C. GSNO/Vaseline primary matrices were mixed with commercial Desitin zinc oxide cream at a 27/73 ratio to achieve 3, 6, and 9 wt% GSNO final matrices. Data represents mean (n = 3).

Table 2.1. Summary of %NO release in 6 h, first order rate constant (k_{obs}), and half-life ($t_{1/2}$) for 3, 6, and 9 wt% GSNO final matrices measured in the dark at 34°C. GSNO/Vaseline primary matrices were mixed with commercial Desitin zinc oxide cream at a 27/73 ratio. (n = 3 separate preparations).

Matrix	% NO release in 6 h	k_{obs} (h^{-1})	$t_{1/2}$ (h)
3 wt% GSNO	77.9 ± 3.8	0.58 ± 0.01	1.18
6 wt% GSNO	75.4 ± 3.8	0.63 ± 0.01	1.10
9 wt% GSNO	74.6 ± 2.2	0.64 ± 0.01	1.08

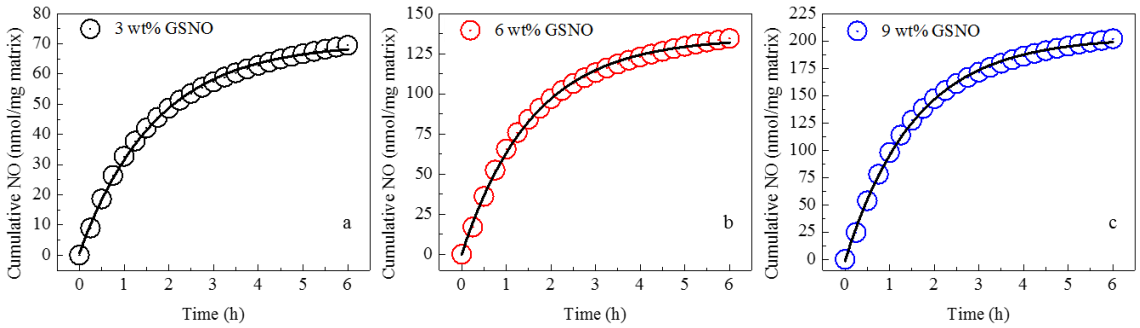

Figure 2.8. Fit of the cumulative NO release versus time of (a) 3 wt% (b) 6 wt%, and (c) 9 wt% GSNO matrices to a first-order rate equation, giving (a) k_{obs} = 0.58 ± 0.01 h^{-1} ($t_{1/2}$ ~ 1.18 h), (b) k_{obs} = 0.63 ± 0.01 h^{-1} ($t_{1/2}$ ~ 1.10 h), (c) k_{obs} = 0.64 ± 0.01 h^{-1} ($t_{1/2}$ ~ 1.08 h). Data represents mean (n = 3).

While it is possible that there could be several different reactions taking place to proliferate NO from GSNO, overall the total %NO release, half-life, and rate constant values are very similar for all three concentrations of GSNO in the final mixtures (Table 2.1). Indeed, the measured rate constants for each concentration of GSNO are very similar, leading to the conclusion that the rate constant is independent of GSNO concentration. However, the actual rate of reaction is time and concentration dependent according to the first-order rate law.

All of the studies described above were completed in the absence of direct light. However, for practical topical application, the creams have a high chance of being exposed to light. Therefore, the NO release kinetics of the highest GSNO concentration in Vaseline/ZnO cream (9 wt% GSNO final cream) were measured in the presence of ambient laboratory light. More specifically, the light source was from fluorescent ceiling lights approximately 2 meters away from the samples tested. In general, the same procedure outlined in Section 2.2.7 was followed. The only changes were that the laboratory light was on during the 6 h NO release measurements, the NOA sample cell was clear glass not amber, and no aluminum foil was used to cover the cell. A direct

comparison of the real-time NO release in the dark versus in ambient room light shows a negligible difference in the rate of NO generation (Fig. 2.9a-b). The %NO released over the first 6 h in the presence of light was 75.1 ± 3.2%, which is very similar to that observed under dark conditions (Table 2.1). The observed first order rate constant in the presence of light was determined in the same manner as described previously, giving k_{obs} = 0.63 ± 0.01 h^{-1} ($t_{1/2}$ ~ 1.10 h), which again is very similar to the in dark scenario (Fig. 2.9c, Table 2.1). One plausible reason why these different scenarios yield similar results could be because only the surface of the opaque cream is exposed to light and not the bulk of the cream. This data concludes that the NO release kinetics are not significantly impacted by the presence of ambient laboratory lighting.

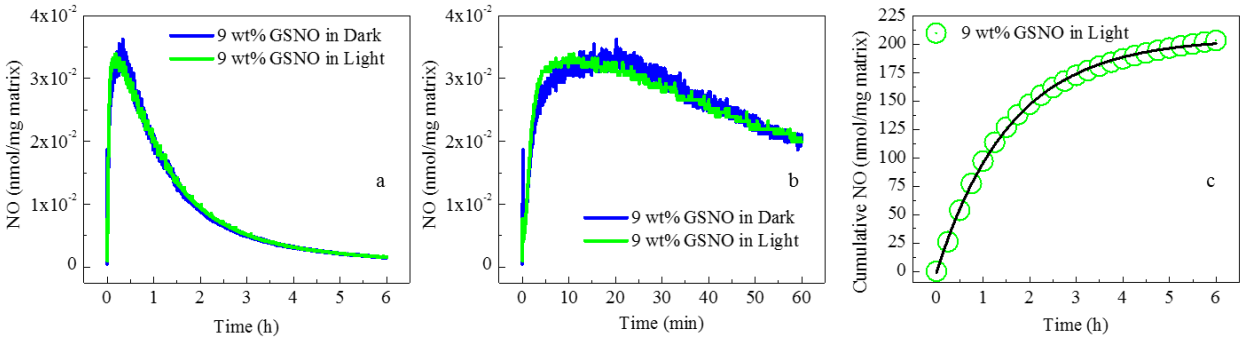

Figure 2.9. Real-time NO release of 9 wt% GSNO matrices in the dark and in ambient room light at 34°C over (a) 6 h and (b) 60 min. (c) Fit of the cumulative NO release versus time of 9 wt% GSNO matrices in ambient room light to a first-order rate equation, giving k_{obs} = 0.63 ± 0.01 h^{-1} ($t_{1/2}$ ~ 1.10 h). GSNO/Vaseline primary matrices were mixed with commercial Desitin zinc oxide cream at a 27/73 ratio to achieve 9 wt% GSNO final matrices. Data represents mean (n = 3).

2.4 Conclusion

The characteristics and capabilities of preparing different NO releasing topical matrices based on storing GSNO as the NO donor in Vaseline have been evaluated. Long-term storage stability was observed for 10 wt% and 33 wt% GSNO mixed in commercial Vaseline at 24°C. The enhanced

stability of GSNO in Vaseline was attributed to the extremely dry storage conditions and the high viscosity of the matrix leading to geminate recombination of the radical pair. Out of four secondary matrices tested to promote NO release when mixed with the GSNO/Vaseline primary matrix, the commercial Desitin zinc oxide-based cream released the highest percentage of NO at both 24°C and 34°C over a 6 h period. The unexpected low rates of NO release from GSNO in the presence of commercial ascorbic acid and copper-containing creams under the same experimental conditions were attributed to interferences in the NO release reaction from other ingredients present in these matrices. First-order NO release kinetics were reported for 3, 6, and 9 wt% GSNO final matrices using the zinc oxide cream as the NO release promoter. Based on the first order rate constants, it was determined that the observed rate constant was independent of GSNO concentration. Comparing the first order rate constants from NO released in the dark versus light revealed that the NO release kinetics are not significantly impacted by ambient light.

2.5 References

(1) Cavanagh, P. R.; Lipsky, B. A.; Bradbury, A. W.; Botek, G. *Lancet* **2005,** *366* (9498), 1725-1735.

(2) Moran, K. A.; Murray, C. K.; Anderson, E. L. *Infect. Control Hosp. Epidemiol.* **2008,** *29* (10), 981-984.

(3) Brisbois, E. J.; Bayliss, J.; Wu, J.; Major, T. C.; Xi, C.; Wang, S. C.; Bartlett, R. H.; Handa, H.; Meyerhoff, M. E. *Acta Biomater.* **2014,** *10* (10), 4136-4142.

(4) Lipsky, B. A.; Hoey, C. *Clin. Infect. Dis.* **2009,** *49* (10), 1541-1549.

(5) Von Döhren, H. *Protein Sci.* **2004,** *13* (11), 3059-3060.

(6) Nathan, C. *Nature* **2004,** *431*, 899.

(7) Fischbach, M. A.; Walsh, C. T. *Science* **2009,** *325* (5944), 1089-1093.

(8) Roca, I.; Akova, M.; Baquero, F.; Carlet, J.; Cavaleri, M.; Coenen, S.; Cohen, J.; Findlay, D.; Gyssens, I.; Heuer, O. E.; Kahlmeter, G.; Kruse, H.; Laxminarayan, R.; Liébana, E.; López-Cerero, L.; MacGowan, A.; Martins, M.; Rodríguez-Baño, J.; Rolain, J. M.; Segovia, C.; Sigauque, B.; Tacconelli, E.; Wellington, E.; Vila, J. *New Microbes New Infect.* **2015,** *6*, 22-29.

(9) Aslam, B.; Wang, W.; Arshad, M. I.; Khurshid, M.; Muzammil, S.; Rasool, M. H.; Nisar, M. A.; Alvi, R. F.; Aslam, M. A.; Qamar, M. U.; Salamat, M. K. F.; Baloch, Z. *Infect. Drug Resist.* **2018,** *11*, 1645-1658.

(10) Food Drug Administration Center for Drug Evaluation Research, Shelf Life/Expieration Dating. FDA Maryland: **2018**.

(11) Food Drug Administration Center for Drug Evaluation Research, New Drug and Antibiotic Regulations [Docket No. 82N-0293]. FDA Maryland, **2018**.

(12) Backlund, C. J.; Worley, B. V.; Schoenfisch, M. H. *Acta Biomater.* **2016,** *29*, 198-205.

(13) Dave, R. N.; Joshi, H. M.; Venugopalan, V. P. *J. Mater. Sci. Mater. Med.* **2012,** *23* (12), 3097-3106.

(14) Hetrick, E. M.; Shin, J. H.; Stasko, N. A.; Johnson, C. B.; Wespe, D. A.; Holmuhamedov, E.; Schoenfisch, M. H. *ACS Nano* **2008,** *2* (2), 235-246.

(15) Lee, W. H.; Ren, H.; Wu, J.; Novak, O.; Brown, R. B.; Xi, C.; Meyerhoff, M. E. *ACS Biomater. Sci. Eng.* **2016,** *2* (9), 1432-1435.

(16) Schanuel, F. S.; Raggio Santos, K. S.; Monte-Alto-Costa, A.; de Oliveira, M. G. *Colloids Surf. B Biointerfaces* **2015,** *130*, 182-191.

(17) Shishido, S. l. M.; Seabra, A. B.; Loh, W.; de Oliveira, M. G. *Biomaterials* **2003,** *24* (20), 3543-3553.

(18) Champeau, M.; Póvoa, V.; Militão, L.; Cabrini, F. M.; Picheth, G. F.; Meneau, F.; Jara, C. P.; de Araujo, E. P.; de Oliveira, M. G. *Acta Biomater.* **2018,** *74*, 312-325.

(19) Fang, F. C. *J. Clin. Invest.* **1997,** *99* (12), 2818-2825.

(20) Liu, X.; Miller, M. J. S.; Joshi, M. S.; Thomas, D. D.; Lancaster, J. R. *Proc. Natl. Acad. Sci.* **1998,** *95* (5), 2175-2179.

(21) Wo, Y.; Brisbois, E. J.; Bartlett, R. H.; Meyerhoff, M. E. *Biomater. Sci.* **2016,** *4* (8), 1161-1183.

(22) Loscalzo, J.; Welch, G. *Prog. Cardiovasc. Dis.* **1995,** *38* (2), 87-104.

(23) Rosselli, M.; Keller, R. J.; Dubey, R. K. *Hum. Reprod. Update* **1998,** *4* (1), 3-24.

(24) Dinerman, J. L.; Lowenstein, C. J.; Snyder, S. H. *Circ. Res.* **1993,** *73* (2), 217-222.

(25) Ghaffari, A.; Miller, C. C.; McMullin, B.; Ghahary, A. *Nitric Oxide* **2006,** *14* (1), 21-29.

(26) Maragos, C. M.; Morley, D.; Wink, D. A.; Dunams, T. M.; Saavedra, J. E.; Hoffman, A.; Bove, A. A.; Isaac, L.; Hrabie, J. A.; Keefer, L. K. *J. Med. Chem.* **1991,** *34* (11), 3242-3247.

(27) Keefer, L. K.; Nims, R. W.; Davies, K. M.; Wink, D. A. "NONOates" (1-substituted diazen-1-ium-1,2-diolates) as nitric oxide donors: Convenient nitric oxide dosage forms. In *Methods in Enzymology*; Academic Press: **1996**; pp 281-293.

(28) Broniowska, K. A.; Diers, A. R.; Hogg, N. *Biochim. Biophys. Acta* **2013,** *1830* (5), 3173-3181.

(29) Kelm, M. *Biochim. Biophys. Acta Bioenerg.* **1999,** *1411* (2), 273-289.

(30) Holmes, A. J.; Williams, D. L. H. *Chem. Commun.* **1998,** (16), 1711-1712.

(31) Dicks, A. P.; Swift, H. R.; Williams, D. L. H.; Butler, A. R.; Al-Sa'doni, H. H.; Cox, B. G. *J. Chem. Soc., Perkin Trans. 2* **1996,** (4), 481-487.

(32) Kashiba-Iwatsuki, M.; Yamaguchi, M.; Inoue, M. *Febs. Lett.* **1996,** *389* (2), 149-152.

(33) Shishido, S. M.; Oliveira, M. G. *Photochem. Photobiol.* **2000,** *71* (3), 273-280.

(34) Singh, S. P.; Wishnok, J. S.; Keshive, M.; Deen, W. M.; Tannenbaum, S. R. *Proc. Natl. Acad. Sci.* **1996,** *93* (25), 14428-14433.

(35) Williams, D. L. H. *Acc. Chem. Res.* **1999,** *32* (10), 869-876.

(36) Wood, P. D.; Mutus, B.; Redmond, R. W. *Photochem. Photobiol.* **1996,** *64* (3), 518-524.

(37) de Souza, G. F. P.; Denadai, J. P.; Picheth, G. F.; de Oliveira, M. G. *Nitric Oxide* **2019,** *84*, 30-37.

(38) Lautner, G.; Stringer, B.; Brisbois, E. J.; Meyerhoff, M. E.; Schwendeman, S. P. *Nitric Oxide* **2019,** *86*, 31-37.

(39) Kołodziejczak-Radzimska, A.; Jesionowski, T. *Materials (Basel)* **2014,** *7* (4), 2833-2881.

(40) Serpone, N.; Dondi, D.; Albini, A. *Inorganica Chim. Acta* **2007,** *360* (3), 794-802.

(41) Siddiqi, K. S.; ur Rahman, A.; Tajuddin; Husen, A. *Nanoscale Res. Lett.* **2018,** *13* (1), 141.

(42) Sirelkhatim, A.; Mahmud, S.; Seeni, A.; Kaus, N. H. M.; Ann, L. C.; Bakhori, S. K. M.; Hasan, H.; Mohamad, D. *Nano-Micro Lett.* **2015,** *7* (3), 219-242.

(43) Hart, T. W. *Tetrahedron Lett.* **1985,** *26* (16), 2013-2016.

(44) Doverspike, J. C.; Zhou, Y.; Wu, J.; Tan, X.; Xi, C.; Meyerhoff, M. E. *Nitric Oxide* **2019,** *90*, 1-9.

(45) Bekker, M.; Louw, N. R.; Jansen Van Rensburg, V. J.; Potgieter, J. *Int. J. Cosmet. Sci.* **2013,** *35* (1), 99-104.

(46) Hogg, N. *Anal. Biochem.* **1999,** *272* (2), 257-262.

(47) Meyer, D. J.; Kramer, H.; Ozer, N.; Coles, B.; Ketterer, B. *Febs. Lett.* **1994,** *345* (2-3), 177-180.

(48) Stubauer, G.; Giuffrè, A.; Sarti, P. *The Journal of biological chemistry* **1999,** *274* (40), 28128-33.

(49) Rabinowitch, E.; Wood, W. C. *Trans. Faraday Soc.* **1936,** *32*, 1381-1387.

(50) Choi, J.-H.; Loftness, V. *Build. Environ.* **2012,** *58*, 258-269.

(51) de Oliveira, M. G.; Shishido, S. M.; Seabra, A. B.; Morgon, N. H. *J. Phys. Chem. A* **2002,** *106* (38), 8963-8970.

(52) Kirsch, M.; Büscher, A.-M.; Aker, S.; Schulz, R.; de Groot, H. *Org. Biomol. Chem.* **2009,** *7* (9), 1954-1962.

(53) Kim, S.; Lee, T. G. *J. Ind. Eng. Chem.* **2018,** *57*, 193-198.

(54) Sheraz, M. A.; Khan, M. F.; Ahmed, S.; Kazi, S. H.; Ahmad, I. *H&PC Today* **2015,** *10* (3), 22-25.

(55) Cui, Y.; Wang, X.; Zhang, Q.; Zhang, H.; Li, H.; Meyerhoff, M. *Anal. Chim. Acta* **2019,** *1053*, 155-161.

(56) Li, X.; Wang, X.; Chen, D.; Chen, S. *Funct. Food Health Dis.* **2011,** *1* (7), 232-244.

(57) Kakkar, S.; Bais, S. *ISRN Pharmacol.* **2014,** *Article ID 952943*, 9 pages.

(58) McCarthy, C. W.; Guillory, R. J.; Goldman, J.; Frost, M. C. *ACS Appl. Mater. Interfaces* **2016,** *8* (16), 10128-10135.

Chapter 3 Antimicrobial Effects of NO Releasing Cream Formulations

3.1 Introduction

In 1941, Selman Waksman was the first to define the term "antibiotic" as any small molecule made by microorganisms that antagonizes the growth of other microbes via a specific Mode-Of-Action.[1, 2] The "golden era" of antibiotic discovery and development occurred from the 1930s to 1960s.[3, 4] Unfortunately, the rise of antibiotic resistant strains caused antibiotic development to rapidly decrease during the following decades mainly due to the abuse and misuse of antibiotics.[3-5] According to organizations such as the World Health Organization (WHO) and Centers for Disease Control (CDC), antimicrobial resistance has evolved into a global crisis.[4-7]

Over the last few decades, several methods have been developed to combat multidrug resistant organisms (MDR). In general, antibiotics are hindered by their specificity toward certain strains/types of bacteria. Therefore, methods such as combination antibiotic therapy have been developed. Combination antibiotic therapy is generalized as using two or more antibiotics to broaden the antibacterial spectrum, treat polymicrobial infections, and provide potential synergistic effects.[3, 8] For topical applications, combination antibiotic therapy is commonly used due to the multitude of bacteria strains/types associated with dermal infections.[9]

Creams/ointments are often the obvious form of treatment/prevention of topical infections. For instance, Neosporin is a commercially available antibiotic cream that utilizes combination

antibiotic therapy. Neosporin cream/ointments contain the antibiotics neomycin, polymyxin B, and/or bacitracin.[10, 11] These are considered as the active ingredients targeting specific bacteria expanding the range of bacteria to kill.[9] Yet, Neosporin and many other creams/ointments still lack the desired broad spectrum antimicrobial killing effects.[12] Therefore, treatments exhibiting non-selective activity are needed. Specifically, an active agent capable of targeting multiple bacteria strains is required.

An agent capable of meeting the above criteria is nitric oxide (NO).[13-20] NO is a free radical molecule, naturally synthesized *in vivo* by the enzyme nitric oxide synthase (NOS).[16, 21, 22] When fighting an infection, the body's immune system macrophages produce NO as a host defense response to serve as an antimicrobial/antiviral agent.[21-23] As a free radical molecule, NO is potent against a broad spectrum of bacteria including antibiotic-resistant strains as it can trigger multiple reactions leading to bacteria cell death.[16, 21, 22] Therefore, assessing the antimicrobial activity of NO releasing creams/ointments is necessary due to their potential impact on society.

This chapter assess the antimicrobial efficacy of previously developed NO releasing cream formulations (see Chapter 2) against *Staphylococcus aureus*, *Staphylococcus epidermidis*, and *Pseudomonas aeruginosa*, which are commonly associated with wound or burn-wound infections.[24-26] First, an indirect application method was used to evaluate the antimicrobial effects of just the NO generated from the GSNO-containing creams. This method eliminated any potential matrix killing effects from the GSNO-containing creams, to focus on the killing effects from only the NO generated. Second, to investigate the antimicrobial effects from both NO and matrix, a direct application study involving pig skin as the model system was conducted. Third, the synergy of combining NO- and antibiotic-containing creams against biofilms was evaluated. Fourth, to further characterize the developed NO releasing formulations, a method was developed to estimate

the pH of the NO releasing cream formulations. Further, the kinetics of NO released from creams with varying pH were reported. Lastly, the antimicrobial efficacy of creams with varying pH were assessed.

3.2 Materials and Methods

3.2.1 Materials

L-Glutathione reduced (GSH), hydrochloric acid (HCl), sodium nitrite, and sodium bicarbonate ($NaHCO_3$) were purchased from Sigma-Aldrich (St. Louis, MO). Acetone was purchased from Fisher Scientific Inc. (Pittsburgh, PA). LB agar and 10 mM phosphate buffered saline (PBS) (pH 7.2) were purchased from ThermoFisher Scientific (Grand Island, NY). Medical grade silicone sheeting (non-reinforced, gloss, 0.0127 cm thick) was purchased from BioPlexus Corp. (Ventura, CA). Vaseline® Jelly, Unilever, Lot 08226JB00 (Vaseline); Neosporin® + Pain Relief Cream, Johnson & Johnson Consumer Inc, Lot 0058LZ; Avalon Organics® Intense Defense with Vitamin C Oil-Free Moisturizer, The Hain Celestial Group Inc, Lot 618747; Desitin® Rapid Relief Cream: Zinc Oxide Diaper Rash Cream, Johnson & Johnson Consumer Inc, Lot 1577LZ/2; Lubriderm Daily Moisture Lotion, Normal to Dry Skin, Fragrance Free, Johnson & Johnson Consumer Inc; and Pond's Dry Skin Cream, Facial Moisturizer, Unilever were products purchased from a local CVS Pharmacy. Osmotics Cosmeceuticals Blue Copper 5®, Osmotics LLC, Lot 4248D7 and Loctite (UK U-05FL) were purchased from Amazon.com. All aqueous solutions were prepared with 18.2 M Ω deionized water using a Milli-Q filter (Milli-q purified water) from EMD Millipore (Billerica, MA). Pork with skin was purchased from a local Chinese supermarket. Staphylococcus aureus ATCC 25923, Staphylococcus epidermidis ATCC 12228, and Pseudomonas aeruginosa ATCC 27853 were obtained from the American Type Culture Collection (Manassas, VA).

3.2.2 S-Nitrosoglutathione (GSNO) synthesis

The method used to prepare GSNO was the same as that described in Chapter 2.

3.2.3 Preparation of various wt% GSNO in Vaseline

The entire preparation of each formulation was completed in the absence of direct light. A mortar and pestle were used to grind GSNO crystals into a fine powder. The desired mass of fine GSNO powder was then weighed out into a mixing vessel. In the same vessel, the desired mass of Vaseline was added. The fine GSNO powder was then mixed thoroughly with the Vaseline using a wooden stirrer for 2.5 min. The resulting mixture was designated as a primary matrix.

3.2.4 Preparation of NO releasing and other matrices

The entire procedure was completed in the absence of direct light. All matrices were mixed together using a wooden stirrer for 2.5 min. The GSNO/Vaseline primary matrix was prepared as described above. For indirect application and direct application antimicrobial studies (3.2.5 and 3.2.7, respectively), the desired mass of a secondary matrix was weighed out into the same mixing vessel such that the ratio of primary to secondary matrix (e.g., commercial 13% ZnO cream) was 27/73. For direct application anti-biofilm studies (3.2.8), the GSNO/Vaseline primary matrix was also mixed with a secondary matrix for a final ratio of 27/73, where the secondary matrix consisted of a 67.5/32.5 ratio of Neosporin/40% ZnO cream (final 13% ZnO after mixing with Neosporin). For the direct application antimicrobial studies of various formulations with varying pH, several additional formulations were prepared. $NaHCO_3$ was added to the GSNO/Vaseline primary matrix such that the final matrix contains 33 wt% GSNO, 16.5 wt% $NaHCO_3$, and 50.5 wt% Vaseline. For this new primary matrix, the amount of $NaHCO_3$ was two molar equivalents of GSNO present.

The GSNO/$NaHCO_3$/Vaseline primary matrix was mixed with the secondary matrix (e.g., commercial 13% ZnO cream) at a 27/73 ratio, yielding 9 wt% GSNO + 4.5 wt% $NaHCO_3$ final concentrations. Another formulation consisted of an equimolar amount of GSH compared to the amount of GSNO described in the previous formulation. GSH was mixed with Vaseline to yield a 30.7 wt% GSH in Vaseline primary matrix. This new primary matrix was mixed with the secondary matrix (e.g., commercial 13% ZnO cream) at a 27/73 ratio, yielding a final concentration of 8.3 wt% GSH. Another formulation was created where $NaHCO_3$ was added to the GSH/Vaseline primary matrix such that the final yields were 30.7 wt% GSH, 16.5 wt% $NaHCO_3$, and 52.8 wt% Vaseline. The GSH/$NaHCO_3$/Vaseline primary matrix was mixed with the secondary matrix (e.g., commercial 13% ZnO cream) at a 27/73 ratio, yielding 8.3 wt% GSH + 4.5 wt% $NaHCO_3$ final concentrations. An additional formulation was created with a primary matrix consisting of 16.5 wt% $NaHCO_3$, and 83.5 wt% Vaseline. This primary matrix was mixed with the secondary matrix (e.g., commercial 13% ZnO cream) at a 27/73 ratio, yielding 4.5 wt% $NaHCO_3$.

3.2.5 Indirect application antimicrobial studies

Overnight grown bacteria cultures were diluted with 1 × PBS buffer (10 mM, pH 7.2) to 1 × 10^5 CFU/mL. Fifty μL of the diluted culture was spread on to a 6 cm diameter LB agar plate and allowed to air dry for 10 min. Squares, 1.5 cm × 1.5 cm, were cut from the inoculated LB agar and place in an empty petri dish. Separately, medical grade silicone sheeting (0.0127 cm thick) was cut into 2.5 cm × 2.5 cm squares. Using a plastic (polystyrene) stencil to define the matrices area (2 cm × 2 cm × 0.033 cm), different mixtures (e.g., GSNO at different wt% in Vaseline mixed with commercial zinc oxide cream (with 13 wt% ZnO)) were spread onto the square silicone sheets

and the excess was scraped away. The average mass of matrix on each silicone sheet was 84.9 ± 3.0 mg (*n*=6). The square silicone sheets with the given matrix mixture were placed on top of the inoculated LB agar squares and the cover was lightly place on the petri dish. Samples were incubated at 34°C, absent from light, for 6 h. After incubation, the silicone sheets were removed from the top of the LB agar squares. A circle (diameter 0.8 cm) was punched out using a biopsy punch (Tru-punch, Fisher Scientific, Hampton, NH) from the center of the LB agar squares. This punched out circle was homogenized in 2 mL of 1 × PBS (10 mM, pH 7.2) in a 15-mL tube using a homogenizer (OMNI TH, OMNI International, Kennesaw, GA) at full speed, and 10-fold serially diluted. Five µL of the dilutions were spread on fresh LB agar plate for overnight culturing and single colonies were numerated. A schematic of the antimicrobial study set-up is shown in Figure 3.1.

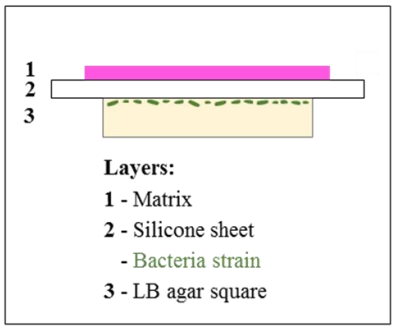

Figure 3.1. Side view schematic of the indirect application antimicrobial study configuration where (1) represents a matrix (NO releasing cream or other), (2) represents a thin silicone membrane/sheet, and (3) represents a LB agar square with bacterial growth cut from a petri dish.

3.2.6 Pig skin treatment

Pork with skin was purchased in a Chinese supermarket. The skin requirements were as follows: hairless, smooth surface, not burned, and not damaged. The flesh attached to the skin was removed using a scalpel. The pig skin was stored at -20°C. Before use in antimicrobial studies, the pig skin

was brought to room temperature (24°C) and cut into pieces (approximately 4 cm × 3 cm). The pig skin surface was sterilized twice using alcohol wipes in a biosafety hood. The sterile pig skin was allowed to dry for 5 min under the biosafety hood ventilation to remove alcohol residue from the pig skin surface. The sterile pig skin pieces were placed in separate Petri dishes.

3.2.7 Direct application antimicrobial studies on pig skin model

Overnight grown bacteria cultures were diluted with 1 × PBS buffer (10 mM, pH 7.2) to 1×10^8 CFU/mL. Fifty μL of the diluted culture was spread on to the surface of each sterile pig skin piece and allowed to air dry for 10 min. Using a plastic (polystyrene) circular stencil to define the matrices area (diameter 1.5 cm, height 0.033 cm), different mixtures (e.g., GSNO at different wt% in Vaseline mixed with commercial zinc oxide cream (with 13% ZnO)) were spread on to the pig skin pieces and the excess was scraped away. The average mass of matrix on each pig skin piece was 68.7 ± 2.7 mg ($n = 6$). The cover was lightly placed on the Petri dish. Samples were incubated at 34°C, absent from light, for 6 h total. After incubation the matrices were removed from the pig skin surface using a razor blade. A circle (diameter 0.8 cm) was punched out using a biopsy punch (Tru-punch, Fisher Scientific, Hampton, NH) from the center of where the matrix was removed from the pig skin piece. This punched out circle was homogenized in 2 mL of 1 × PBS (10 mM, pH 7.2) in a 15-mL tube using a homogenizer (OMNI TH, OMNI International, Kennesaw, GA) at full speed, and 10-fold serially diluted. Fifty μL of the dilutions were spread on fresh LB agar plates for overnight culturing and single colonies were numerated.

3.2.8 Direct application anti-biofilm studies on pig skin model

The biofilm on pig skin model was adapted from Wang *et al*..[27] Briefly, after the pig skin was cut, separated, and sterilized (as described above), a sterile 1.5 mL Eppendorf tube was cut to a height of 1.5 cm and the top side was glued to the pig skin surface using Loctite (UK U-05FL). 1% of overnight grown bacterial culture (*Staphylococcus aureus*, *Staphylococcus epidermidis*, or *Pseudomonas aeruginosa*) was inoculated into fresh LB broth and 0.5 mL of this suspension was transferred to the tube glued on to the pig skin surface. The samples were incubated at 37°C for 24 h. After 24 h, the liquid and tubing were carefully removed from the pig skin surface. The biofilm developed on the pig skin surface was now ready for testing. Cream application and bacteria enumeration were performed using the same procedure described above (2.2.7).

3.2.9 Measuring relative pH of various cream formulations

Five hundred mg of all cream formulations were created in triplicate and prepared in separate 15 mL conical sterile polypropylene centrifuge tubes. Each sample was mix thoroughly with a wooden applicator for 2.5 min. Milli-q purified water (4.5 mL) was added to each vessel and hand shaken for 3 min. Each sample was centrifuged at 14,000 rpm for 3 min. Four mL of the supernatant fluid was put into separate glass dram vials. The pH of each solution was measured using a pH electrode InLab Routine Pro from Mettler Toledo.

3.2.10 Measuring wt% water within the creams

Creams were weighed out into glass sample vials. The entire mass of the matrix plus the sample vial was measured. The samples were dried under vacuum for 7 days. On the 7th day, samples

were re-weighed and the masses subtracted from the original masses on day 0. Results are shown in Table 3.3 (see Results and Discussion section).

3.2.11 Preparation of matrices for NO release measurements

The entire procedure was completed in the absence of direct light. After the desired matrix was created as described in Section 2.2.4, a small aliquot of the resulting matrix was placed inside of a plastic (polystyrene), circular stencil (diameter 5.85 mm, height 0.33 mm), on top of a glass slide. The excess matrix was scraped away from the top and the stencil was removed, leaving the matrix at a defined sample size.

3.2.12 Measuring NO release from matrices

Nitric oxide release from various mixed matrices was measured using a Sievers Chemiluminescence Nitric Oxide Analyzer (NOA) 280i (Boulder, CO). The NOA was calibrated before via a two-point calibration of N_2 gas passed through a NOA zero air filter and a standard of 44.3 ppm NO in N_2 gas. The test matrix mixture was prepared and put onto a small glass slide as described above (2.2.11). The glass slide was then placed into an amber NOA sample cell. The bottom of the amber NOA sample cell was filled with Milli-q purified water, and the glass slide was placed on top of a stage above the water line such that the matrix mixture did not come in contact with the water. The water reservoir was bubbled with N_2 gas at a rate of 50 mL/min to humidify the NOA sample cell to prevent the matrix from drying out. The amber NOA sample cell was placed in a 34°C water bath. The NO generated from the GSNO within the Vaseline/cream mixture was swept into the NOA by N_2 sweep gas. All amber NOA sample cells were wrapped in aluminum foil to shield the samples from light exposure.

3.3 Results and Discussion

3.3.1 Indirect application antimicrobial studies

Indirect application antimicrobial studies were conducted to demonstrate the killing effect of only NO released from the 3, 6 and 9 wt% GSNO test mixtures with the Desitin cream containing 13% ZnO against *Staphylococcus aureus*, *Staphylococcus epidermidis*, and *Pseudomonas aeruginosa*. These three bacteria strains were chosen because they have been shown to be common bacteria associated with wound or burn-wound infections.[25, 26] The initial concentration of bacteria (1×10^5 CFU/mL) was chosen because it is often associated with infection for open wounds and hindering wound closure.[28] Figure 3.1 shows a schematic of how the antimicrobial studies were performed. A silicone sheet was employed to keep the matrices from coming into direct contact with the bacteria on agar plates such that no additional killing effects from the matrix itself (e.g., ZnO particles) would be observed.[29] Silicone films were chosen because Ren *et al.* reported that silicone rubber polymers have the highest rate of NO diffusion compared to several other biomedical grade polymers.[30] The antimicrobial studies were completed in the dark at 34°C with an incubation/application period of 6 h.

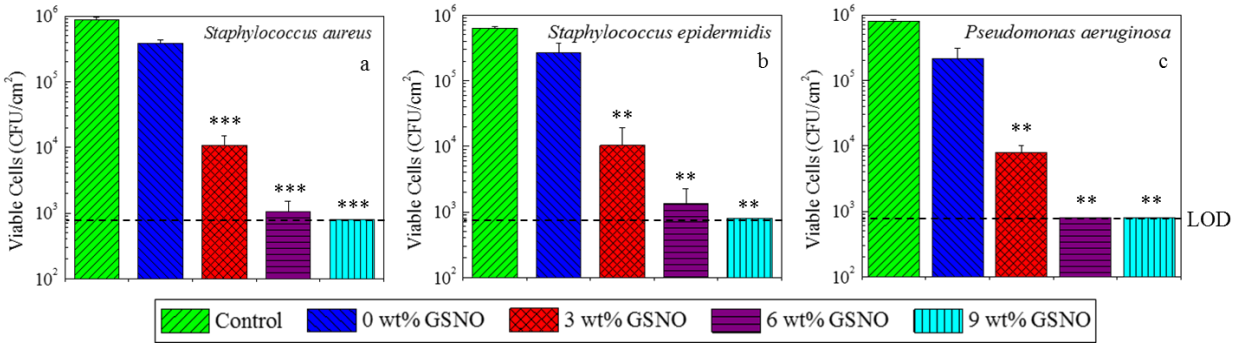

Figure 3.2. (a-c) Antimicrobial study results for Control and 0, 3, 6, and 9 wt% GSNO final matrices indirectly applied (with silicone sheet between) to (b) *S. aureus*, (c) *S. epidermidis*, and (d) *P. aeruginosa* inoculated LB agar plates in the dark at 34°C for 6 h. Control means nothing was applied to the surface of the inoculated LB agar. GSNO/Vaseline primary matrices were mixed with Desitin zinc oxide cream at a 27/73 ratio to achieve 0, 3, 6, and 9 wt% GSNO final matrices. Viable cells were determined via plate counting. Horizontal dashed line represents the LOD (7.96×10^2 CFU/cm^2). No error bar means the LOD was reached for each trial. Data represents the mean ± SD (n = 3). * $p < 0.05$, ** $p < 0.025$, *** $p < 0.01$, 0 wt% GSNO vs. 3, 6, and 9 wt% GSNO.

"Control" in Fig. 3.2 means nothing was applied to the surface of the inoculated LB agar. The 0 wt% GSNO sample used in this study served as a second control to determine how much bacteria were lost when removing the silicone sheeting from the surface of the LB agar plate (Fig. 3.2a-c). All log reduction values of bacterial counts are reported in the order *S. aureus*, *S. epidermidis*, *P. aeruginosa*. Comparing the "Control" columns versus the "0 wt% GSNO" columns in Fig. 3.2a-c, the average log reduction after removing the silicone sheeting was calculated to be 0.36, 0.37, and 0.57, respectively. Therefore, when no NO is present and the bacteria are only in contact with the silicone sheet, very little killing effects are observed. In Figure 3.2a-c, the columns that do not display an error bar indicate that all of the bacteria of that strain were killed for each trial (n = 3), hence reaching the limit of detection for this study (7.96×10^2 CFU/cm^2). The average log reduction between the 0 wt% GSNO and 3 wt% GSNO matrices were 1.55, 1.41, and 1.44; between 0 wt% GSNO and 6 wt% GSNO matrices the log reductions were 2.56, 2.31, and 2.44;

and between the 0 wt% GSNO and 9 wt% GSNO matrices the log reductions were 2.68, 2.53, and 2.44, for each of the bacteria examined, respectively.

In general, the amount of NO released from the 3, 6, and 9 wt% GSNO samples were able to kill each bacterial strain (more NO yields greater log reduction). However, the amount of NO released from the 9 wt% GSNO matrix always killed all of the bacteria, therefore reaching the limit of detection for this antimicrobial assay. The true killing potential of the 9 wt% GSNO matrix is, therefore, likely greater than that illustrated in Figure 3.2a-c. Nonetheless, the current study demonstrates that NO produced from the ZnO particle enhanced reaction with GSNO is capable of killing both gram-positive (*S. aureus* and *S. epidermidis*) and gram-negative (*P. aeruginosa*) bacteria to a significant degree. This phenomenon is not surprising and has been reported several times in prior publications because there are multiple mechanisms by which NO can be toxic to bacteria.[31-36]

3.3.2 Direct application antimicrobial studies on pig skin model

Direct application antimicrobial studies were performed to determine the killing effect of the matrices and NO released from the 3, 6, and 9 wt% GSNO mixtures with the Desitin cream containing 13% ZnO against *Staphylococcus aureus*, *Staphylococcus epidermidis*, and *Pseudomonas aeruginosa*. The killing effect of a commonly used antibiotic cream (Neosporin) was also determined against each bacteria strain as a comparison. Neosporin cream contains the active antibiotics neomycin and polymyxin B which are mainly effective against gram-negative bacteria strains.[9] The indirect application antimicrobial studies did not allow the matrices to come in to direct contact with the bacteria. Therefore, any killing effect observed was only from the NO and not from the matrices. For the current study, the matrices were spread directly on the surface

of inoculated pig skin. Thus, any killing effects from the matrices (e.g., ZnO particles, antibiotics) would be observed in addition to NO (if present). The direct application antimicrobial studies were completed in the absence of light at 34 °C with an incubation/application period of 6 h. The same matrices studied in the indirect application antimicrobial studies were used for the current study in addition to Neosporin.

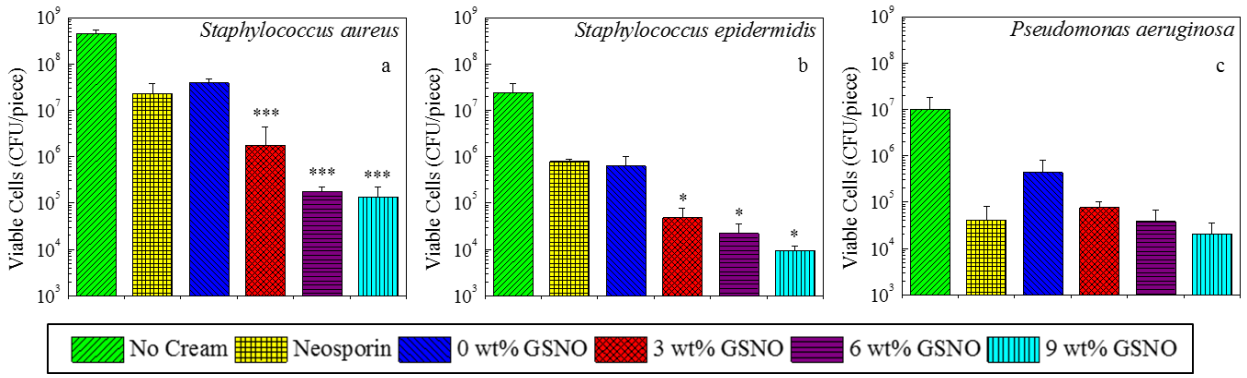

Figure 3.3. (a-c) Antimicrobial study results for No Cream, Neosporin, and 0, 3, 6, and 9 wt% GSNO final matrices directly applied to (a) *S. aureus*, (b) *S. epidermidis*, and (c) *P. aeruginosa* inoculated pig skin pieces in the dark at 34°C for 6 h. No Cream means nothing was applied to the surface of the inoculated pig skin. GSNO/Vaseline primary matrices were mixed with Desitin zinc oxide cream at a 27/73 ratio to achieve 0, 3, 6, and 9 wt% GSNO final matrices. Viable cells were determined via plate counting. Data represents the mean ± SD (n = 3). * $p < 0.05$, ** $p < 0.025$, *** $p < 0.01$, 0 wt% GSNO vs. 3, 6, and 9 wt% GSNO.

"No Cream" in Figure 3.3 means nothing was applied to the surface of the inoculated pig skin. The 0 wt% GSNO sample used in this study served as a control to determine how much bacteria were killed when in direct contact with just the ZnO-containing cream and no NO or antibiotics present (Fig. 3.3a-c). All log reduction values of bacterial counts are reported in the order *S. aureus*, *S. epidermidis*, *P. aeruginosa*. Comparing the "No Cream" columns versus the "0 wt% GSNO" columns in Fig. 3.3a-c, the average log reduction was calculated to be 1.07, 1.58, and 1.36, respectively. Therefore, ZnO present in the commercial Desitin cream does induce a >1 log unit reduction for all bacteria strains. These observations are not surprising, the killing effect that ZnO has on several different bacteria strains has been previously reported.[29, 37] The average log

reduction between the 0 wt% GSNO and Neosporin matrices were 0.23, N/A, and 1.02; between 0 wt% GSNO and 3 wt% GSNO matrices the log reduction values were 1.35, 1.12, and 0.76; between 0 wt% GSNO and 6 wt% GSNO matrices they were 2.34, 1.45, and 1.06; and between the 0 wt% GSNO and 9 wt% GSNO matrices the log reduction values were were 2.47, 1.83, and 1.34, for each of the bacteria examined, respectively.

The data presented in Fig. 3.3 shows that the NO releasing creams can match or exceed the killing effect of a commonly used antibiotic cream (Neosporin), especially for *S. aureus* and *S. epidermidis* (both are gram-positive strains). As mentioned previously, the active antibiotics present in Neosporin are mainly effective against gram-negative bacteria strains such as *P. aeruginosa*.[9] This phenomenon is confirmed by the data shown in Fig. 3.3. Overall, NO releasing creams directly applied to inoculated pig skin exhibit greater killing effects on *S. aureus*, *S. epidermidis*, and *P. aeruginosa* compared to Neosporin.

3.3.3 Evaluate synergy of combining NO and antibiotics to kill biofilm

Ren *et al.* showed that using NO and antibiotics together was able to kill much more bacteria than just NO alone.[38] This prior report demonstrated significant synergy when combining NO release with various antibiotics. Therefore, the goal for the current study was to evaluate the synergy of combining NO- and antibiotic-containing creams. Direct application anti-biofilm studies were performed to determine the synergy of combining NO- and antibiotic-containing creams against 24 h *Staphylococcus aureus*, *Staphylococcus epidermidis*, and *Pseudomonas aeruginosa* biofilms on a pig skin model. A moisturizer cream was used as a control to evaluate how much biofilm was removed/killed during the removal of any cream from the pig skin surface because it contains no anti-biofilm agents. Neosporin containing the active antibiotics neomycin and polymyxin B

was evaluated against each biofilm. The NO releasing cream utilized for the current study was the 9 wt% GSNO final matrix used in both the indirect and direct application antimicrobial studies (Sections 3.3.1 and 3.3.2) and designated as formulation (**a**) in Fig. 3.4. The NO- and antibiotic-containing cream formulation used for this study was described in detail in Section 3.2.4. This formulation contains GSNO, ZnO, and Neosporin in the final matrix and is designated as formulation (**b**) in Fig. 3.4. Note that both formulation (**a**) and (**b**) contain the same wt% of GSNO and ZnO. The direct application anti-biofilm studies were completed in the absence of light at 34 °C with an incubation/application period of 6 h.

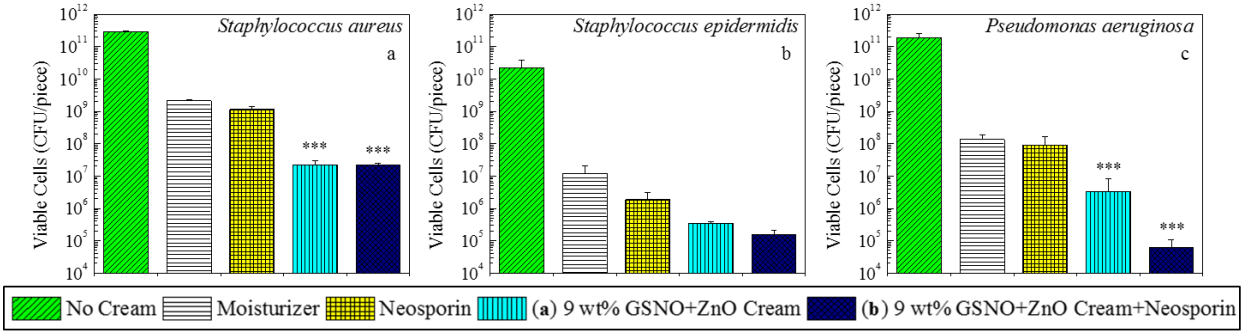

Figure 3.4. (a-c) Anti-biofilm study results for No Cream, Moisturizer, Neosporin, formulation (**a**), and formulation (**b**) matrices directly applied to 24 h (a) *S. aureus*, (b) *S. epidermidis*, and (c) *P. aeruginosa* biofilms on pig skin pieces in the dark at 34°C for 6 h. No Cream means nothing was applied to the surface of biofilms. Formulations (**a**) = 9 wt% GSNO + ZnO Cream: GSNO-Vaseline/13% ZnO cream mixed at 27/73 ratio. Formulation (**b**) = 9 wt% GSNO + ZnO Cream + Neosporin: Neosporin cream/40% ZnO cream, 67.5/32.5; GSNO-Vaseline/Neosporin-ZnO cream mixed at 27/73 ratio. Viable cells were determined via plate counting. Data represents the mean ± SD (n = 3). * $p < 0.05$, ** $p < 0.025$, *** $p < 0.01$, 0 wt% GSNO vs. 3, 6, and 9 wt% GSNO.

"NO Cream" in Fig. 3.4 means nothing was applied to the surface of the biofilm on the pig skin piece. The "Moisturizer" sample was used to determine how much biofilm was removed/killed during the removal of any cream from the pig skin surface (Fig. 3.4a-c). All log reduction values of bacterial counts are reported in the order *S. aureus*, *S. epidermidis*, *P. aeruginosa*. Comparing the "No Cream" columns versus the "Moisturizer" columns in Fig. 3.4a-c, the average log reduction was calculated to be 2.13, 3.28, and 3.14, respectively. Therefore, a significant amount

of bacteria is removed/killed during removal of a cream from the surface of the pigskin/biofilm. However, greater log reductions are observed for all other formulations utilized during this study (Fig. 3.4). Comparing the Moisturizer control versus the Neosporin sample demonstrates the killing effect of only antibiotics neomycin and polymyxin B have against the biofilms. The average log reduction was calculated to be 0.27, 0.81, and 0.17, respectively. These relatively low log reduction values are to be expected, because biofilms inherently resist antibiotics.[39] Comparing the Moisturizer control versus formulation (**a**) demonstrates the killing effect of only NO and ZnO against the biofilms. The average log reduction was calculated to be 1.98, 1.55, and 1.16, respectively. These results show that NO and ZnO have a greater anti-biofilm killing effect compared to only the antibiotics neomycin and polymyxin B present in Neosporin. Comparing the Moisturizer control versus formulation (**b**) demonstrates the killing effect of combining NO, ZnO, and antibiotics (neomycin and polymyxin B) have against biofilms. The average log reduction was calculated to be 2.00, 1.89, and 3.34, respectively. The log reduction values that formulation (**a**) achieved compared to formulation (**b**) indicates that only the killing effect against the *P. aeruginosa* biofilm was significant. This phenomenon make sense because *P. aeruginosa* is a gram-negative bacteria and the antibiotics neomycin and polymyxin B are mainly effective against gram-negative bacteria.[9] Therefore, the significantly greater synergistic killing effect of combining NO plus the antibiotics neomycin and polymyxin B against *P. aeruginosa* was to be expected because *S. aureus* and *S. epidermidis* are both gram-positive bacteria strains.

3.3.4 Evaluate pH of NO releasing creams

Traditionally, GSNO is synthesized from its parent thiol glutathione (GSH) under acidic conditions to yield a fully protonated product (Section 3.2.2). The most acidic carboxylic acid on GSH has a

predicted pKa of 1.94 according to ChemAxon. After conversion to GSNO, the predicted pKa lowers to 1.60. The pH of 1 mM solutions of GSNO and GSH are <4 (Table 3.1). This knowledge draws concern to the relative pH of the NO releasing creams containing GSNO when potentially used for direct application to the skin. The final 9 wt% GSNO formulation created from 33 wt% GSNO in Vaseline mixed with 13% ZnO Desitin cream at a 27/73 ratio, is 20.0 ± 1.5 wt% water (Table 3.3). Based on the solubility of GSNO in water (20 mg/mL), the aqueous phase is super saturated with GSNO. Therefore, the relative pH of the final 9 wt% GSNO matrix is potential highly acidic.

Table 3.1. Average pH of 1 mM GSNO, GSH, and SNAP solutions. Data represents the mean ± SD (n = 3).

Solution (1 mM)	pH
GSNO	3.36 ± 0.01
GSH	3.61 ± 0.03

This formulation is considered a water-in-oil emulsion (w/o) because the dominate phase is oil-based. For w/o emulsions, the pH cannot be accurately determined by submerging a traditional pH probe in an aliquot of the w/o emulsion because the dominant phase is not aqueous-based. As consequence, to assess the relative pH of the w/o emulsion NO releasing cream, the most extreme condition in which all of the GSNO saturates the aqueous phase of the cream was considered and the pH was measured. Refer to Section 3.2.9 for the specific procedure. Briefly, each formulation was diluted at a 1:10 ratio in purified water, hand shaken for 3 min, centrifuged for 5 min, and then the pH of the supernatant (aqueous phase) was measured using a calibrated pH electrode/meter (Table 3.2). The pH of several moisturizers and other commercially available creams/emulsions were measured as controls using this method.

It was determined that the relative pH of the final 9 wt% GSNO matrix was 2.92 ± 0.02. This pH was considered too acidic and therefore needed to be increased to a more neutral pH for potential topical skin applications. To increase the relative pH, sodium bicarbonate ($NaHCO_3$) was added because it is a weak base and is commonly used to control the acid-base balance in cosmetic formulations. To achieve a neutral pH, the amount of $NaHCO_3$ added to the existing formulation was 2 molar equivalents of the amount of GSNO (Table 3.2). More specifically, $NaHCO_3$ was added to the 33 wt% GSNO in Vaseline primary matrix to achieve a new primary matrix of 33 wt% GSNO and 16.5 wt% $NaHCO_3$ in Vaseline. Then, this new primary matrix was mixed at a 27/73 ratio with the 13% ZnO Desitin cream to yield the final neutral pH NO releasing cream formulation of 9 wt% GSNO + 4.5 wt% $NaHCO_3$.

Table 3.2. Average pH of formulations diluted 1:10 in purified water. Data represents the mean ± SD (n = 3).

Formulation	pH
9 wt% GNSO: 27/73 ratio of 33 wt% GSNO in Vaseline/13% ZnO Desitin cream	2.92 ± 0.02
Avalon Organics® Intense Defense with Vitamin C Oil-Free Moisturizer	4.87 ± 0.02
Osmotics Cosmeceuticals Blue Copper 5®	4.96 ± 0.02
Neosporin® Dual Action Cream + Pain Relief	5.30 ± 0.04
9 wt% GNSO + 4.5 wt% $NaHCO_3$: 27/73 ratio of 33 wt% GSNO and 16.5 wt% $NaHCO_3$ in Vaseline/13% ZnO Desitin cream	6.98 ± 0.01
Milli-q purified water	6.98 ± 0.04
Desitin® Rapid Relief Cream: Zinc Oxide Diaper Rash Cream	7.44 ± 0.06
Lubriderm® Daily Moisture Lotion	7.56 ± 0.06
Pond's® Dry Skin Cream	7.70 ± 0.08

Table 3.3. Summary of wt% water content for various creams/emulsions and their corresponding classifications of water-in-oil (w/o) or oil-in-water (o/w) emulsions. Data represents the mean ± SD (n = 3).

Matrix	wt% water	Classification
9 wt% GNSO: 27/73 ratio of 33 wt% GSNO in Vaseline/13% ZnO Desitin cream	20.0 ± 1.5	w/o
Avalon Organics® Intense Defense with Vitamin C Oil-Free Moisturizer	71.1 ± 0.3	o/w
Osmotics Cosmeceuticals Blue Copper 5®	72.9 ± 2.5	o/w
Neosporin® Dual Action Cream + Pain Relief	73.8 ± 0.1	o/w
9 wt% GNSO + 4.5 wt% $NaHCO_3$: 27/73 ratio of 33 wt% GSNO and 16.5 wt% $NaHCO_3$ in Vaseline/13% ZnO Desitin cream	20.5 ± 1.9	w/o
Desitin® Rapid Relief Cream: Zinc Oxide Diaper Rash Cream	27.7 ± 2.2	w/o
Lubriderm® Daily Moisture Lotion	85.2 ± 0.5	o/w
Pond's® Dry Skin Cream	66.3 ± 0.3	o/w

3.3.5 NO release kinetics from neutral pH cream containing GSNO and ZnO

The NO release kinetics were investigated for the neutral pH NO releasing cream formulation to determine if the addition of $NaHCO_3$ had any significant effect. The NO release kinetics of the acidic 9 wt% GSNO containing cream was previously report and will be used here for comparison.[24] An aliquot of the appropriate wt% of GSNO and $NaHCO_3$ in Vaseline was mixed with the 13% Zinc Oxide Desitin cream at a 27/73 ratio. NO release was measured at 34°C for 6 h revealing that the NO release profile for the neutral pH NO releasing cream was similar to that of the acidic NO releasing cream (Fig. 3.5a,b).

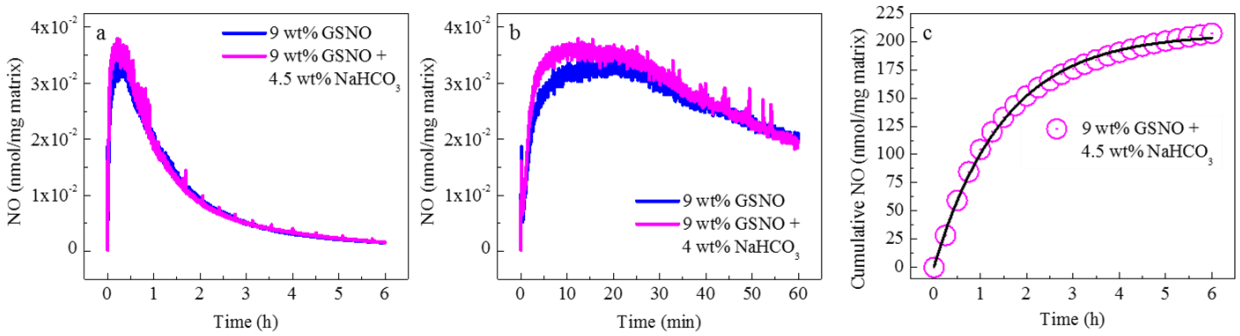

Figure 3.5. Real-time NO release of 9 wt% GSNO (acidic pH) and 9 wt% GSNO + 4.5 wt% $NaHCO_3$ (neutral pH) matrices in the dark at 34°C over (a) 6 h and (b) 60 min.[24] (c) Fit of the cumulative NO release versus time for the 9 wt% GSNO + 4.5 wt% $NaHCO_3$ matrix to a first-order rate equation, giving k_{obs} = 0.66 ± 0.01 h^{-1} ($t_{1/2}$ ~ 1.05 h). Data represents mean (n = 3).

Table 3.4. Comparison summary of %NO release in 6 h, first order rate constant (k_{obs}), and half-life ($t_{1/2}$) for 9 wt% GSNO and 9 wt% GSNO + 4.5 wt% $NaHCO_3$ matrices measured in the dark at 34°C.[24] Data represents the mean ± SD (n = 3 separate preparations).

Matrix	% NO release in 6 h	k_{obs} (h^{-1})	$t_{1/2}$ (h)
9 wt% GSNO	74.6 ± 2.2	0.64 ± 0.01	1.08
9 wt% GSNO + 4.5 wt% $NaHCO_3$	79.5 ± 2.3	0.66 ± 0.01	1.05

Cumulative NO release of the neutral pH cream plotted versus time reveal apparent first-order kinetics (Fig. 3.5c). Integration of the neutral pH NO releasing cream plot in Fig. 3.5a showed that 79.5 ± 2.3% of the total theoretical NO available was released over the 6 h test period, which is similar to that of the acidic NO releasing cream (Table 3.4). The observed first order rate constant of k_{obs} = 0.66 ± 0.01 h^{-1} ($t_{1/2}$ ~ 1.05 h) for the overall NO release kinetics of the neutral pH NO releasing cream was determined by the cumulative moles of NO release versus time (Fig. 3.5c, Table 3.4). The observed first order rate constants for the acidic and neutral pH NO releasing cream are very similar, leading to the conclusion that NO release kinetics are not significantly impacted by the addition of $NaHCO_3$.

3.3.6 Direct application bacteria studies of neutral pH NO releasing cream on pig skin

To determine if the antimicrobial effects observed from the previous direct application antimicrobial studies were from the relative acidity of the matrices or the NO released, further direct application antimicrobial studies with the neutral pH NO releasing matrices were conducted. These new direct application antimicrobial studies were performed using the same protocol as the first direct application antimicrobial studies (Section 3.3.2). The bacteria strains tested against were *Staphylococcus aureus*, *Staphylococcus epidermidis*, and *Pseudomonas aeruginosa*.

The trials labeled no cream, Neosporin, 0 and 9 wt% GSNO are the same matrices utilized in the first direct application antimicrobial studies (Fig. 3.6). The new matrices tested were 9 wt% GSNO + 4.5 wt% $NaHCO_3$, 8.3 wt% GSH, 8.3 wt% GSH + 4.5 wt% $NaHCO_3$, and 4.5 wt% $NaHCO_3$ (Fig. 3.6). The latter three matrices were tested as controls. The 8.3 wt% GSH matrix contains GSH at an equimolar amount of GSNO in the 9 wt% GSNO-containing matrices. Therefore, the acidity of the GSH-containing matrix should be similar because GSH and GSNO only differ in molecular structure by the NO moiety. The 8.3 wt% GSH + 4.5 wt% $NaHCO_3$ matrix again contains GSH at an equimolar amount of GSNO in the 9 wt% GSNO-containing matrices and also two molar equivalents of $NaHCO_3$. This control matrix was neutral in pH and without NO release. The 4.5 wt% $NaHCO_3$ matrix contained $NaHCO_3$ at two molar equivalents compared to the amount of GSNO in the 9 wt% GSNO-containing matrices. This control matrix was slightly basic in pH and without NO release. The 9 wt% GSNO + 4.5 wt% $NaHCO_3$ contained $NaHCO_3$ at two molar equivalents compared to the amount of GSNO. This matrix was the neutral pH NO releasing cream.

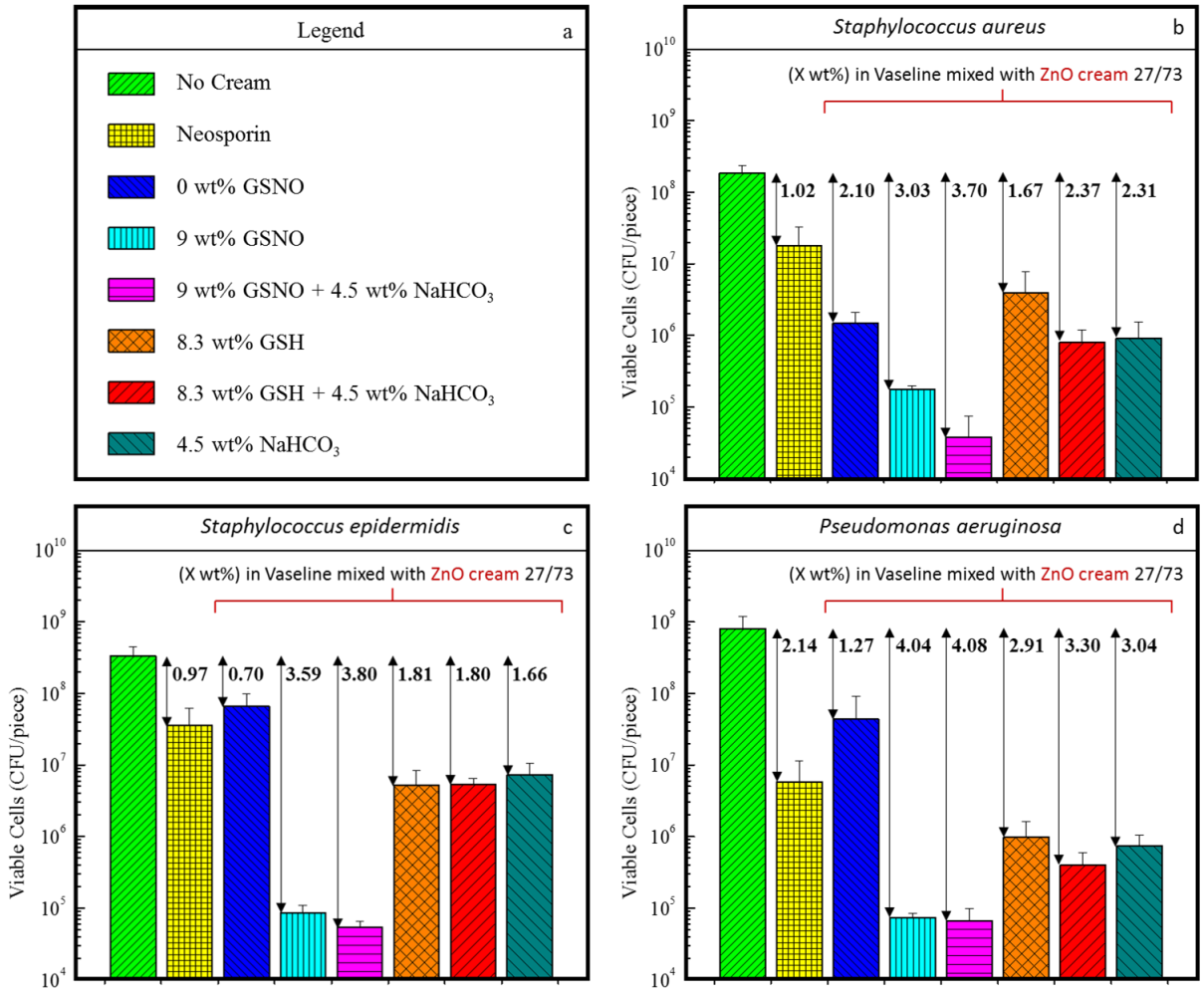

Figure 3.6. (a) Legend for bar graphs b-d. (b-d) Antimicrobial study results for various matrices (see below for detailed matrix list) directly applied to (b) *S. aureus*, (c) *S. epidermidis*, and (d) *P. aeruginosa* inoculated pig skin pieces at 34°C, absent from light, for 6 h. Values above bars represent log reduction between that sample bar and No Cream sample bar. Data represents the means ± SD (n = 3).

Detailed Matrix List:

- No Cream = no cream applied to pig skin
- Neosporin = antibiotic cream containing the active antibiotics neomycin and polymyxin B
- 0 wt% GSNO = Vaseline/13% ZnO Desitin cream mixed at a 27/73 ratio
- 9 wt% GSNO = GSNO-Vaseline/13% ZnO Desitin cream mixed at a 27/73 ratio
- 9 wt% GSNO + 4.5 wt% $NaHCO_3$ = GSNO-$NaHCO_3$-Vaseline/13% ZnO Desitin cream mixed at a 27/73 ratio (amount of $NaHCO_3$ is two molar equivalents of the amount GSNO)
- 8.3 wt% GSH = GSH-Vaseline/13% ZnO Desitin cream mixed at a 27/73 ratio (amount of GSH is equimolar to the amount of GSNO in the 9 wt% GSNO matrices)
- 8.3 wt% GSH + 4.5 wt% $NaHCO_3$ = GSH-$NaHCO_3$-Vaseline/13% ZnO Desitin cream mixed at a 27/73 ratio (amount of $NaHCO_3$ is two molar equivalents of the amount GSH)
- 4.5 wt% $NaHCO_3$ = $NaHCO_3$-Vaseline/13% ZnO Desitin cream mixed at a 27/73 ratio (amount of $NaHCO_3$ is two molar equivalents of the amount GSNO in the 9 wt% GSNO matrices)

For *S. aureus*, the addition of $NaHCO_3$ to the 9 wt% GSNO matrix increased the killing effect. Sodium bicarbonate has inherent antimicrobial properties, leading to the increased killing effect observed.[40] For *S. epidermidis*, the neutral pH NO releasing cream does not reduce the killing effect compared to the acidic NO releasing cream. The same effect was observed for *P. aeruginosa*. Overall, the neutral pH NO releasing cream (9 wt% GSNO + 4.5 wt% $NaHCO_3$) met or exceeded the killing effect of the acidic NO releasing cream (9 wt% GSNO) for all three bacteria strains. Therefore, this data justifies that the first direct application antimicrobial studies using only the acidic NO releasing matrices are valid because the relative acidity has no major killing effect.

3.4 Conclusion

The indirect application antimicrobial studies demonstrated the killing effect of only NO released from 3, 6, and 9 wt% GSNO final matrices prepared by mixing Desitin zinc oxide cream with the GSNO/Vaseline mixture in the dark at 34°C with an application period of 6 h. *S. aureus*, *S. epidermidis*, and *P. aeruginosa* were all affected by the NO released from each NO releasing matrix. In general, the more GSNO present (larger amount of NO released) lead to a greater killing effect. The direct application antimicrobial studies on a pig skin model demonstrated the killing effect of the matrices and NO released from the 3, 6, and 9 wt% GSNO final matrices. The performance of the NO releasing matrices were compared to a common commercially available antibiotic-containing cream, Neosporin. At minimum, one NO releasing cream formulation was able to exceed the killing effect obtained by Neosporin for *S. aureus*, *S. epidermidis*, and *P. aeruginosa*. Combining NO- and antibiotic-containing creams together showed the most synergistic killing effect against *P. aeruginosa* because the antibiotics utilized are mainly effective

at killing gram-negative bacteria strains. Evaluating the relative pH of the final 9 wt% GSNO matrix revealed that the cream was acidic because of the acidic nature of GSNO. However, a neutral pH NO releasing formulation was created by adding an appropriate amount of $NaHCO_3$. First-order NO release kinetics were examined for the neutral pH NO releasing cream and compared to the acidic NO releasing cream, revealing very similar characteristics and kinetics. The addition of $NaHCO_3$ to the acidic 9 wt% GSNO cream did not significantly impact the NO release kinetics. A repeat of the first direct application antimicrobial studies on pig skin with the addition of the neutral pH NO releasing cream also revealed that the neutral pH NO releasing cream was able to match or exceed the killing effect of the acidic pH NO releasing cream for *S. aureus, S. epidermidis,* and *P. aeruginosa*. Thus, the relative acidity has no major killing effect.

3.5 References

(1) Clardy, J.; Fischbach, M. A.; Currie, C. R. *Curr Biol* **2009,** *19* (11), R437-R441.

(2) Ribeiro da Cunha, B.; Fonseca, L. P.; Calado, C. R. S. *Antibiotics* **2019,** *8* (2), 45.

(3) Nathan, C.; Cars, O. *New England Journal of Medicine* **2014,** *371* (19), 1761-1763.

(4) Aslam, B.; Wang, W.; Arshad, M. I.; Khurshid, M.; Muzammil, S.; Rasool, M. H.; Nisar, M. A.; Alvi, R. F.; Aslam, M. A.; Qamar, M. U.; Salamat, M. K. F.; Baloch, Z. *Infect. Drug Resist.* **2018,** *11*, 1645-1658.

(5) Roca, I.; Akova, M.; Baquero, F.; Carlet, J.; Cavaleri, M.; Coenen, S.; Cohen, J.; Findlay, D.; Gyssens, I.; Heuer, O. E.; Kahlmeter, G.; Kruse, H.; Laxminarayan, R.; Liébana, E.; López-Cerero, L.; MacGowan, A.; Martins, M.; Rodríguez-Baño, J.; Rolain, J. M.; Segovia, C.; Sigauque, B.; Tacconelli, E.; Wellington, E.; Vila, J. *New Microbes New Infect.* **2015,** *6*, 22-29.

(6) Michael, C. A.; Dominey-Howes, D.; Labbate, M. *Front Public Health* **2014,** *2*, 145-145.

(7) Spellberg, B.; Srinivasan, A.; Chambers, H. F. *JAMA* **2016,** *315* (12), 1229-1230.

(8) Ahmed, A.; Azim, A.; Gurjar, M.; Baronia, A. K. *Indian J Crit Care Med* **2014,** *18* (5), 310-314.

(9) Lipsky, B. A.; Hoey, C. *Clin. Infect. Dis.* **2009,** *49* (10), 1541-1549.

(10) Akin Polat, Z.; Vural, A. *Parasitology Research* **2012,** *110* (5), 1945-1950.

(11) Sharma, S.; Srinivasan, M.; George, C. *Archives of Ophthalmology* **1990,** *108* (5), 676-678.

(12) Wilkinson, R. D.; Carey, W. D. *International Journal of Dermatology* **1988,** *27* (7), 514-515.

(13) Brisbois, E. J.; Bayliss, J.; Wu, J.; Major, T. C.; Xi, C.; Wang, S. C.; Bartlett, R. H.; Handa, H.; Meyerhoff, M. E. *Acta Biomater.* **2014,** *10* (10), 4136-4142.

(14) Backlund, C. J.; Worley, B. V.; Schoenfisch, M. H. *Acta Biomater.* **2016,** *29*, 198-205.

(15) Dave, R. N.; Joshi, H. M.; Venugopalan, V. P. *J. Mater. Sci. Mater. Med.* **2012,** *23* (12), 3097-3106.

(16) Hetrick, E. M.; Shin, J. H.; Stasko, N. A.; Johnson, C. B.; Wespe, D. A.; Holmuhamedov, E.; Schoenfisch, M. H. *ACS Nano* **2008,** *2* (2), 235-246.

(17) Lee, W. H.; Ren, H.; Wu, J.; Novak, O.; Brown, R. B.; Xi, C.; Meyerhoff, M. E. *ACS Biomater. Sci. Eng.* **2016,** *2* (9), 1432-1435.

(18) Schanuel, F. S.; Raggio Santos, K. S.; Monte-Alto-Costa, A.; de Oliveira, M. G. *Colloids Surf. B Biointerfaces* **2015,** *130*, 182-191.

(19) Shishido, S. l. M.; Seabra, A. B.; Loh, W.; de Oliveira, M. G. *Biomaterials* **2003,** *24* (20), 3543-3553.

(20) Champeau, M.; Póvoa, V.; Militão, L.; Cabrini, F. M.; Picheth, G. F.; Meneau, F.; Jara, C. P.; de Araujo, E. P.; de Oliveira, M. G. *Acta Biomater.* **2018,** *74*, 312-325.

(21) Wo, Y.; Brisbois, E. J.; Bartlett, R. H.; Meyerhoff, M. E. *Biomater. Sci.* **2016,** *4* (8), 1161-1183.

(22) Ghaffari, A.; Miller, C. C.; McMullin, B.; Ghahary, A. *Nitric Oxide* **2006,** *14* (1), 21-29.

(23) Fang, F. C. *J. Clin. Invest.* **1997,** *99* (12), 2818-2825.

(24) Doverspike, J. C.; Zhou, Y.; Wu, J.; Tan, X.; Xi, C.; Meyerhoff, M. E. *Nitric Oxide* **2019,** *90*, 1-9.

(25) Gallagher, J. J.; Williams-Bouyer, N.; Villarreal, C.; Heggers, J. P.; Herndon, D. N. Chapter 12 - Treatment of infection in burns. In *Total Burn Care (Third Edition)*; Herndon, D. N., Ed.; W.B. Saunders: Edinburgh, **2007**; pp 136-176.

(26) Bessa, L. J.; Fazii, P.; Di Giulio, M.; Cellini, L. *Int. Wound J.* **2015,** *12* (1), 47-52.

(27) Wang, Y.; Tan, X.; Xi, C.; Phillips, K. S. *npj Biofilms and Microbiomes* **2018,** *4* (1), 16.

(28) Edwards, R.; Harding, K. G. *Curr. Opin. Infect. Dis.* **2004,** *17* (2), 91-96.

(29) Sirelkhatim, A.; Mahmud, S.; Seeni, A.; Kaus, N. H. M.; Ann, L. C.; Bakhori, S. K. M.; Hasan, H.; Mohamad, D. *Nano-Micro Lett.* **2015,** *7* (3), 219-242.

(30) Ren, H.; Bull, J. L.; Meyerhoff, M. E. *ACS Biomater. Sci. Eng.* **2016,** *2* (9), 1483-1492.

(31) Feelisch, M. *Naunyn Schmiedebergs Arch. Pharmacol.* **1998,** *358* (1), 113-122.

(32) Bogdan, C. *Nat. Immunol.* **2001,** *2*, 907.

(33) Deupree, S. M.; Schoenfisch, M. H. *Acta Biomater.* **2009,** *5* (5), 1405-1415.

(34) Heilman, B. J.; Halpenny, G. M.; Mascharak, P. K. *J. Biomed. Mater. Res. Part B Appl. Biomater.* **2011,** *99B* (2), 328-337.

(35) Privett, B. J.; Broadnax, A. D.; Bauman, S. J.; Riccio, D. A.; Schoenfisch, M. H. *Nitric Oxide* **2012,** *26* (3), 169-173.

(36) Pant, J.; Gao, J.; Goudie, M. J.; Hopkins, S. P.; Locklin, J.; Handa, H. *Acta Biomater.* **2017,** *58*, 421-431.

(37) Siddiqi, K. S.; ur Rahman, A.; Tajuddin; Husen, A. *Nanoscale Res. Lett.* **2018,** *13* (1), 141.

(38) Ren, H.; Wu, J.; Colletta, A.; Meyerhoff, M. E.; Xi, C. *Front Microbiol* **2016,** *7*, 1260-1260.

(39) Wolcott, R. D.; Rumbaugh, K. P.; James, G.; Schultz, G.; Phillips, P.; Yang, Q.; Watters, C.; Stewart, P. S.; Dowd, S. E. *Journal of Wound Care* **2010,** *19* (8), 320-328.

(40) Dobay, O.; Laub, K.; Stercz, B.; Kéri, A.; Balázs, B.; Tóthpál, A.; Kardos, S.; Jaikumpun, P.; Ruksakiet, K.; Quinton, P. M.; Zsembery, Á. *Front Microbiol* **2018,** *9* (2245).

Chapter 4 Investigation of Enhanced NO Release from GSNO in the Presence of ZnO

X-ray photoelectron spectroscopy (XPS) experiments were conducted by Dr. Molly MacInnes whose name will appear on any future publication of the research described in this chapter.

4.1 Introduction

Over the past few decades, several ways have been discovered to enhance the rate of NO release from *S*-nitrosoglutathione (GSNO) and other *S*-nitrosothiols (RSNOs). Some of these methods include photolysis, thermal cleavage, the use of metal ions, and the use of reducing agents.[1-11] In Chapter 2, a commercial zinc oxide (ZnO)-containing cream demonstrated the ability to significantly enhance NO generation from GSNO. Therefore, further actions/experiments are needed to determine the specie(s) responsible for the enhanced NO generation.

As mentioned above, prior literature has reported the capabilities of various metal ions to enhance or suppress NO release from GSNO. There is a strong likelihood that trace Zn^{2+} ions are present within the commercial ZnO-containing cream used in the studies reported in Chapter 2. There are conflicting reports in the literature whether or not Zn^{2+} ions are capable of enhancing NO release from GSNO or other RSNOs.[12-15] A portion of this chapter addresses this discrepancy.

Another component studied in detail within this chapter is zinc oxide. ZnO nanoparticles are the key component present in the commercial ZnO cream. ZnO has many unique physical and chemical properties that make it a useful substance for several applications. Specifically, ZnO is a piezo- and pyroelectric metal oxide with high thermal and mechanical stability.[16, 17] Its wide band gap (3.37 eV) makes ZnO an ideal semiconductor to be used for different sensor and electronic applications.[16, 17] ZnO particles are also used in cosmetics, sunscreens, and diaper rash creams because of its inherent antimicrobial properties, its ability to absorb UVA and UVB sunlight radiation, and its relatively low toxicity towards humans and the environment.[18, 19]

This chapter is a more detailed follow-up to Chapter 2, focusing on identifying the component in commercial zinc oxide cream responsible for the observed enhanced NO proliferation from GSNO. The following topics were studied in detail. First, NO release from GSNO in the presence of Zn^{2+} ions was monitored for their potential enhancement or suppression of NO release. Second, each other component present in the commercial zinc oxide cream was tested for their individual potential to enhance NO release from GSNO. Third, NO release kinetics of 30, 50, and 200 nm size ZnO nanoparticles were evaluated under simplistic reaction conditions (dark, 24°C, 7.4 pH). Fourth, experimental conditions were simulated to purposely inhibit/block the surface of ZnO to gain insight into the manner in which GNSO and ZnO interact. Lastly, surface analysis of the ZnO nanoparticles after interaction with GSNO were completed via X-ray photoelectron spectroscopy (XPS) to assess whether any GSH or other product species remained adhered to the surface of the particles.

4.2 Materials and Methods

4.2.1 Materials

L-Glutathione reduced (GSH), hydrochloric acid (HCl), phosphoric acid (H_3PO_4), sodium nitrite, zinc chloride, copper chloride, glycerol, poly(ethylene glycol) (avg. MW=300) (PEG-300), magnesium sulfate, alpha tocopheryl acetate, 1,2-octanediol, 1,2-hexanediol, tropolone, Trizma base, and potassium hydroxide were purchased from Sigma-Aldrich (St. Louis, MO). Acetone was purchased from Fisher Scientific Inc. (Pittsburgh, PA). Zinc oxide nanoparticles with an APS of 30, 50 and 200 nm were purchased from EPRUI Biotech Co. Ltd. (ShangHai, China). All aqueous solutions were prepared with 18.2 M Ω deionized water using a Milli-Q filter (Milli-q purified water) from EMD Millipore (Billerica, MA).

4.2.2 S-Nitrosoglutathione (GSNO) synthesis

The method used to prepare GSNO was the same as that described in Chapter 2.

4.2.3 Measuring NO release from GSNO in the presence of Zn^{2+} ions

All solutions were made with 10 mM Tris-HCl buffer, pH 7.4. NO release was measured using a Sievers Chemiluminescence Nitric Oxide Analyzer (NOA) 280i (Boulder, CO). The NOA was calibrated before via a two-point calibration of N_2 gas passed through a NOA zero air filter and a standard of 44.3 ppm NO in N_2 gas. The reaction mixtures were analyzed for NO release in the absence of light at 24°C. Two mL of a 1 mM GSNO solution in buffer was added to an amber

NOA sample cell (bulk). After a 1 min equilibration period, 100 μL of 1 mM $ZnCl_2$ was added to the bulk. For the control, 100 μL of the buffer (10 mM Tris-HCl, pH 7.4) was added into the test solution. After 9.5 min, 100 μL of 1 mM $CuCl_2$ was added to the bulk as a positive control. Each solution was bubbled with N_2 gas at a rate of 50 mL/min. NO generated was carried into the NOA by a N_2 sweep gas.

4.2.4 Measuring NO release from GSNO for component studies

All solutions were made with 10 mM Tris-HCl buffer, pH 7.4. NO release was quantitated using a NOA in the absence of light at 34°C. The components studied were the same or similar to those known to be present in the commercial zinc oxide cream (Desitin® Rapid Relief Cream: Zinc Oxide Diaper Rash Cream). These included 30 nm ZnO nanoparticles, glycerol, magnesium sulfate, tocopheryl acetate, PEG-300, 1,2-octanediol, 1,2-hexanediol, tropolone, and potassium hydroxide. The experimental scheme employed was as follows: 2 mL of a solution containing one component was first placed inside of an amber NOA sample cell (bulk solution) at 34°C. Then, 100 μL of a GSNO solution was added to the same sample cell. The bulk solutions contained 10 μmol of the given test component and the GSNO solution contained 1 μmol of GSNO. The final mole ratio of test component to GSNO was 10:1 μmol. For each of the aqueous-soluble components, 5 mM bulk solutions were made in advance in buffer (e.g., glycerol, magnesium sulfate, PEG-300, 1,2-octanediol, 1,2-hexanediol, tropolone, and potassium hydroxide). The 30 nm ZnO nanoparticles and tocopheryl acetate are not soluble in aqueous buffer and therefore prepared in a different manner to make the bulk solutions. For the ZnO nanoparticles, 0.82 mg were added to 2 mL of the buffer (0.41 mg ZnO/mL buffer) inside the amber NOA sample cell

and sonicated for 20 s. For testing tocopheryl acetate, 4.92 μL was added to 2 mL of the buffer (2.36 mg tocopheryl acetate/mL buffer) inside the NOA sample cell and sonicated for 20 s. The amber NOA sample cell containing the bulk solution(s) was submerged in a 34°C water bath and allowed to equilibrate for 1 min. After 1 min, 100 μL of a 10 mM GSNO solution was added into this bulk solution. As previously described, the solutions inside the sample cells were bubbled with N_2 gas at a rate of 50 mL/min and the NO generated was carried into the NOA by a N_2 sweep gas.

4.2.5 NO release kinetics from GSNO using 30, 50, and 200 nm ZnO nanoparticles

All solutions were made with 100 mM Tris-HCl buffer, pH 7.4. NO release was quantitated using the NOA in the absence of light at 24°C for 10 h. ZnO nanoparticles (4.1 mg) with diameters of 30, 50, or 200 nm were added to 2 mL of buffer inside an amber NOA sample cell (bulk solution). After achieving a stable baseline, 100 μL of 50 mM GSNO in buffer was added to the reaction cell (2.38 mM final concentration of GSNO after addition to bulk solution). Each solution was bubbled with N_2 gas at a rate of 50 mL/min and the NO generated was carried into the NO by a N_2 sweep gas.

4.2.6 NO release from GSNO in the presence 30 nm ZnO in Tris–HCL or –H_3PO_4 buffer

Nitric oxide release was quantitated using a NOA in the absence of light at 24°C for 25 min. Thirty nm size ZnO nanoparticles (4.1.mg) were added to 2 mL of either 100 mM Tris-HCL or 100 mM Tris-H_3PO_4 buffer, pH 7.4, inside an amber NOA sample cell (bulk solution). Upon attaining a stable baseline, 100 μL of 50 mM GSNO in either 100 mM Tris-HCL or 100 mM Tris-H_3PO_4

buffer, pH 7.4, was added to the respective reaction cells (2.38 mM GSNO final concentration). Each solution was bubbled with N_2 gas at a rate of 50 mL/min and the NO generated was carried into the NOA by a N_2 sweep gas.

4.2.7 ZnO nanoparticle preparation for surface analysis via XPS

All solutions were prepared using 100 mM Tris-HCl buffer, pH 7.4. The entire procedure and reaction was completed in the dark at room temperature (24°C). ZnO nanoparticles (16.4 mg of 30 nm particles) were added to 8 mL of buffer inside a 15 mL glass test tube. Then, 400 μL of 50 mM GSNO was added to the test tube that was then capped with a rubber septa. The solution was stirred using a stir bar and continuously bubbled with N_2 gas at a rate of 50 mL/min via a glass pipet. For a control sample, the same steps were followed as described above, except 400 μL of buffer was added to the test tube and not 400 μL of 50 mM GSNO. The control sample was not exposed to GSNO at any point. Both control and GSNO-containing samples were stopped after 5 h. Contents from each test tube were transferred to 15 mL polypropylene conical centrifuge tubes separately. Each glass test tube was washed 3 times with 1 mL of purified water and the contents were added to their respective centrifuge tube. Each tube was centrifuged at 4000 rpm for 1 min. The supernatant was decanted off from each tube. Five mL of purified water was added to each centrifuge tube, hand shaken for 10 s, and then centrifuged again. This washing process was completed three times total for both samples. After washing was completed, both samples were dried under vacuum at 24°C for 24 h. After drying was completed, both samples were ready for XPS analysis.

4.2.8 X-ray photoelectron spectroscopy (XPS)

Using a monochromatic Al K alpha source, X-ray photoelectron spectra were collected with a Kratos AXIS system with base pressure below 10^{-9} torr. To obtain survey and high-resolution spectra, pass energies of 160 and 20 eV were used, respectively. All collected data were referenced to the binding energy of adventitious carbon (284.6 eV).[20]

4.3 Results and Discussion

4.3.1 Investigation of NO release from GSNO in the presence of Zn^{2+} ions

An aqueous phase study was undertaken to determine if Zn^{2+} ions can increase NO proliferation from GSNO in the dark at 24°C. McCarthy *et al*. reported the NO generation potential of several different metal ions from SNAP under physiological pH conditions.[12] They discovered that three transition metal ions including Co^{2+}, Ni^{2+}, and Zn^{2+} increased NO release rates, while Fe^{3+}, Mg^{2+}, Mn^{2+}, and Pt^{2+} displayed significantly less NO release enhancement.[12] In contrast, Krężel *et al*. reported that the stability of GSNO in HEPES buffer (pH 7.4) actually increases in the presence of Zn^{2+} due to the formation of simple coordination complexes.[13] Askew *et al*. observed no catalysis capability of Zn^{2+} on SNAP to proliferate NO, although no data was shown to assess whether a non-catalytic reaction can occur.[14] More recently, Lutzke *et al*. reported the NO releasing capabilities of over twenty different metal ion species when mixed with GSNO, and Zn^{2+} ions was shown to exhibit no activity.[15] In light of these conflicting reports, further investigation was needed to better understand the substantial increase in the rate of NO release when the ZnO cream is mixed with the GSNO/Vaseline mixture reported in Chapter 2.

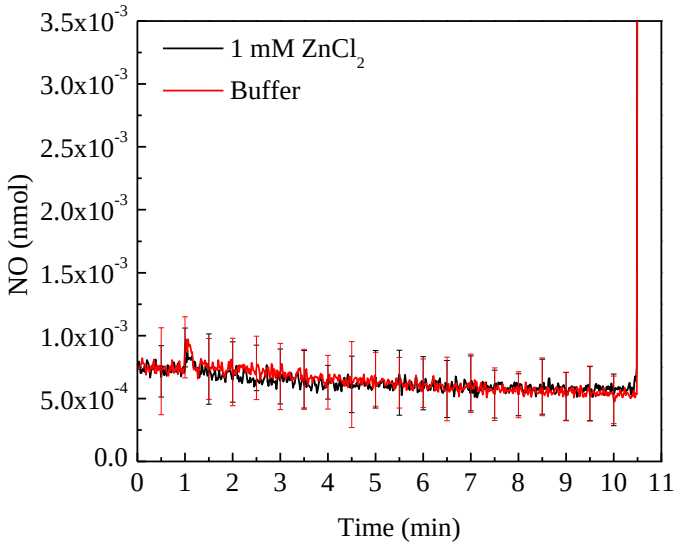

Figure 4.1. Real-time NO release from 2 mL of 1 mM GSNO after addition of either 100 µL of 1 mM $ZnCl_2$ or 100 µL of the buffer. Completed in the dark at 24°C. All solutions made with the buffer 10 mM Tris-HCl (pH 7.4). At *t*=10.5 min, 100 uL of 1 mM $CuCl_2$ was added as a positive control (The $ZnCl_2$ black plot is hidden behind the red plot at *t*=10.5 min). Data represents the mean ± SD (*n* = 3).

For the current study, $ZnCl_2$ was chosen as the source of Zn^{2+} ions. Figure 4.1 shows NO release from GSNO in solution as a function of time with and without Zn^{2+} ions present in solution. At t=1 min, 100 µL of 1 mM $ZnCl_2$ was added to the bulk solution containing 2 mL of 1 mM GSNO resulting in a very small, insignificant burst of NO. The same insignificant burst was observed when the buffer (10 mM Tris-HCl, pH 7.4) was added to the bulk solution. As a positive control, 100 µL of 1 mM $CuCl_2$ was added to each scenario at t=10.5 min and a very large burst in NO release was observed. A comparison of these two scenarios reveals that Zn^{2+} ions do not appreciably increase NO proliferation from GSNO. This data supports the findings of Krężel *et al.* and Lutzke *et al.*[13, 15]

4.3.2 Component study of Desitin® Rapid Relief Cream: Zinc Oxide Diaper Rash Cream

An aqueous phase study was undertaken to determine which agent or agents within the Desitin cream were responsible for the accelerated NO release from GSNO discovered in Chapter 2. A simplified system was employed to monitor and measure NO release when GSNO is mixed with various components/ingredients present in the commercial zinc oxide cream. Some ingredients present in the Desitin cream were omitted due to their low water solubility (mineral oil, petrolatum, beeswax, microcrystalline wax). The experiments were performed in the presence of 10 mM Tris-HCl buffer, pH 7.4, at 34°C. Nine components were studied at a 10:1 μmol ratio with GSNO in aqueous solution. Figure 4.2 shows NO release versus time when 100 μL of 10 mM GSNO was added into different bulk solutions containing a given component. Only the first 10 min of each reaction was monitored to determine which component is responsible for the enhanced NO release from GSNO. As shown clearly in Figure 4.2, which compares the NO release profiles of each of the components, only the 30 nm ZnO nanoparticles yield a significantly enhanced and prolonged NO release from GSNO. The NO release profiles of the other eight components demonstrate a similar profile to the buffer control, where no added components are present. Moreover, this study demonstrates that the other eight components present in the Desitin cream are not significantly involved in the enhanced NO release from GSNO.

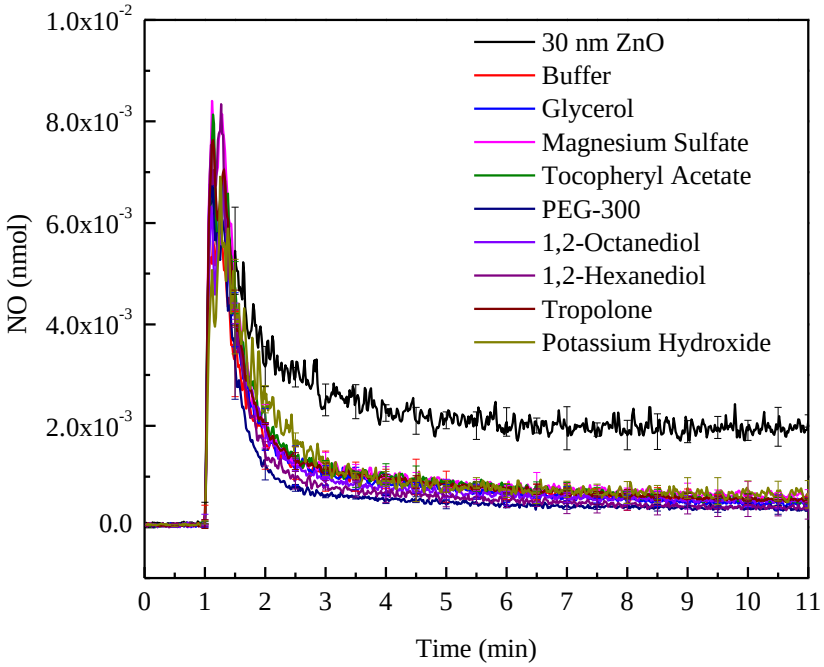

Figure 4.2. Real-time NO release after addition of 100 µL of 10 mM GSNO into 2 mL bulk solutions containing a given component. Experiments were completed in the dark at 34°C. All solutions were made with a 10 mM Tris-HCl buffer (pH 7.4). The final ratio of component to GSNO was 10:1 µmol. Data represents the mean ± SD (n = 3).

Promoting NO release from GSNO using ZnO nanoparticles has not been reported previously. However, very recently Singha *et al.* demonstrated enhanced and prolonged NO release from SNAP-doped CarboSil films with an additional top coating consisting of CarboSil and ZnO nanoparticles.[21] This demonstrates that ZnO nanoparticles could be capable of promoting NO release from other RSNOs. The data shown here (Fig. 4.2) clearly demonstrates that ZnO nanoparticles enhance the NO release from GSNO.

4.3.3 NO release kinetics from GSNO using 30, 50, and 200 nm ZnO nanoparticles

To study the NO release kinetics from GSNO in the presence of different sized ZnO nanoparticles, a simplistic reaction model was developed to limit external GSNO decomposition. Traditionally, *S*-nitrosothiols decompose in the presence of light, at higher temperatures, and in acidic or basic solutions.[1, 5, 9-11] Thus, the reaction kinetics between GSNO and ZnO nanoparticles were studied in the dark, at room temperature (~24°C), and in 100 mM Tris-HCl buffer solution, pH 7.4. Plotting cumulative NO release versus time (10 h) when adding 100 μL of 50 mM GSNO to 2.0 mL of buffer containing 4.1 mg of 30, 50, or 200 nm size ZnO nanoparticles reveals zero order reaction kinetics, meaning that the reaction rate is equal to the rate constant (k_{obs}) (Fig. 4.3). The relative ZnO surface area available during each reaction is not directly proportional to the reaction rate (Table 4.1). The presence of the 30 nm size ZnO nanoparticles increases the reaction rate by a factor of 2.78 compared to having no ZnO present. Overall, the reaction rate does increase as ZnO nanoparticle size decreases.

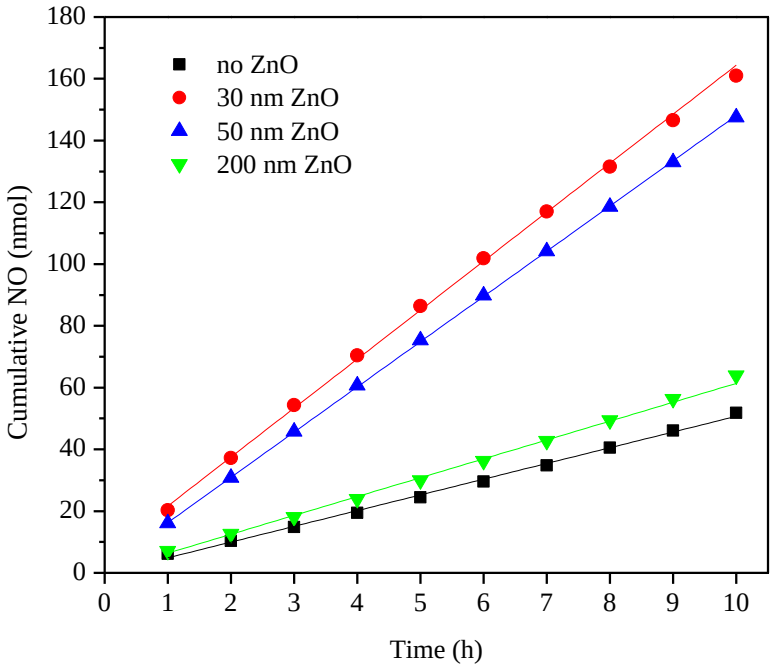

Figure 4.3. Cumulative NO release vs. time for no ZnO, 30, 50, and 200 nm size ZnO nanoparticles in the dark, at 24°C, in 100 mM Tris-HCL, pH 7.4 (buffer). At t=0 min, 100 µL of 50 mM GSNO was introduced to 2.0 mL of buffer containing 4.1 mg of 30, 50, or 200 nm size ZnO nanoparticles. No ZnO means no ZnO was present and NO release was caused by natural GSNO decomposition in the dark, at 24°C, in 100 mM Tris-HCL buffer, pH 7.4. The first hour of NO release was removed due to inconsistent initial NO release rates. Error bars were omitted for clarity. Data represents mean (n = 3).

Table 4.1. Summary of rate constant (k_{obs}) measured and the available surface area of ZnO present for trials containing no ZnO, 30, 50, and 200 nm size ZnO nanoparticles; where at t=0 min, 100 µL of 50 mM GSNO was introduced to 2.0 mL of 100 mM Tris-HCL buffer, pH 7.4, containing 4.1 mg of 30, 50, or 200 nm size ZnO nanoparticles. Trials were completed in the dark at 24°C. No ZnO means no ZnO was present. Data represents the mean ± SD (n = 3).

ZnO size (nm)	k_{obs} (nmol h^{-1})	Surface area of ZnO (cm^2)
no ZnO	5.07 ± 0.09	N/A
30	15.86 ± 0.18	1461.68
50	14.65 ± 0.04	877.01
200	6.10 ± 0.10	219.25

4.3.4 Comparing NO release from GSNO using ZnO under Tris–HCl and –H_3PO_4

A study was completed to determine if GSNO needs to have unblocked access to the surface of ZnO in order to promote NO release. Literature has shown that phosphoric acid (H_3PO_4) or like groups (HPO_4^{2-}) readily adsorb and interact with the surface of ZnO at neutral pH.[17, 22] Hence, utilizing a Tris-based buffer where the acid component can be interchanged between –HCl and –H_3PO_4, will reveal if GSNO needs unblocked access to the ZnO surface to enhance NO release. Figure 4.4 shows the real-time NO release when 100 μL of GSNO is added to a 100 mM Tris-HCl or –H_3PO_4 buffer solution (pH 7.4) containing 30 nM ZnO nanoparticles or when no ZnO is present. When using 100 mM Tris-HCl buffer (pH 7.4), there is a clear difference in the NO release profiles when ZnO is present versus when ZnO is not present (Fig. 4.4a). However, when using 100 mM Tris-H_3PO_4 the NO release profiles are very similar for both scenarios (Fig. 4.4b). By changing one chemical of the buffer solution from HCl to H_3PO_4, the NO release profile changes drastically. Since H_3PO_4/HPO_4^{2-} favorably interact/adsorb to the ZnO surface at pH 7.4, the promoted NO release reaction between GSNO and ZnO does not occur. This data suggests that GSNO needs uninhibited access to the surface of ZnO to promote NO release.

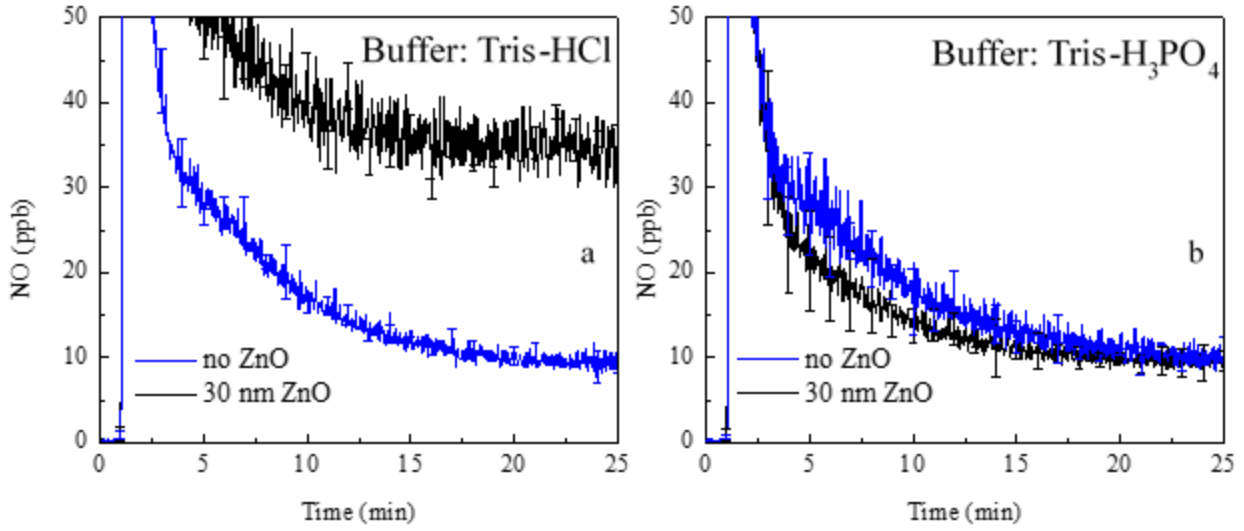

Figure 4.4. Real-time NO release after addition of 100 µL of 50 mM GSNO (t=1 min) into 2 mL of (a) 100 mM Tris-HCL or (b) 100 mM Tris-H_3PO_4 buffer (pH 7.4) containing no ZnO or 4.1 mg of 30 nm size ZnO nanoparticles. Completed in the dark at 24°C. Data represents the mean ± SD (n = 3).

4.3.5 Surface analysis of ZnO nanoparticles via X-ray photoelectron spectroscopy

To characterize the surface of ZnO after NO release from GSNO, X-ray photoelectron spectroscopy (XPS) was employed. There are literature reports of gold and platinum nanoparticles catalyzing NO generation from RSNOs.[23-25] Jia *et al.* reported the enhanced rate of NO release from GSNO via reaction of gold nanoparticles in a dose-dependent manner.[23] Later, Taladriz-Blanco *et al.* showed that due to the affinity between gold and thiols, the RS-NO bond breaks when in the presence of gold nanoparticles, and subsequently the gold surface is functionalized with the corresponding thiol species (as a sub-monolayer).[24] More recently, Cao *et al.* reported enhanced NO generation from SNAP and GSNO using 3 nm platinum nanoparticles, and suggested evidence of Pt-S bond formation during the reaction.[25] Therefore, surface analysis of ZnO after reaction with GSNO to promote NO release is necessary to reveal potential evidence of glutathione (thiol) attachment to the ZnO surface or Zn-S bond formation.

ZnO nanoparticles exposed and not exposed to GSNO were analyzed by XPS. The specific procedure of how each were prepared can be found in Section 4.2.7, above. Briefly, 400 µL of 50 mM GSNO was added to 16.4 mg of 30 nm ZnO nanoparticles in 8 mL of 100 mM Tris-HCl buffer, pH 7.4, in the dark at 24°C. The reaction was stopped after 5 h and the ZnO nanoparticles were thoroughly washed and dried under vacuum for XPS analysis. Control ZnO nanoparticles were prepared in the same manner except, 400 µL of buffer was added and not 400 µL of 50 mM GSNO. The control ZnO nanoparticles were not exposed to GSNO.

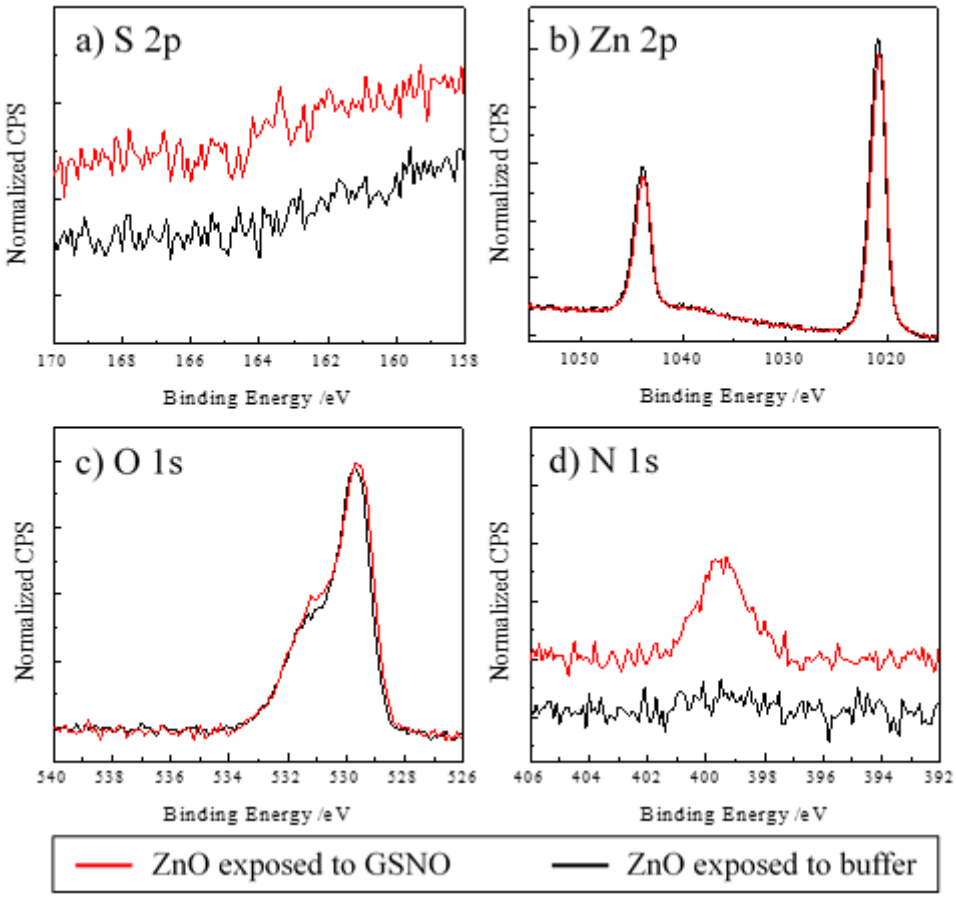

Figure 4.5. High-resolution (a) S 2p, (b) Zn 2p, (c) O1s, and (d) N 1s XP spectra of 30 nm size ZnO nanoparticles exposed and not exposed to GSNO in 100 mM Tris-HCl buffer (pH 7.4) in the dark at 24°C for 5 h.

The S 2p spectra for both ZnO nanoparticles exposed and not exposed to GSNO detect no signal (Fig 4.5a). No detection means that glutathione (thiol) is not adsorbed or bonded to the surface of ZnO. If there was evidence of Zn-S bond, there would be an S $2p_{3/2}$ and S $2p_{1/2}$ doublet between 162-167 eV.[26-29] The Zn $2p_{3/2}$ and Zn $2p_{1/2}$ signals at ~1021 and 1044 eV are consistent with ZnO (Fig. 4.5b).[27] The O 1s spectra are consistent with a signal at ~530 eV from lattice oxygen (O^{2-}) in ZnO and the signal at ~532.7 is from hydroxyl groups or chemisorbed oxygen (Fig. 4.5c).[27] There is a difference in the N 1s spectra between the ZnO exposed and not exposed to GSNO (Fig 4.5d). For the ZnO exposed to GSNO, the N 1s signal spans from 397-401 eV and corresponds to the combination of two peaks assigned to N-H and N-C bonds (Fig. 4.5d).[30] Since there is no S 2p signal from the ZnO that was exposed to GSNO, the N 1s signal must originate from the primary amine in the Tris buffer. Therefore, because there is no N 1s signal from the ZnO not exposed to GSNO and only exposed to the buffer, means that when ZnO and GSNO react to promote NO release, it allows the buffer to more favorably adsorb to the surface of ZnO. The lack of any S 2p signal from the ZnO exposed to GSNO suggests no thiol attachment post-NO proliferation as seen previously when using gold or platinum nanoparticles.

4.4 Conclusion

It was determined that Zn^{2+} ions have little or no effect on NO proliferation from GSNO in pH 7.4 buffer at 24°C. Further, a thorough component study of the Desitin zinc oxide cream suggests that the ZnO nanoparticles present are primarily responsible for increased NO proliferation from GSNO. A study of the NO release kinetics from GSNO in the presence of 30, 50, and 200 nm size ZnO nanoparticles in the dark, at 24°C, and in neutral pH conditions revealed zero order kinetics

during the first 10 h of reaction. Also, the available ZnO surface area is not directly proportional to the reaction rate, but the reaction rate does increase as ZnO nanoparticle size decreases. A study comparing the NO release profiles of using Tris-HCl buffer versus Tris-H_3PO_4 buffer revealed that GSNO needs uninhibited access to the surface of ZnO to promote NO release because H_3PO_4/HPO_4^{2-} adsorb to the ZnO surface and cause NO release to significantly decrease. Lastly, surface analysis of ZnO using XPS after exposure to GSNO showed no evidence of thiol attachment or Zn-S bond formation.

4.5 References

(1) Broniowska, K. A.; Diers, A. R.; Hogg, N. *Biochim. Biophys. Acta* **2013,** *1830* (5), 3173-3181.

(2) Holmes, A. J.; Williams, D. L. H. *Chem. Commun.* **1998,** (16), 1711-1712.

(3) Dicks, A. P.; Swift, H. R.; Williams, D. L. H.; Butler, A. R.; Al-Sa'doni, H. H.; Cox, B. G. *J. Chem. Soc., Perkin Trans. 2* **1996,** (4), 481-487.

(4) Kashiba-Iwatsuki, M.; Yamaguchi, M.; Inoue, M. *Febs. Lett.* **1996,** *389* (2), 149-152.

(5) Shishido, S. M.; Oliveira, M. G. *Photochem. Photobiol.* **2000,** *71* (3), 273-280.

(6) Siddiqi, K. S.; ur Rahman, A.; Tajuddin; Husen, A. *Nanoscale Res. Lett.* **2018,** *13* (1), 141.

(7) Singh, S. P.; Wishnok, J. S.; Keshive, M.; Deen, W. M.; Tannenbaum, S. R. *Proc. Natl. Acad. Sci.* **1996,** *93* (25), 14428-14433.

(8) Williams, D. L. H. *Acc. Chem. Res.* **1999,** *32* (10), 869-876.

(9) Wood, P. D.; Mutus, B.; Redmond, R. W. *Photochem. Photobiol.* **1996,** *64* (3), 518-524.

(10) de Souza, G. F. P.; Denadai, J. P.; Picheth, G. F.; de Oliveira, M. G. *Nitric Oxide* **2019,** *84*, 30-37.

(11) Lautner, G.; Stringer, B.; Brisbois, E. J.; Meyerhoff, M. E.; Schwendeman, S. P. *Nitric Oxide* **2019,** *86*, 31-37.

(12) McCarthy, C. W.; Guillory, R. J.; Goldman, J.; Frost, M. C. *ACS Appl. Mater. Interfaces* **2016,** *8* (16), 10128-10135.

(13) Krężel, A.; Bal, W. *Chem. Res. Toxicol.* **2004,** *17* (3), 392-403.

(14) Askew, S. C.; Barnett, D. J.; McAninly, J.; Williams, D. L. H. *J. Chem. Soc., Perkin Trans. 2* **1995,** (4), 741-745.

(15) Lutzke, A.; Melvin, A. C.; Neufeld, M. J.; Allison, C. L.; Reynolds, M. M. *Nitric Oxide* **2019,** *84*, 16-21.

(16) Kołodziejczak-Radzimska, A.; Jesionowski, T. *Materials (Basel)* **2014,** *7* (4), 2833-2881.

(17) Hotchkiss, P. J.; Malicki, M.; Giordano, A. J.; Armstrong, N. R.; Marder, S. R. *Journal of Materials Chemistry* **2011,** *21* (9), 3107-3112.

(18) Serpone, N.; Dondi, D.; Albini, A. *Inorganica Chim. Acta* **2007,** *360* (3), 794-802.

(19) Sirelkhatim, A.; Mahmud, S.; Seeni, A.; Kaus, N. H. M.; Ann, L. C.; Bakhori, S. K. M.; Hasan, H.; Mohamad, D. *Nano-Micro Lett.* **2015,** *7* (3), 219-242.

(20) Chen, J. J.; Winograd, N. *Surface Science* **1995,** *326* (3), 285-300.

(21) Singha, P.; Workman, C. D.; Pant, J.; Hopkins, S. P.; Handa, H. *J. Biomed. Mater. Res. A* **2019,** *0* (0).

(22) Luo, Z.; Zhu, S.; Liu, Z.; Liu, J.; Huo, M.; Yang, W. *Journal of Water and Health* **2015,** *13* (3), 704-713.

(23) Jia, H. Y.; Liu, Y.; Zhang, X. J.; Han, L.; Du, L. B.; Tian, Q.; Xu, Y. C. *J. Am. Chem. Soc.* **2009,** *131* (1), 40-41.

(24) Taladriz-Blanco, P.; Pastoriza-Santos, V.; Pérez-Juste, J.; Hervés, P. *Langmuir* **2013,** *29* (25), 8061-8069.

(25) Cao, G.-J.; Fisher, C. M.; Jiang, X.; Chong, Y.; Zhang, H.; Guo, H.; Zhang, Q.; Zheng, J.; Knolhoff, A. M.; Croley, T. R.; Yin, J.-J. *Nanoscale* **2018,** *10* (23), 11176-11185.

(26) Singh, J.; Im, J.; Whitten, J. E.; Soares, J. W.; Steeves, D. M. *Chemical Physics Letters* **2010,** *497* (4), 196-199.

(27) Fouetio Kengne, B.-A.; Karmakar, S.; Kaura, M.; Sai, V. V. R.; Corti, G.; Niraula, I. B.; Larin, A.; Hall, J.; Sowell, D.; Hrdlicka, P. J.; Dobrokhotov, V.; McIlroy, D. N. *ACS Appl. Mater. Interfaces* **2014,** *6* (16), 13355-13366.

(28) Sadik, P. W.; Pearton, S. J.; Norton, D. P.; Lambers, E.; Ren, F. *Journal of Applied Physics* **2007,** *101* (10), 104514.

(29) Singh, J.; Im, J.; Watters, E. J.; Whitten, J. E.; Soares, J. W.; Steeves, D. M. *Surface Science* **2013,** *609*, 183-189.

(30) Jana, J.; Chung, J. S.; Hur, S. H. *ACS Omega* **2019,** *4* (16), 17031-17038.

Chapter 5 Hub Region Disinfecting NO Releasing Insert for Tunnel Dialysis Catheters

The content of this chapter includes experiments conducted by Shale Mack, Amy Lou, and Blake Stringer. These individuals were undergraduate researchers in the Meyerhoff laboratory working under the direction of this Ph.D. candidate, and their names will appear on any future publication of the research described in this chapter.

5.1 Introduction

Tunneled dialysis catheters (TDCs) are commonly utilized for patients with End Stage Renal Disease (ESRD) that require hemodialysis (HD) treatments. Even though it is generally accepted that TDCs are the least desirable form of dialysis vascular access, in 2010 approximately 80% of patients started HD treatment using a TDC and it has remained relatively unchanged since then.[1] One of the major complications associated with TDCs is blood stream infections (BSIs). BSIs caused by TDCs has continued to be an important clinical issue that leaves patients with substantial morbidity, mortality, expense, and a decrease in their quality of life.[2]

For long-term TDCs, BSIs predominately occur from bacteria/biofilm growth via the intraluminal route because of hub contamination.[3] The most favored treatment of foreign body-related infection is removal of the foreign body (TDC), however this may not be practical for the patient. Thus, methods and devices have been developed that treat/prevent BSIs related to TDCs. A few notable treatment/prevention methods include antimicrobial lock therapy, Tego Needlefree Hemodialysis Connector plus Curos Disinfecting Cap for Tego, and a ClearGuard HD Antimicrobial Barrier Cap.

Antimicrobial lock therapy (ALT) involves infusing a highly concentrated antibiotic solution into the catheter lumen for a minimum of 2-4 h.[2, 4] Although there is no Food and Drug Administration (FDA) approved ALT, ALT practice has exhibited significant benefit to those with TDC.[2] Difficulty arises for ALT when microbial biofilm is already present in the catheter lumen due to the inability of antibiotics to penetrate and kill a biofilm. Certain chemicals like citrate and ethylenediaminetetraacetic acid (EDTA) have been added to help disrupt the biofilm, but high rates of ALT failure still occur with *Staphylococcus aureus*, *Pseudomonas aeruginosa*, and *Candida* bacteria.[2, 5, 6]

A recent study compared the performance of two FDA approved devices in relation to the rate of BSIs. These devices included the combination of Tego Needlefree Hemodialysis Connector (Tego) plus Curos Disinfecting Cap for Tego (Curos) and ClearGuard HD Antimicrobial Barrier Cap (ClearGuard).[7] Tego is a device that attaches to the hub and aims to prevent infection by using a "closed" system by reducing catheter hub manipulation.[7, 8] Curos is a port protector that utilizes 70% isopropanol to kill bacteria on the surface of Tego.[7, 9] ClearGuard is a device with a protruding rod and threads that are coated with chlorhexidine.[7, 10] Chlorohexidine is a well-known, broad spectrum antimicrobial agent with minimal risk of developing resistant bacteria strains.[7, 10] After a 13 month long study, the ClearGuard had a significantly lower BSI rate of 0.28 positive blood cultures (PBC) per 1000 TDC-days versus 0.75 PBC per 1000 TDC-days for Tego + Curos.[7] The potential downfall of the Tego + Curos device is that only the outer surface of the catheter hub is targeted. A potential downfall of the ClearGuard product is that chlorhexidine has trouble dispersing and killing biofilms.[11]

A device that retains the positive characteristics (effective broad spectrum antimicrobial agent, minimal risk of developing resistant bacteria strains) to prevent BSIs but also solves prior device

short-comings (effectiveness against biofilms) is one that involves the use of nitric oxide. Nitric oxide (NO) is an endogenously produced, free radical gas molecule that is synthesized by the enzyme nitric oxide synthase (NOS).[12-15] The body naturally produces NO when fighting an infection via immune system macrophages.[13, 14] NO is highly effective against a broad spectrum of bacteria including antibiotic-resistant strains because there are several mechanisms/reactions that can lead to cell death.[12, 13, 16]

Nitric oxide is also effective at dispersing/displacing biofilms.[17-20] One example involves NO released from intravascular catheters fabricated with *S*-nitroso-*N*-acetyl-D-penicillamine (SNAP) doped CarboSil polymer against *S. aureus* biofilms.[20] The amount of bacteria were evaluated after catheter segments were subjected to 7 d in a drip-flow bioreactor. A 5 log unit reduction was achieved compared to control catheters with no NO release.[20] Therefore, a NO releasing insert device that could disinfect the inner lumen of TDCs has great potential for preventing BSIs because of its inherent antimicrobial non-specificity, as well as biofilm dispersal and killing capabilities.

Herein, the NO releasing characteristics of various NO releasing insert devices are evaluated as well as their antimicrobial efficacy against *S. aureus* in a simulated catheter hub model. The most promising NO releasing insert was also evaluated for stability of the NO-donor molecule after subjection to different sterilization methods. The antimicrobial efficacy of the most promising NO releasing insert formulation was tested in real hemodialysis catheter hubs against both gram-negative (*P. aeruginosa*) and gram-positive (*S. aureus*) bacteria strains. Further, two 14-d long sheep studies compared the antimicrobial/anti-biofilm capabilities of the chosen NO releasing insert versus a control of a normal hemodialysis catheter cap and versus a commercially available antimicrobial cap that utilizes the antimicrobial agent chlorhexidine.

5.2 Materials and Methods

5.2.1 Materials

L-Glutathione reduced (GSH), hydrochloric acid (HCl), sodium nitrite, and polyethylene glycol (MW = 3,350) were purchased from Sigma-Aldrich (St. Louis, MO). Acetone; DOWSIL 3140, MIL-A-46146 RTV Silicone Coating; Dow Corning Silastic Laboratory Tubing (ID 0.058" × OD 0.077", 2415542); and Helix Medical Inc. Silicone Tubing (0.125" × 0.250", 6001121) were purchased from Fisher Scientific Inc. (Pittsburgh, PA). Male Luer Lock Injection Site caps (80149) were purchased from Qosina (Ronkonkoma, NY). LB agar and 10 mM phosphate buffered saline (PBS) (pH 7.2) were purchased from ThermoFisher Scientific (Grand Island, NY). Zinc oxide nanoparticles (APS 30 nm in diameter) were purchased from EPRUI Biotech Co. Ltd. (ShangHai, China). All aqueous solutions were prepared with 18.2 M Ω deionized water using a Milli-Q filter (Milli-q purified water) from EMD Millipore (Billerica, MA). Staphylococcus aureus ATCC 25923 and Pseudomonas aeruginosa ATCC 27853 were obtained from the American Type Culture Collection (Manassas, VA).

5.2.2 S-Nitrosoglutathione (GSNO) synthesis

The method used to prepare GSNO was the same as that described in Chapter 2.

5.2.3 Fabrication of NO releasing inserts

The entire procedure involving GSNO was completed in the absence of direct light. Silicone tubing (ID 0.058″, OD 0.077″) was cut to ~3 cm and sealed at one end using an adhesive glue (DOWSIL 3140, MIL-A-46146 RTV Coating) and allowed to dry for 24 h. Then, 12 ± 0.2 mg of a desired dry powder formulation was dispensed into the tubing using a glass funnel pipet. The

dry powder formulations used included (a) 75% GSNO : 25% 30 nm size ZnO nanoparticles; (b) 25% GSNO : 75% 30 nm size ZnO nanoparticles; (c) 60% GSNO : 20% 30 nm size ZnO nanoparticles : 20% solid polyethylene glycol (MW = 3,350) (PEG); (d) 75% GSNO : 25% fumed silica. Before use, the GSNO was crushed into a fine powder using a mortar and pestle and mixed with the other components by vortexing for 1 min to achieve a homogeneous dry powder mixture. After filling the tubing with the desired powdered formulation (~12 mg = ~1.8 cm fill length), the end that was employed to fill the tubing was cut to achieve ~0.2 cm head space above the fill powder. Lastly, adhesive glue was used to seal the open end and allowed to dry for 24 h. The final length of the inserts are ~ 2.0 cm.

5.2.4 Measuring real-time NO release from inserts

Nitric oxide release from the NO releasing inserts was measured using a Sievers Chemiluminescence Nitric Oxide Analyzer (NOA) 280i (Boulder, CO). The NOA was calibrated before via a two-point calibration of N_2 gas passed through a NOA zero air filter and a standard of 44.3 ppm NO in N_2 gas. Saline solution (0.9% sodium chloride) was made using 18.2 M Ω deionized water using a Milli-Q filter (Milli-q purified water) from EMD Millipore (Billerica, MA). The NOA sample cell was filled with 11 mL of saline solution and the NO releasing insert was placed below a floating polypropylene barrier to keep the insert fully submerged at all times. The saline solution reservoir was bubbled with N_2 gas at a rate of 50 mL/min to allow the NO generated from GSNO to escape from the solution and be carried into the NOA by the N_2 sweep gas. All NOA sample cells were wrapped in aluminum foil to shield the samples from light exposure. NO release was continuously monitored for 72 h at room temperature (24°C).

5.2.5 In vitro simulated catheter hub antimicrobial assay

To simulate the hub region of a catheter, 3 cm of silicone tubing (ID 0.125″, OD 0.250″) was employed. A volume of 0.3 mL of overnight grown bacteria cultures (1×10^8 CFU/mL) in 10% LB broth was transferred into the simulated hub clamped at one end. Then, a NO releasing insert was placed inside of the simulated hub and the other end clamped shut. For control samples, no NO releasing insert was added. Each sample was incubated at room temperature (24°C) in the dark, for 72 h, on a shaker at low speed. After 72 h of incubation, 20 µL of bacteria culture liquid was retrieved from each simulated hub and 10-fold serially diluted. Fifty µL of each dilution was spread on LB agar plates and incubated at 37°C overnight for colony-forming unit (CFU) counting. The simulated hub was also sliced into small pieces and the inside was stained with BacLight Live/Dead staining kit in the dark for 15 min to assess the degree of biofilm. Microscopic images were obtained by using a fluorescent microscope with appropriate filter sets (488/520 nm for SYTO-9 and 493/636 nm for propidium iodide.

5.2.6 Sterilization studies: Ethylene oxide (EO) vs. hydrogen peroxide (H_2O_2)

Nitric oxide releasing inserts (formulation (a)) were prepared as described in Section 5.2.3, individually packaged into separate pouches, and sent to the University of Michigan hospital sterilization facility for ethylene oxide (EO) or hydrogen peroxide (H_2O_2) treatment. For EO treatment, the NO releasing inserts undergo a 1 h preconditioning and humidification process (54°C, 40-80% humidity), followed by 3 h of exposure to ethylene oxide gas under the same temperature and humidity. Then, a 2 h ethylene oxide gas evacuation process occurs, followed by 12 h of air washes. For H_2O_2 treatment or STERRAD®, the process takes approximately 45 min total. Under vacuum, 59% (nominal) aqueous H_2O_2 is vaporized to cover the NO releasing inserts.

Diffusion of the gaseous H_2O_2 occurs while the pressure is reduced, forming low-temperature H_2O_2 gas plasma after radio frequency (RF) energy is applied. The H_2O_2 gas plasma generated sterilizes the NO releasing inserts. Control NO releasing inserts were prepared as described in Section 5.2.3, but not sterilized. The amount/stability of GSNO within each insert was measured by releasing all of the NO from GSNO via shining UV light on them and detecting/quantitating the total amount of NO released using a NOA. Specifically, 2 mL of Milli-q purified water was added to an NOA sample cell. After a steady baseline was achieved, a NO releasing insert was cut open and the powder filling was transferred into the sample cell using another 2 mL of Milli-q purified water. An additional 1 mL of Milli-q purified water was used to rinse all remaining powder on the NOA sample cell walls, down into the bulk solution (total 5 mL of Milli-q purified water). The GSNO/ZnO containing solution was bubbled with N_2 gas at a rate of 50 mL/min to escape from the solution and be carried into the NOA by the N_2 sweep gas. UV light was used to irradiate the sample until NO release from GSNO was exhausted, marked by a return to the original baseline. The amount of NO released from each NO releasing insert was directly converted to GSNO because the mole ratio is 1:1. The highest amount of GSNO measured from the three NO releasing control inserts (not sterilized) was assumed to be 100% recovery of GSNO; therefore. all other samples (sterile and non-sterile) were normalized to this value. Thus, >100% GSNO recovery was possible.

5.2.7 Stability Study

Nitric oxide releasing inserts using formulation (a) (75% GSNO : 25% 30 nm size ZnO nanoparticles) were prepared. Three NO releasing inserts were measure for their amount of GSNO on Day 0 without any sterilization processes. On Day 0 the remaining NO releasing inserts were sterilized using the H_2O_2 sterilization method described above. After sterilization was completed

on Day 0, each sterile insert remained in their individual sterilization pouches and were stored in a sealed glass jar with desiccant, in the dark, at room temperature (24°C) until further use. The %GSNO recovery from an NO releasing insert on any given day was achieved using the method outlined in Section 5.2.6. Briefly, the NO releasing inserts were cut open and the powder washed into a NOA sample cell. All the NO was exhausted from GSNO using UV light. The NO was quantitated and measured by a NOA. All recovery values obtained were normalized to the highest amount of GSNO obtained from one of the three control NO releasing inserts (not sterilized).

5.2.8 In vitro catheter hub antimicrobial assay

The catheters utilized for this assay were 28 cm long Permcath™ Pediatric Silicone Chronic Dual Lumen Oval Catheters, Covidien/Medtronic (Ref 8815543001, Lot 1611800146). The clamp on the catheter's hub region was clamped shut and 0.3 mL of overnight grown bacteria cultures (1×10^8 CFU/mL) in 10% LB broth was added. A NO releasing insert (pre-sterilized by the H_2O_2 sterilization method mentioned above) was inserted inside of the catheter hub and sealed by a cap. For control samples, no NO releasing insert was added. Each catheter was incubated at room temperature (24°C) in the dark, for 72 h, on a shaker at low speed. After 72 h of incubation, 20 µL of bacteria culture liquid was retrieved from each hub region and 10-fold serially diluted. Fifty µL of each dilution was spread on LB agar plates and incubated at 37°C overnight for colony-forming unit (CFU) counting.

5.2.9 Sheep studies - general procedure

This study including animal handling and surgical procedures that were approved by the University of Michigan Committee on Use and Care of Animals (24 h fasting and pre-surgical analgesia with

Fentanyl transdermal patch 100 µg/h) in accordance with university and federal regulations. Adult sheep weighing 45-50 kg were utilized. Under general anesthesia, 28 cm long (13 cm cuff to proximal tip) Permcath™ Pediatric Silicone Chronic Dual Lumen Oval Catheters, Covidien/Medtronic (8815543001) were placed using the Seldinger wire technique in the right and left jugular veins (3-5 cm above the subclavian), aiming to place the proximal tip in the RA-SVC junction. Caution was taken not to expose or manipulate the vessels. Catheters were secured to the skin and covered with a sterile dressing. After catheter placements, the sheep were recovered from anesthesia and housed in a barn (non-sterile conditions) for the remainder of the experiment. All catheters were capped and filled with 2,000 U heparinized saline solution (2 mL) injected via the distal end of the lumen. The NO releasing inserts used for both sheep studies were made using formulation (a) 75% GSNO : 25% 30 nm size ZnO nanoparticles. The NO releasing inserts were attached to male luer lock injection site caps, Qosina (80149), using the same adhesive glue used in Section 5.2.3, and allowed to dry for 24 h (Fig. 5.1a). Each NO releasing insert cap was individually packaged and sterilized using the H_2O_2 sterilization method described previously. The sterile NO releasing insert caps were stored at room temperature (24°C) and shielded from light until further use.

Prior to necropsy (day 14), 10,000 U bolus of heparin was given via a cephalic vein angiocath, followed by FatalPlus IV injection. Each catheter was procured using sterile techniques. The external surface of each catheter was sterilized by wiping with a 70% ethanol solution. One cm length sections were cut from each section of catheter as shown in Figure 5.1b. Each section was homogenized in 2 mL of 1 × PBS (10 mM, pH 7.2) in a 15-mL tube using a homogenizer (OMNI TH, OMNI International, Kennesaw, GA) at full speed to remove all bacteria/biofilm adhered to the inner lumen walls, and the resulting solution was 10-fold serially diluted. Fifty µL of each

dilution was spread on LB agar plates and incubated at 37°C overnight for CFU counting. Additionally, >0.5 cm length sections were cut from each section of catheter described in Figure 5.1b, and the inner lumen surfaces were stained with BacLight Live/Dead staining kit in the dark for 15 min. Microscopic images were obtained by using a fluorescent microscope with appropriate filter sets (488/520 nm for SYTO-9 and 493/636 nm for propidium iodide.

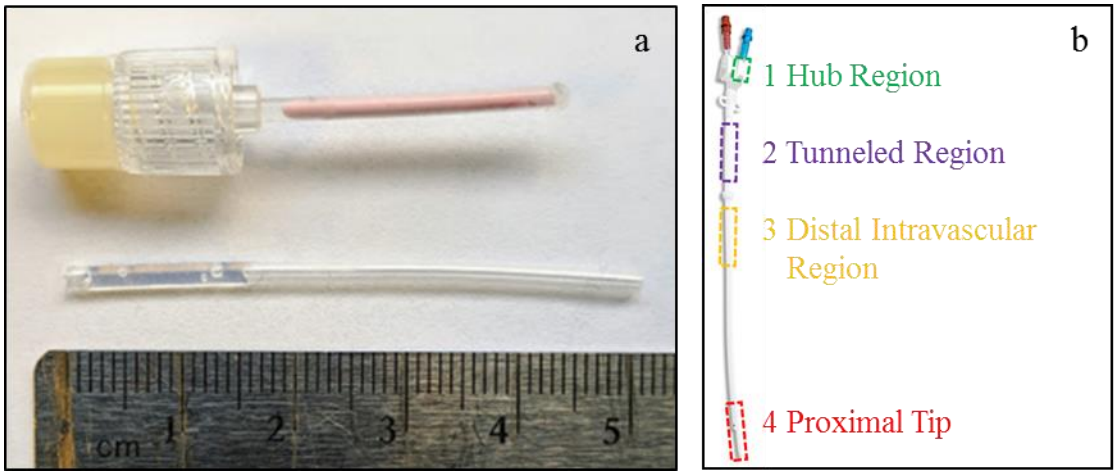

Figure 5.1. (a) (top) NO releasing insert cap used in Sheep Study #1 and #2 and (bottom) the silicone tubing filled partially with adhesive glue prior to gluing it to cap (pre-glued section is inside of cap). (b) Regions of catheter studied in Sheep Study #1 and #2.

5.2.10 Sheep Study #1

Two adult sheep were studied during Sheep Study #1. One sheep was designated as control (n = 4 catheter hubs total, no NO releasing inserts) and the other sheep was designated as experimental (n = 4 catheter hubs total, using NO releasing insert caps). On postoperative days 0, 2, 4, 7, 9, 11, and 14, 50 µL of liquid from the hub region of each catheter lumen was taken for CFU counting. Then, 3.5 mL of blood was drawn from each lumen, the lumens were then locked with 2,000 U heparinized saline solution (2 mL), and both NO releasing insert caps and control caps were replaced with new caps, respectively.

5.2.11 Sheep Study #2

Two adult sheep were studied during Sheep Study #2. Use of a commercially available antimicrobial cap with chlorhexidine as the antimicrobial agent was studied and compared to use of the new NO releasing insert device. For one sheep, the catheter implanted in the right jugular vein was designated for the commercial chlorhexidine caps and the catheter implanted in the left jugular vein was designated for the NO release insert caps. For the second sheep, the designations were reversed such that right jugular vein was designated for the NO release insert caps and the catheter implanted in the left jugular vein was designated for the chlorhexidine caps. In total, for chlorhexidine caps there were $n = 4$ catheter hubs and for the NO releasing insert caps there were also $n = 4$ catheter hubs. On postoperative days 0, 2, 3, 6, 8, 10, 12, and 14, 50 µL of liquid from the hub region of each catheter lumen was taken for CFU counting. Then, 3.5 mL of blood were drawn from each lumen, locked with 2,000 U heparinized saline solution (2 mL), and both NO releasing insert caps and chlorhexidine caps were replaced with new caps, respectively.

5.3 Results and Discussion

5.3.1 Design of NO releasing inserts

The dimensions of the NO releasing insert were designed based on the hub dimensions of commonly used hemodialysis catheters (Fig. 5.2). *S*-nitrosoglutathione (GSNO) was chosen as the NO donor molecule because it is endogenously produced and fairly stable when stored as a powder in the absence of moisture.[21, 22] ZnO nanoparticles (30 nm diameter) were chosen to enhance the NO release from GSNO.[23] Silicone rubber tubing was chosen because the high diffusivity of NO through silicone rubber compared to other biomedical grade polymers and its

relatively low hardness allows moisture to pass through its walls to initiate NO release from GSNO.[24]

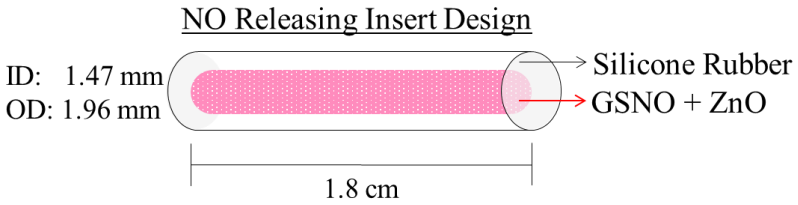

Figure 5.2. Design of NO releasing insert.

5.3.2 Characterizing real-time NO release of NO releasing insert formulations

The real-time NO release of four different NO releasing insert formulations was evaluated to determine each formulation's NO release characteristics. Nitric oxide release was measured from each NO releasing insert over a 72 h period while submerged in saline solution in the dark at room temperature (24°C). The measurement conditions were as close to "real-world" conditions of hemodialysis catheter hubs as possible. Measuring over a 72 h period was chosen because hemodialysis treatments normally occur every 2-3 days, enabling the NO release insert to be changed at each dialysis session. The other conditions were chosen because catheter hubs are located outside of the body, opaque, and locked with a saline lock solution.

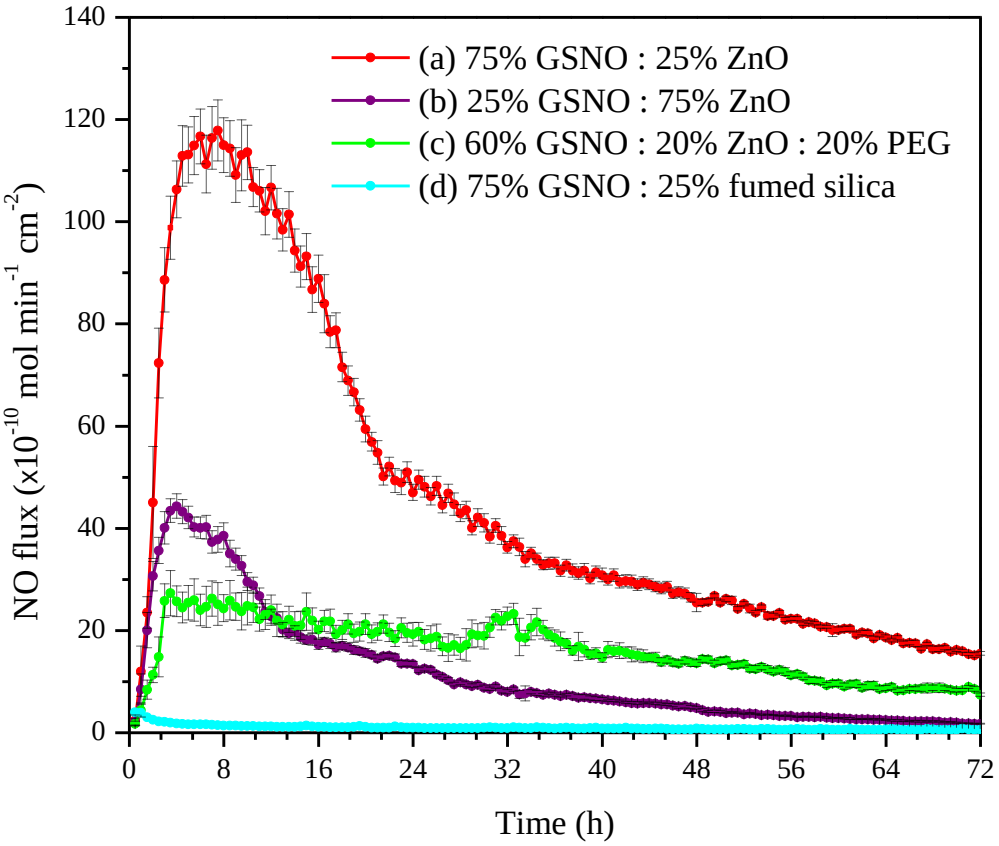

Figure 5.3. Real-time NO flux of inserts prepared with different formulations a-d in the dark at 24°C over a 72 h period. Data represents the mean ± SD (*n* = 3).

Four different NO releasing insert formulations were tested for their NO release characteristics under real world conditions (Fig. 5.3). The dry powder NO releasing formulations studied include (a) 75% GSNO : 25% 30 nm size ZnO nanoparticles; (b) 25% GSNO : 75% 30 nm size ZnO nanoparticles; (c) 60% GSNO : 20% 30 nm size ZnO nanoparticles : 20% solid polyethylene glycol (MW = 3,350) (PEG); and (d) 75% GSNO : 25% fumed silica. Formulation (a) yielded a large burst of NO over the first 24 h and tapered off until the 72 h mark was reached (Fig. 5.3). For formulation (b), the percentages of GSNO and ZnO were reversed compared to formulation (a). Formulation (b) demonstrated a similar NO release profile compared to formulation (a), however the initial burst lasted only 12 h and tapered off significantly afterwards due to the lower amount

of GSNO initially present (Fig. 5.3). In attempt to level/smooth out the NO release profile of formulation (a), polyethylene glycol (MW=3,350) (PEG) was added to increase the viscosity of the insert's internal components (GSNO and ZnO). The addition of PEG should increase the internal viscosity upon moisture absorption, imposing a cage effect on the thiyl and NO radical pair such that they recombine to form GSNO and slow the rate of NO release.[25, 26] The addition of PEG led to formulation (c) and still includes GSNO and ZnO. The expected leveling/smoothing effect was achieved, leading to a more consistent NO release rate over 72 h (Fig. 5.3). To prove that ZnO was necessary to enhance NO release in each formulation, fumed silica particles were substituted in place of ZnO as an inert agent that does not react with GSNO. The NO release profile of formulation (d) shows minimal NO release over 72 h (Fig. 5.3). This data definitively proves that ZnO is needed to achieve significant NO release from GSNO contained within the silicone tubing.

5.3.3 Antimicrobial effects of NO releasing formulations (a-c) inserts in simulated catheter hubs

Formulations (a-c) displayed unique NO releasing profiles over 72 h. Therefore, each was tested for their bactericidal effects using a "Simulated Hub" antimicrobial experiment. This experiment was designed to mimic the conditions of a real hemodialysis catheter hub. Silicone tubing with a similar inner diameter to that of an actual hemodialysis catheter hub was utilized as the "Simulate Hub". A detailed description of this study can be found in Section 5.2.5. Briefly, a given concentration of *Staphylococcus aureus* (*S. aureus*) in 10% LB broth was put inside of the silicone tubing that was sealed at one end. The NO releasing inserts were place inside of the simulated hub and the opposite end closed. The controls contained no NO releasing insert. The prepared simulated hubs were subjected to real world ambient conditions as stated previously (24°C, dark,

72 h, and on a shaker). After 72 h, the amount of bacteria in the liquid broth was enumerated for each sample and the inner lumen wall of the simulated hub was imaged for bacteria/biofilm adhered to its surface.

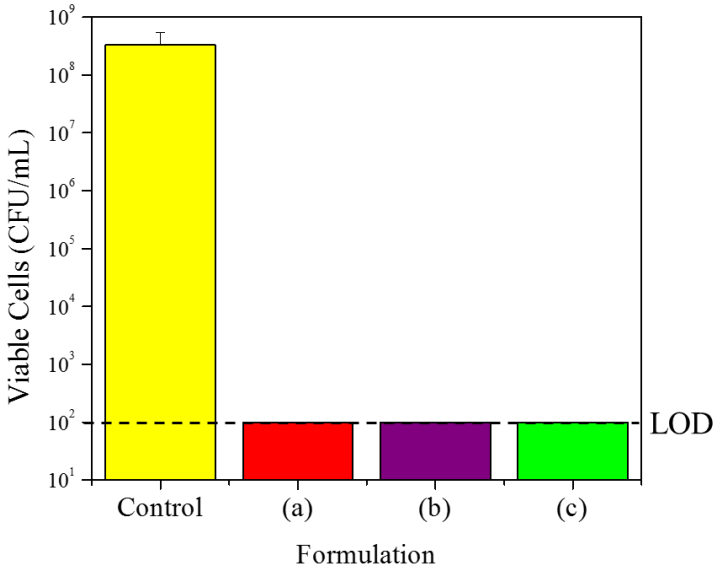

Figure 5.4. Viable cell counts of *S. aureus* from the liquid broth of simulated catheter hubs after 72 h of exposure to control (no insert) and NO release inserts with formulations (a), (b), and (c), in the dark at 24°C. The horizontal dashed line represents the LOD (100 CFU/mL) for the assay. Data represents the mean ± SD (n = 3).

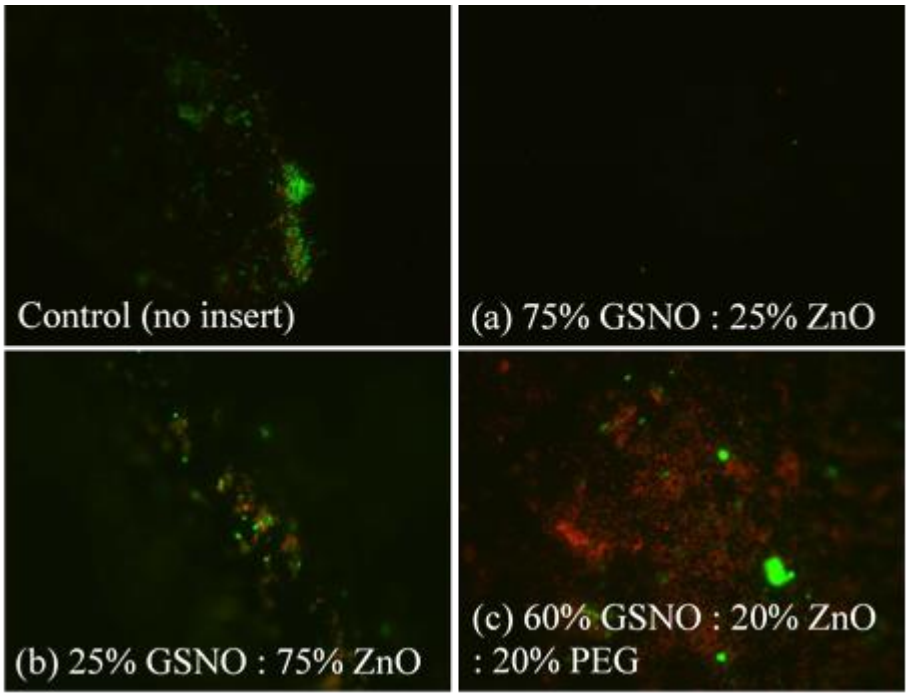

Figure 5.5. Fluorescent microscopic images of *S. aureus* bacteria/biofilm adhered to the inner lumen wall of the simulated hub after exposure to no insert (control) or NO releasing inserts with formulations (a-c) for 72 h in the dark at 24°C. Live/Dead dye stain was used where green = alive cells and red = dead cells.

Each NO releasing insert formulation (a-c) killed all of the bacteria present in the liquid broth of each simulated hub, leading to a 6.4 log reduction of bacteria compared to control (no NO releasing insert) (Fig. 5.4). This data indicates that formulations (a-c) are capable of killing *S. aureus* bacteria cells in the liquid broth of a simulated catheter hub region. Fluorescent microscopic images were taken of the inner lumen wall of each simulated hub and representative images are pictured in Figure 5.5. The control as well as formulations (b) and (c) displayed evidence of *S aureus* bacteria/biofilm adhered to the inner lumen wall of the simulated hubs (Fig. 5.5). However, formulation (a) showed no evidence of significant *S aureus* bacteria/biofilm adhesion (Fig. 5.5). The data from formulation (a) suggests that having a large burst of NO over the first 24 h is needed to prevent biofilm formation. Therefore, formulation (a), 75% GSNO : 25% 30 nm ZnO

nanoparticles, was chosen as the formulation to continue testing because of its excellent antimicrobial/anti-biofilm characteristics.

5.3.4 Sterilization and Stability Testing

Sterilization of the NO releasing inserts would be needed for animal testing. GSNO naturally reacts to release NO in the presence of light, heat, metal ions, and water.[21, 22, 25, 27-31] Thus, different sterilization methods were tested to see if they had any negative effects on GSNO stability. Again, the NO releasing formulation (a) insert was utilized in these studies. Two common sterilization methods were tested as described in Section 5.2.6 (above), ethylene oxide (EO) gas and hydrogen peroxide (H_2O_2) plasma. EO sterilization is a traditional sterilization method that takes place at a temperature of 54°C and requires several hours to complete. H_2O_2 sterilization is a relatively new method of sterilization that occurs at a temperature of 40°C and takes ~45 min to complete.

To test if the sterilization methods effected the stability of GSNO inside of the silicone insert tubing, the amount of GSNO (%recovery of GSNO) was measured for NO releasing formulation (a) inserts subjected to no sterilization (control), H_2O_2 sterilization, and EO sterilization. Since each NO releasing insert was made by hand and the amount of GSNO inevitably varies somewhat. Thus, the highest amount of GSNO measured from the three NO releasing control inserts (not sterilized) was assumed to be 100% recovery of GSNO (Table 5.1). All other NO releasing inserts tested were normalized to this value, and hence >100% recovery values were possible. The results of this study are shown in Table 5.1. Ultimately, H_2O_2 sterilization was chosen as the best method compared to EO sterilization because of lower standard deviation and quicker turn-around period.

Table 5.1. %Recovery of GSNO after no sterilization (control), hydrogen peroxide (H_2O_2) sterilization, or ethylene oxide (EO) sterilization processes. Values are normalized to the highest amount of GSNO recovered from the control (no sterilization) trials. Data represents the mean ± SD (n = 3).

Control (no sterilization)	H_2O_2 Sterilization	EO Sterilization
98.4 ± 1.6%	100.2 ± 2.4%	95.3 ± 10.1%

After the sterilization method was selected, it was important to test the long-term stability of the GSNO inside of the NO releasing inserts. For this study, NO releasing formulation (a) inserts were fabricated and sterilized via H_2O_2. However, three NO releasing inserts were not sterilized (control) and the amount of GSNO in each insert was determined on Day 0 using the method described in Section 5.2.7. After H_2O_2 sterilization was completed on Day 0 for the remaining inserts, they remained in their individual sterilization pouches and stored in a sealed glass jar with desiccant, in the dark, at room temperature (24°C) until further use. After nearly 2 months of storage, the GSNO inside of the NO releasing formulation (a) inserts was found to degrade by an average of 4.3% (Fig. 5.6). Therefore, GSNO is relatively stable when stored dry with ZnO nanoparticles inside of the silicone insert devices at room temperature.

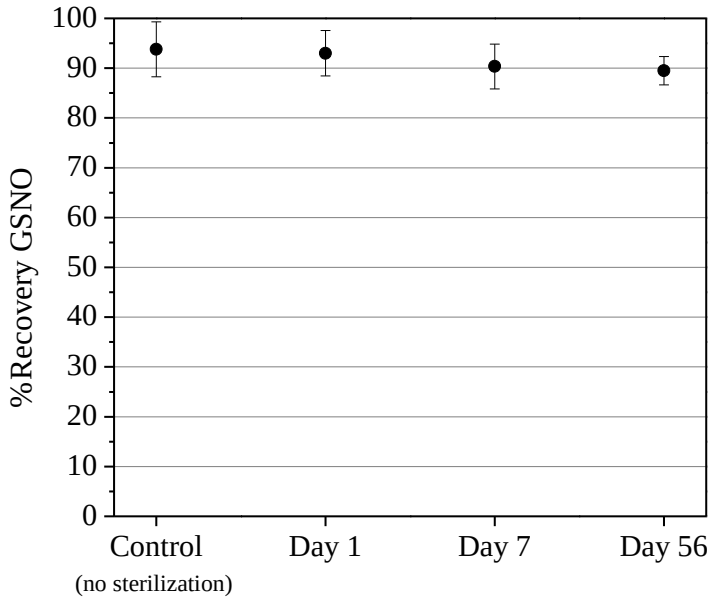

Figure 5.6. %Recovery of GSNO measured on Day 1, 7, and 56 from NO releasing inserts using formulation (a), stored in the dark at 24°C after hydrogen peroxide (H_2O_2) sterilization. Control (no sterilization) NO releasing inserts using formulation (a) were measure for %recovery of GSNO on Day 0. Data represents the mean ± SD (n = 3).

5.3.5 Antimicrobial effects of NO releasing formulation (a) inserts in hemodialysis catheter hubs

The antimicrobial efficacy of NO releasing formulation (a) inserts in real hemodialysis catheter hubs were tested against gram-positive and gram-negative strains, *S. aureus*, and *P. aeruginosa*, respectively. A detailed procedure can be found in Section 5.2.8, above. Briefly, a given concentration of bacteria in 10% LB broth was added to a real hemodialysis catheter hub region and the hub region was closed at the proximal end of the hub region using the pre-existing clamp. H_2O_2 sterilized NO releasing inserts were then placed inside of the catheter hubs and closed via the attached cap. The control trials contained no NO releasing inserts, just a normal hub cap. The hemodialysis catheter hubs were then subjected to real world conditions as stated previously (24°C, dark, 72 h, and on a shaker). Upon completions of the 72 h study, bacteria counts were obtained from the liquid broth inside of the catheter hubs containing the NO releasing formulation

(a) inserts versus the controls with no inserts. This led to a log reduction of 6.6 and 6.7 (compared to controls) against *S. aureus* and *P. aeruginosa*, respectively. This data suggests that the NO releasing inserts containing formulation (a) are extremely effective at killing both gram-positive and gram-negative strains.

5.3.6 Sheep Study #1

The purpose of Sheep Study #1 was to evaluate the antimicrobial/anti-biofilm performance of the NO releasing formulation (a) insert caps versus normal hemodialysis catheter caps by replacing each cap every 2-3 d over a 14 d long period. Detailed procedures for Sheep Study #1 can be found in Sections 5.2.9 and 5.2.10. Briefly, two sheep were studied during Sheep Study #1 with one sheep designated as a control (no NO release inserts) and the other sheep experimental (NO releasing inserts). Each sheep had two surgically implanted dual-lumen TDC catheters for a total of four catheter hubs each. The NO releasing formulation (a) inserts were glued to catheter caps for convenience (Fig. 5.1a). During the 14 d study the sheep were housed in a barn at the U of M farm. Control and experimental caps were changed every 2-3 d and blood was drawn through each lumen to simulate the average time between dialysis treatments and blood exposure. Bacteria cultures from the liquid in each hub region were taken prior to replacing the caps. After 14 d, the study was terminated and each hemodialysis catheter was evaluated for the amount of bacteria/biofilm present on the inside wall of four separate regions of the catheter (Fig. 5.1b).

The results of the bacteria counts taken from the liquid within the hub region every 2-3 days are summarized in Figure 5.7. On particular days, some unforeseen circumstances prevented obtaining a proper liquid sample from each hub region (Day 7, and 11) (Fig. 5.7). However, the

data remains consistent where the control sheep displayed significant bacteria counts after Day 4 and the experimental sheep (NO releasing insert caps) showed no bacteria on any day, therefore reaching the limit of detection (220 CFU/mL) after each day of testing (Fig. 5.7). A log reduction of 3.88 was already observed by Day 4 and increased to 5.42 by Day 14 for experimental sheep versus control (Fig 5.7). This data suggests that the NO releasing formulation (a) insert caps have a significant antimicrobial effect against bacteria present in the liquid of the hub region under real world conditions.

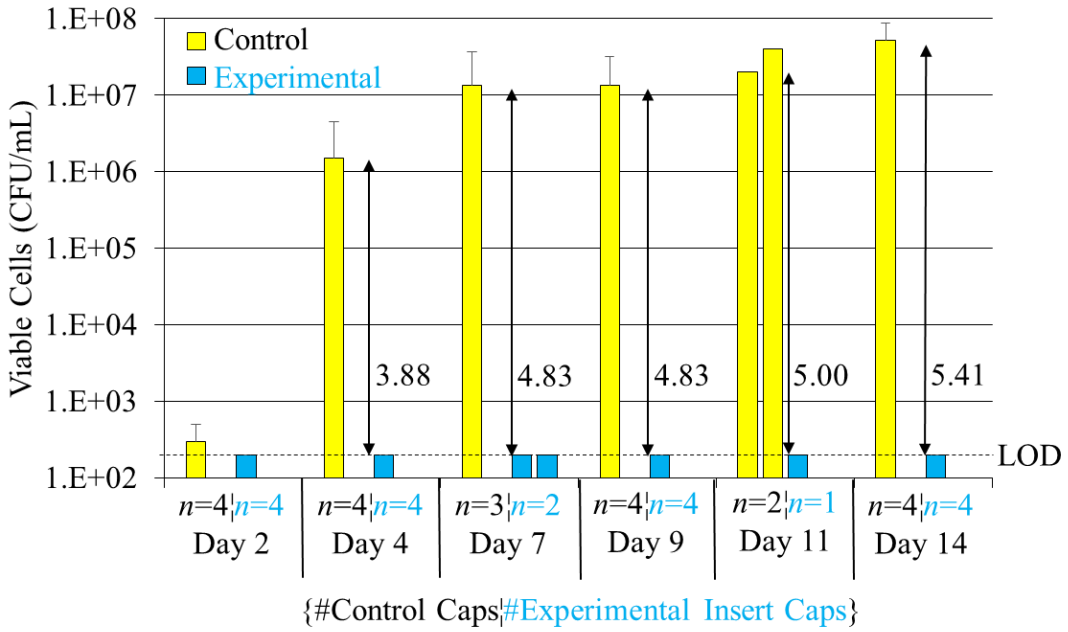

Figure 5.7. Sheep Study #1 bacteria counts from the hub solution on days 2, 4, 7, 9, 11, and 14 using normal catheter caps (Control) and NO releasing insert caps (Experimental). Dashed line is the limit of detection (200 CFU/mL). Log reduction values are given for Experimental vs. Control. The number of samples (n = X) is specified for each day. Data with an error bar represents the mean ± SD.

Upon completion of the 14 d study, four regions of each catheter were tested for bacteria/biofilm adhered to the inner lumen walls (Fig. 5.1b). This test was conducted by first sterilizing the outside of the catheter, cutting out the specific sections, and using a homogenizer to remove all of the

adhered bacteria/biofilm from the inner lumen wall for bacteria enumeration. The results of this study are summarized in Figure 5.8. For the control catheters, all four regions of the catheters had a significant amount of bacteria/biofilm present. For catheters with the experimental NO releasing insert caps, no bacteria were detected in any of the four regions (Fig. 5.8). Interestingly, bacteria/biofilm prevention was observed in all regions of the catheter and not just the hub region (where the NO is locally released). This data quantitatively suggests that bacteria can migrate to the proximal regions of the catheter from the hub region and that the NO releasing formulation (a) insert caps have significant antibacterial/anti-biofilm potential throughout all regions of a catheter during a real world situation.

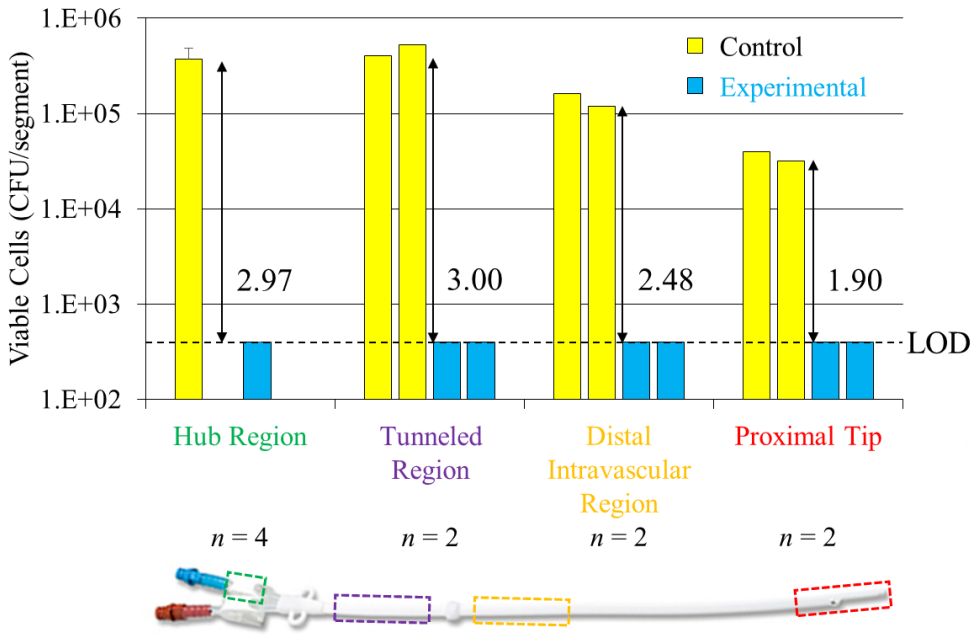

Figure 5.8. Sheep Study #1 bacteria/biofilm adhered to the inner lumen wall of the hub region, tunneled region, distal intravascular region, and proximal tip of catheters using normal catheter caps (Control) and NO releasing insert caps (Experimental). Dashed line is the limit of detection (400 CFU/segment). Log reduction values are given for Experimental vs. Control. The number of samples (n = X) are specified for each section of catheter. Data with an error bar represents the mean ± SD.

Fluorescent microscopic images were taken of the inner lumen walls of each region of the catheters using Live/Dead dye stain upon termination of the study (Fig. 5.9). Experimental catheters (NO releasing insert caps) displayed minimal to no bacteria adhered to the inner lumen walls in all regions (Fig. 5.9). The control catheters displayed significant bacteria/biofilm adhesion in all four regions (Fig. 5.9). This data qualitatively suggests that the NO releasing formulation (a) insert cap prevents bacteria/biofilm formation in each catheter region during a real world study.

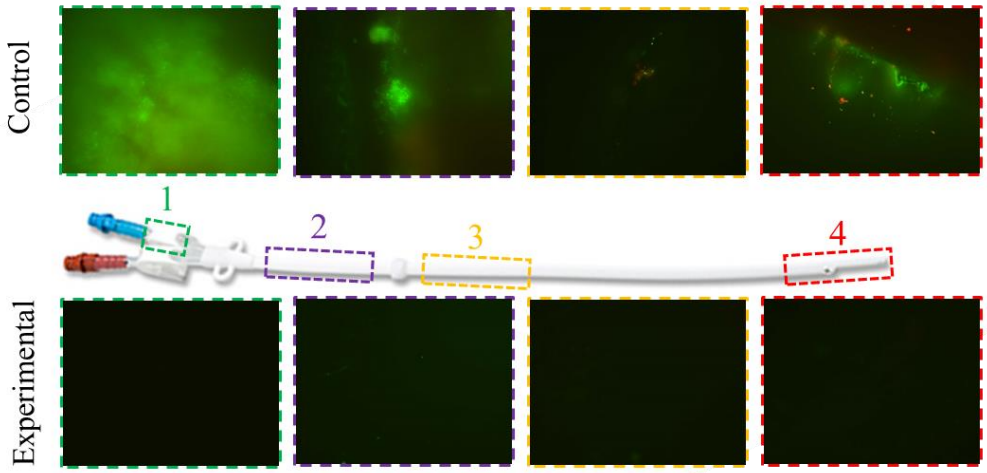

Figure 5.9. Sheep Study #1 fluorescent microscopic images of bacteria/biofilm adhered to the inner lumen wall of the (1) hub region, (2) tunneled region, (3) distal intravascular region, and (4) proximal tip of catheters using normal catheter caps (Control) and NO releasing insert caps (Experimental). Live/Dead dye stain was used where green = alive cells and red = dead cells.

5.3.7 Sheep Study #2

The purpose of Sheep Study #2 was to compare the antimicrobial/anti-biofilm performance the NO releasing formulation (a) insert cap versus a commercially available antimicrobial cap that utilizes chlorhexidine as the antimicrobial agent. For both type of inserts, each cap was replaced every 2-3 d over a 14 d long period. Detailed procedures for Sheep Study #2 can be found in sections 5.2.9 and 5.2.11. Briefly, two sheep were studied and for one sheep the dual-lumen catheter was surgically implanted in the right jugular vein and it was designated for use with the

chlorhexidine caps, while the dual-lumen catheter implanted in the left jugular vein was designated for the NO release insert caps. For the second sheep, the cap designations were reversed to the opposite jugular veins. Both sheep were housed in a barn during the 14 d study. The same procedures were performed in Sheep Study #1 as were performed in Sheep Study #2. Chlorhexidine and experimental NO release caps were changed every 2-3 d and blood was drawn through each lumen to simulate the average time between dialysis treatments and blood exposure. Bacteria cultures were taken from the liquid in each hub region prior to replacing the caps. After the study was terminated on Day 14, each hemodialysis catheter was evaluated for the amount of bacteria/biofilm present in four different regions of the catheter (Fig. 5.1b).

The bacteria counts taken from the liquid of the hub region every 2-3 days yielded no bacteria detected on any day for both chlorhexidine and experimental catheters. This data suggests that chlorhexidine caps display significant antimicrobial effects against bacteria present in the liquid phase of the hub region. This data also confirms the results obtained in Sheep Study #1 for the NO releasing formulation (a) insert cap because the same results (no bacteria detected on any day) were obtained in Sheep Study #2.

After the 14 d study was completed, four regions of each catheter were tested for bacteria/biofilm adhered to the inner lumen walls (Fig. 5.1b). The outside of each catheter was sterilized, then the specific sections of the catheter were cut out and bacteria/biofilm adhered to the inner lumen walls were removed using a homogenizer for bacteria enumeration. The results of this study are summarized in Figure 5.10. For the experimental catheters, minimal bacteria were detected in the hub and tunneled regions and no bacteria were detected in the distal intravascular region and proximal tip (Fig. 5.10). For the chlorhexidine catheters, bacteria/biofilm was detected in all four regions (Fig. 5.10). The tunneled region of the catheter had the largest log reduction of bacteria

(3.82) for the experimental versus chlorhexidine catheters (Fig. 5.10). Overall, this data suggests that the NO releasing formulation (a) insert caps are much more capable at preventing bacteria/biofilm formation in all four regions of a hemodialysis catheter compared to commercially available chlorhexidine caps.

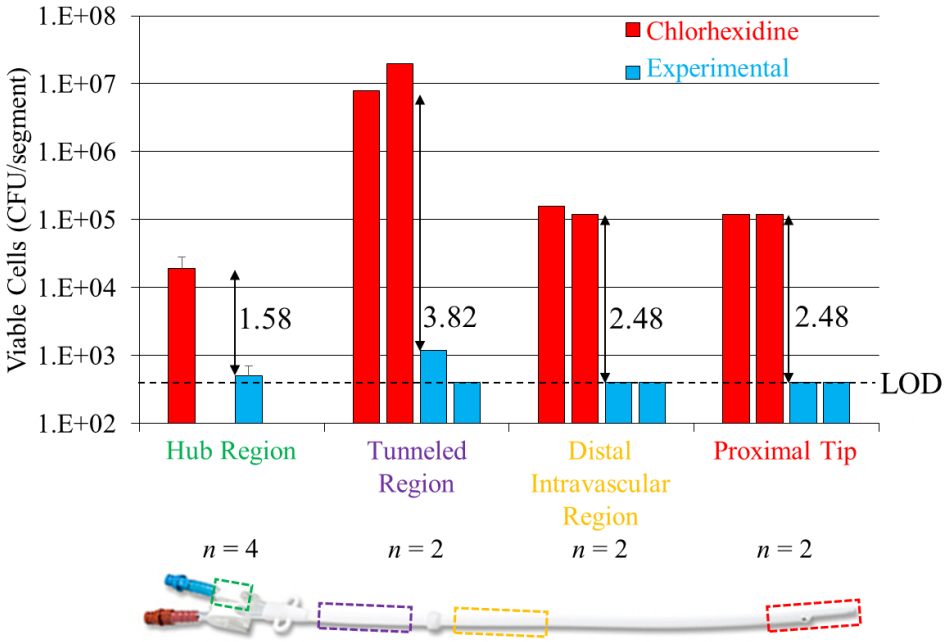

Figure 5.10. Sheep Study #2 bacteria/biofilm adhered to the inner lumen wall of the hub region, tunneled region, distal intravascular region, and proximal tip of catheters using normal catheter caps (Control) and NO releasing insert caps (Experimental). Dashed line is the limit of detection (400 CFU/segment). Log reduction values are given for Experimental vs. Control. The number of samples (n = X) are specified for each section of catheter. Data with an error bar represents the mean ± SD.

Fluorescent microscopic images were taken of the inner lumen walls of each region of the catheters using Live/Dead dye stain after study termination (Fig. 5.11). The chlorhexidine catheters displayed significant bacteria/biofilm adhered to the inner lumen wall of the tunneled region, which corresponds to the elevated bacteria/biofilm counts obtained from the tunneled region (Fig. 5.10, Fig. 5.11). The experimental catheters (NO releasing insert caps) displayed minimal to no bacteria adhered to the inner lumen walls of all four regions (Fig. 5.11). This data indicates that

the NO releasing formulation (a) insert cap prevents more bacteria/biofilm formation in each catheter region compared to the commercially available chlorhexidine cap.

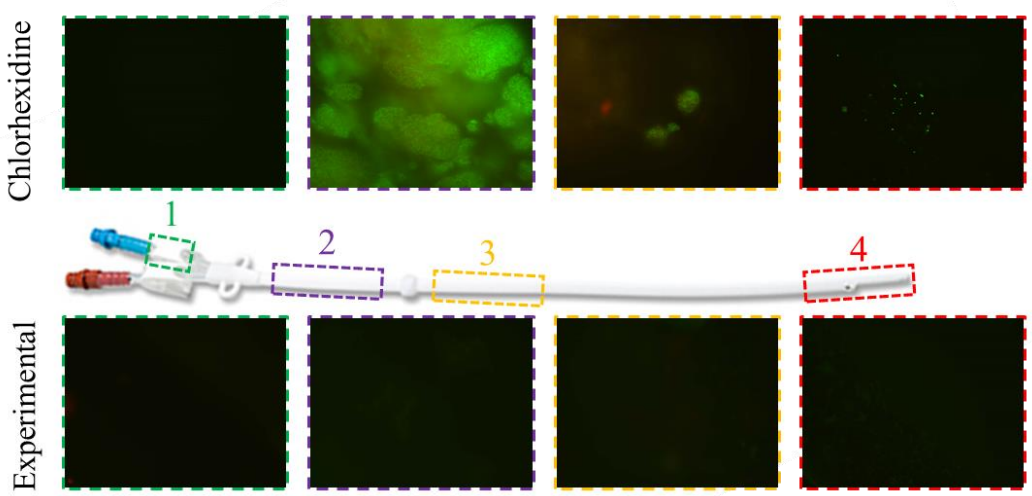

Figure 5.11. Sheep Study #2 fluorescent microscopic images of bacteria/biofilm adhered to the inner lumen wall of the (1) hub region, (2) tunneled region, (3) distal intravascular region, and (4) proximal tip of catheters using chlorhexidine caps (Chlorhexidine) and NO releasing insert caps (Experimental). Live/Dead dye stain was used where green = alive cells and red = dead cells.

5.4 Conclusion

The real-time NO releasing characteristics of four different NO releasing insert formulations were determined under real world conditions (24°C, dark, 72 h, submerged in saline). Formulation (a) demonstrated high initial NO flux levels compared to the other formulations. Formulation (b) demonstrated similar characteristics to formulation (a), however the NO fluxes were significantly lower. Formulation (c) contained PEG to smooth/level out the NO flux over the 72 h period. Formulation (d) contained no ZnO and displayed minimal NO release, therefore further proving that ZnO is needed in the formulation to display significant NO release capability. Testing the antimicrobial/anti-biofilm efficacy of formulations (a-c) using an simulated catheter hub assay against *S. aureus* revealed that formulation (a) was the best at preventing biofilm formation because of the large initial burst of NO that formulation (a) provides. Testing the %recovery of

GSNO from inside of the NO releasing formulation (a) inserts after different sterilization techniques revealed that minimal to no GSNO decomposition occurs during the H_2O_2 sterilization process. Thus, due to minimal GSNO decomposition and faster sample turn-around time, H_2O_2 sterilization was chosen as the main sterilization procedure. A preliminary shelf-life stability study of H_2O_2 sterilized NO releasing formulation (a) inserts showed minimal degradation of GSNO (4.3%) after 56 d of being stored at 24°C, in the dark, and in the presence of desiccant. It was also discovered that H_2O_2 sterilized NO releasing formulation (a) inserts are highly effective at killing both gram-negative (*P. aeruginosa*) and gram-positive (*S. aureus*) strains (6.7 and 6.6 log reduction, respectively) from the liquid present in actual catheter hubs under real world conditions (24°C, dark, 72 h). Sheep Study #1 revealed that the NO releasing formulation (a) insert caps are highly effective at killing/preventing bacteria and biofilm formation at all regions of a hemodialysis catheter compared to the control that had a normal catheter cap. Sheep Study #2 confirmed the results of Sheep Study #1 for the NO releasing formulation (a) insert cap. Sheep Study #2 also revealed that the NO releasing formulation (a) insert cap prevents bacteria growth and biofilm formation better than a commercially available antimicrobial cap that utilizes chlorhexidine. Overall, this research has clearly demonstrated that the NO releasing formulation (a) insert cap demonstrates significant antimicrobial/anti-biofilm effects and should be useful in significantly decreasing the risk of infection for dialysis patients that have TDCs in place.

5.5 References

(1) Lok, C. E.; Foley, R. *Clinical Journal of the American Society of Nephrology* **2013,** *8* (7), 1213-1219.

(2) Rupp, M. E.; Karnatak, R. *Infectious Disease Clinics of North America* **2018,** *32* (4), 765-787.

(3) Buetti, N.; Timsit, J. F. *Semin. Respir. Crit. Care. Med.* **2019,** *40* (4), 508-523.

(4) Justo, J. A.; Bookstaver, P. B. *Infect. Drug Resist.* **2014,** *7*, 343-363.

(5) Banin, E.; Brady, K. M.; Greenberg, E. P. *Applied and Environmental Microbiology* **2006,** *72* (3), 2064-2069.

(6) Raad, I. I.; Fang, X.; Keutgen, X. M.; Jiang, Y.; Sherertz, R.; Hachem, R. *Curr. Opin. Infect. Dis.* **2008,** *21* (4), 385-392.

(7) Brunelli, S. M.; Van Wyck, D. B.; Njord, L.; Ziebol, R. J.; Lynch, L. E.; Killion, D. P. *Journal of the American Society of Nephrology* **2018,** *29* (4), 1336-1343.

(8) Brunelli, S. M.; Njord, L.; Hunt, A. E.; Sibbel, S. P. *Int J Nephrol Renovasc Dis* **2014,** *7*, 131-139.

(9) Sweet, M. A.; Cumpston, A.; Briggs, F.; Craig, M.; Hamadani, M. *American Journal of Infection Control* **2012,** *40* (10), 931-934.

(10) Hymes, J. L.; Mooney, A.; Van Zandt, C.; Lynch, L.; Ziebol, R.; Killion, D. *American Journal of Kidney Diseases* **2017,** *69* (2), 220-227.

(11) Bonez, P. C.; dos Santos Alves, C. F.; Dalmolin, T. V.; Agertt, V. A.; Mizdal, C. R.; Flores, V. d. C.; Marques, J. B.; Santos, R. C. V.; Anraku de Campos, M. M. *American Journal of Infection Control* **2013,** *41* (12), e119-e122.

(12) Hetrick, E. M.; Shin, J. H.; Stasko, N. A.; Johnson, C. B.; Wespe, D. A.; Holmuhamedov, E.; Schoenfisch, M. H. *ACS Nano* **2008,** *2* (2), 235-246.

(13) Wo, Y.; Brisbois, E. J.; Bartlett, R. H.; Meyerhoff, M. E. *Biomater. Sci.* **2016,** *4* (8), 1161-1183.

(14) Ghaffari, A.; Miller, C. C.; McMullin, B.; Ghahary, A. *Nitric Oxide* **2006,** *14* (1), 21-29.

(15) Loscalzo, J.; Welch, G. *Prog. Cardiovasc. Dis.* **1995,** *38* (2), 87-104.

(16) Fang, F. C. *J. Clin. Invest.* **1997,** *99* (12), 2818-2825.

(17) Barraud, N.; Hassett, D. J.; Hwang, S.-H.; Rice, S. A.; Kjelleberg, S.; Webb, J. S. *J Bacteriol* **2006,** *188* (21), 7344-7353.

(18) Barraud, N.; Storey, M. V.; Moore, Z. P.; Webb, J. S.; Rice, S. A.; Kjelleberg, S. *Microb Biotechnol* **2009,** *2* (3), 370-378.

(19) Xu, L.-C.; Wo, Y.; Meyerhoff, M. E.; Siedlecki, C. A. *Acta Biomater.* **2017,** *51*, 53-65.

(20) Wo, Y.; Li, Z.; Brisbois, E. J.; Colletta, A.; Wu, J.; Major, T. C.; Xi, C.; Bartlett, R. H.; Matzger, A. J.; Meyerhoff, M. E. *ACS Appl. Mater. Interfaces* **2015,** *7* (40), 22218-22227.

(21) Broniowska, K. A.; Diers, A. R.; Hogg, N. *Biochim. Biophys. Acta* **2013,** *1830* (5), 3173-3181.

(22) Lautner, G.; Stringer, B.; Brisbois, E. J.; Meyerhoff, M. E.; Schwendeman, S. P. *Nitric Oxide* **2019,** *86*, 31-37.

(23) Doverspike, J. C.; Zhou, Y.; Wu, J.; Tan, X.; Xi, C.; Meyerhoff, M. E. *Nitric Oxide* **2019,** *90*, 1-9.

(24) Ren, H.; Bull, J. L.; Meyerhoff, M. E. *ACS Biomater. Sci. Eng.* **2016,** *2* (9), 1483-1492.

(25) Shishido, S. M.; Oliveira, M. G. *Photochem. Photobiol.* **2000,** *71* (3), 273-280.

(26) Rabinowitch, E.; Wood, W. C. *Trans. Faraday Soc.* **1936,** *32*, 1381-1387.

(27) Dicks, A. P.; Swift, H. R.; Williams, D. L. H.; Butler, A. R.; Al-Sa'doni, H. H.; Cox, B. G. *J. Chem. Soc., Perkin Trans. 2* **1996,** (4), 481-487.

(28) Singh, S. P.; Wishnok, J. S.; Keshive, M.; Deen, W. M.; Tannenbaum, S. R. *Proc. Natl. Acad. Sci.* **1996,** *93* (25), 14428-14433.

(29) Williams, D. L. H. *Acc. Chem. Res.* **1999,** *32* (10), 869-876.

(30) Wood, P. D.; Mutus, B.; Redmond, R. W. *Photochem. Photobiol.* **1996,** *64* (3), 518-524.

(31) de Souza, G. F. P.; Denadai, J. P.; Picheth, G. F.; de Oliveira, M. G. *Nitric Oxide* **2019,** *84*, 30-37.

Chapter 6 Conclusions and Future Directions

6.1 Conclusions

This dissertation research has focused on examining the characteristics and antimicrobial properties of newly devised NO releasing creams and devices. Furthermore, a novel method for enhancing NO release from GSNO using ZnO nanoparticles was introduced and investigated. Overall, each project had the goal of preventing/treating infections in the biomedical field. Therefore, practicality of each application led to the heavy utilization of a natural/endogenous NO donor, GSNO.

In Chapter 2, enhanced, long-term stability of GSNO when stored in Vaseline was observed. The enhanced stability was attributed to the dry storage conditions as well as the hydrophobicity, and high viscosity of Vaseline. Four secondary creams were evaluated for their ability to proliferate NO from GSNO stored in Vaseline. A commercially available ZnO-containing cream yielded the most NO released during the initial 6 h test period at both 24°C and 34°C. The NO release kinetics using the commercial ZnO-containing cream to initiate NO release from GSNO in Vaseline displayed first-order NO release kinetics. The observed rate constants for NO releasing formulations with 3, 6, and 9 wt% GSNO revealed that the rate of NO release was independent of GSNO concentration. Lastly, measuring NO release from the GSNO-Vaseline-ZnO cream in the presence of ambient light versus dark, revealed no significant impact on the rate of NO release.

Chapter 3 evaluated the antimicrobial effects of the NO releasing two-part creams introduced in Chapter 2. The 3, 6, and 9 wt% GSNO in Vaseline/ZnO cream were tested against *S. aureus*, *S.*

epidermidis, and *P. aeruginosa* using an indirect application assay, where there was a thin silicone membrane between the NO releasing cream and the bacteria grown on LB agar plates. Overall, the more NO produced yielded a greater killing effect for each bacteria strain. The various NO releasing creams were also tested against the same bacteria using a direct application assay on pig skin. The killing effect on both types of surface matrices (pig skin and agar gels) was similar. Compared to a commercially available antibiotic-containing cream (Neosporin), each NO releasing cream formulation was able to exceed or match the killing effect achieved by Neosporin for all three bacteria strains examined. The NO releasing cream was combined with an antibiotic-containing cream and tested using direct application on pig skin of pre-grown *S. aureus*, *S. epidermidis*, and *P. aeruginosa* biofilms. The NO + antibiotic cream formulation proved most effective against the *P. aeruginosa* biofilm because the antibiotics present are known to be highly potent against gram-negative bacteria strains. The relative pH of the NO releasing formulation was determined to be quite acidic. Therefore, $NaHCO_3$ was added to create a more neutral pH NO releasing cream to prevent any negative consequences (e.g., burning sensation on skin, etc.) of the acidic pH of the original formulation. First-order NO release kinetics were observed for the new neutral pH NO releasing cream compared to the kinetics of the acidic pH NO releasing cream evaluated in Chapter 2. The results indicated that the addition of $NaHCO_3$ has no major influence on the observed NO release kinetics. The neutral pH NO releasing cream was tested using the direct application assay on pig skin against *S. aureus*, *S. epidermidis*, and *P. aeruginosa*. This test revealed that the relative acidity of the initial NO releasing creams tested had no major contribution to the killing effects observed.

In Chapter 4, it was determined that Zn^{2+} ion, potentially formed from slight dissolution of ZnO or present as impurities in ZnO preparations, have little or no effect on enhancing NO release from

GSNO. A component study was performed that tested all the compounds present in the commercial ZnO cream for their potential to enhance NO release from GSNO. ZnO nanoparticles were found to be the primary component responsible for enhancing NO release from GSNO. NO release kinetics from GSNO in the presence of different sized ZnO nanoparticles revealed zero-order NO release kinetics during the first 10 h of reaction in the dark, at 24°C, and under neutral pH conditions. Also, it was discovered that the NO release rate does increase with decreasing ZnO nanoparticle size, but not in a directly proportional manner. The NO release profiles observed using Tris-HCl buffer versus Tris-H_3PO_4 buffer in the presence of GSNO and ZnO nanoparticles revealed that GSNO needs uninhibited access to the surface of ZnO to enhance NO release. Indeed, it appears that some equilibrium form of phosphate ions may interact with the surface and reduce access of the GSNO species from reaching the surface to react with the ZnO. Lastly, XPS was used to analyze the surface of ZnO nanoparticles after exposure to GSNO. This experiment detected no trace of thiol attachment or Zn-S bond formation.

Chapter 6 introduced a NO releasing insert device that disinfects the hub region of tunnel dialysis catheters (TDCs). The real-time NO release characteristics of four different NO releasing formulations (a-d) were evaluated using real world conditions for a TDC (24°C, dark, 72 h, and submerged in saline). These tests revealed that ZnO must be present to enhance NO release from GSNO. Testing the antimicrobial capabilities of formulations (a-c) using a simulated hub assay revealed that each formulation was capable of killing all of the *S. aureus* bacteria present in the liquid broth of a simulated hub after 72 h of exposure at 24°C. *S. aureus* bacteria/biofilm adhered to the inner lumen wall of the simulated hub were evaluated using a Live/Dead dye stain and taking fluorescent microscopic images upon completion of the 72 h study. The fluorescent microscopic images revealed that the characteristic of a large burst of NO during the first 24 h of incubation

displayed by formulation (a) was necessary to kill all bacteria, such that none adhered to the inner lumen wall as biofilm. Two sterilization techniques were evaluated to see which method decomposed the most GSNO during the respective procedures. It was determined that sterilization via H_2O_2 gas resulted in minimal GSNO decomposition. A short term shelf-life stability study was completed for the NO releasing formulation (a) inserts after being H_2O_2 sterilized and stored in the dark at 24°C, and in the presence of desiccant. After 56 d, the GSNO present in the NO releasing inserts only degraded by 4.3% on average. The H_2O_2 sterilized NO releasing formulation (a) inserts were subjected to another antimicrobial test using real catheter hubs inoculated with a solution containing either *S. aureus* (gram-positive) or *P. aeruginosa* (gram-negative) bacteria. The test resulted in a 6.6 and 6.7 log unit reduction from the liquid present in actual catheter hubs under real world conditions (24°C, dark, 72 h) for *S. aureus* and *P. aeruginosa*, respectively. The 14 d long Sheep Study #1 tests revealed that the NO releasing formulation (a) insert caps are effective at killing a preventing bacteria and biofilm growth in all regions of a TDC versus the control of a normal catheter cap. Sheep Study #2 tested the NO releasing formulation (a) insert caps against commercially available antimicrobial caps that utilize chlorhexidine as the antimicrobial agent. Both NO release caps and commercial caps kill all bacteria present in the liquid phase within the hub region during the 14 d study. However, the NO releasing insert caps were also able to prevent biofilm growth on the inner lumen of the entire catheter to a much greater extent than the commercial chlorhexidine coated cap.

6.2 Future Directions

6.2.1 Goals for future directions

To continue the research reported in this thesis, there are a few important goals. The first goal is to assess if the NO releasing cream is safe/non-toxic to human skin. Hence, the safety of the NO releasing cream needs to be evaluated using a living animal model. The second goal is to understand the fundamentals of the mechanism of the reaction between GSNO and ZnO nanoparticles. That is exactly how does the GSNO interact with the ZnO surface that leads to acceleration of the NO release from this *S*-nitrosothiol species. The third goal is to ensure that none of the components present inside of the NO releasing insert, leach out of the insert while being used inside of a catheter hub. Leaching studies will evaluate the relative safety of using the NO releasing inserts in humans. Detailed suggestions for studies to examine these areas are described below.

6.2.2 Cytotoxicity study of NO releasing two-part cream via live pig models

It is necessary to understand whether the NO produced locally by the GSNO-based NO release creams developed in this thesis work exhibits any toxicity toward live skin cells and whether the creams have other biomedical applications (beyond treating dermal infections, etc.). Therefore, a project is now being planned to collaborate with Dr. Raimon Duran-Struuck, Assistant Professor and Director of Laboratory Animal Medicine Residency Program at the University of Pennsylvania. The overall goal of this project is to prevent/reduce the effects of graft-versus-host disease (GVHD) after hematopoietic cell transplantations (HCT). GVHD is a common problem caused by HTC, leaving patients with high risk of infection and potential long term side effects.[1, 2] GVHD targets organs such as the liver, gastrointestinal tract, and skin, with the most common target being the skin.[3] Acute GVHD is an immunologically mediated process where donor T cells

attack host tissue, commonly causing eczema, rosacea, and psoriasis.[4, 5] Past preventions strategies include blocking inflammatory cascades that activate donor T cells, however these therapies are not fully effective because the immunosuppression drugs also non-selectively inhibit host regulatory T cells (Tregs) that are important for controlling GVHD.[6]

It has been hypothesized that there are potential interactions between the skin microbiome and the immune system that likely influences the development of skin-GVHD post HCT. Chronic inflammatory and autoimmune disorders such as atopic dermatitis (AD), rosacea and psoriasis have been linked to commensal microbiota in skin.[5, 7, 8] Skin bacteria can act as endogenous adjuvants, and can shape T cell responses through their capacity to modulate the local milieu (i.e. IL-1 production) and by promoting the overgrowth of *S. aureus*, thereby inducing flares in AD.[8, 9] Recent studies have shown that ultraviolet (UV) therapy can modify the skin microflora to improve sclerotic skin conditions.[10] The mechanism of the antimicrobial effects from UV irradiation is not clear, however the skin contains large stores of nitric oxide (NO) that release upon UV irradiation (likely, in part, from endogenous RSNO species).[11] NO is a potent antimicrobial, anti-biofilm, and antifungal agent that is naturally produced endogenously by the enzyme nitric oxide synthase (NOS) and is responsible for several regulatory body functions.[12-18] Therefore, a hypothesis is that applying the NO releasing two-part cream developed in Chapters 2 and 3 may decrease the bacterial burden fueling GVHD.

Three pigs will receive an allogenic bone marrow transplant (BMT) for the induction of GVHD. One week prior to transplant, the NO releasing cream will be applied near the surgical area. After transplant, the NO releasing cream will be applied daily for one month. Three additional pigs will receive daily treatments of the NO releasing cream without receiving a BMT (GVHD-free control) for one month as well. Blood immunophenotype, microbiome, and skin biopsy samples will be

analyzed weekly. Histology samples will be taken weekly and will be assessed for any cytotoxic effects the NO releasing creams (seen on control/GVHD-free pigs).

6.2.3 Determination of mechanism between GSNO and ZnO nanoparticles

The experiments performed in Chapter 4 established that ZnO nanoparticles were the responsible component present in the ZnO commercial cream for the enhanced NO release observed from GSNO incorporated within Vaseline. Further studies suggested that GSNO needs uninhibited access to the surface of the ZnO particles and that the ZnO surface is not modified with thiol moieties post reaction with GSNO. The mechanism by which ZnO reacts with GSNO to enhance NO release is unknown. However, a hypothesized mechanism involves oxygen vacancies present on the ZnO nanoparticle surface (Fig. 6.1).

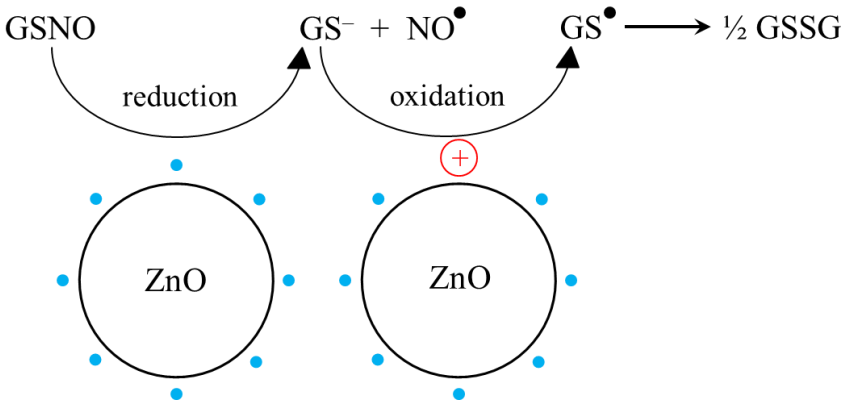

Figure 6.1. Proposed scheme for the mechanism by which ZnO nanoparticles react with GSNO to enhance NO release. Blue dots represent electrons trapped in oxygen vacancies on the surface of ZnO. The red positive sign represents a net positive area that remains in the oxygen vacancy after the trapped electron facilitates a reduction reaction with GSNO.

The rationale behind this hypothesized mechanism is as follows. ZnO nanoparticles can contain defects known as singly ionized oxygen vacancies (i.e. oxygen vacancy with one electron).[19, 20] Prasanna *et al.* demonstrated that a superoxide radical can form by atmospheric oxygen reacting

with an electron from the surface of ZnO while in the dark (Fig. 6.2).[19] Therefore, the hypothesis that GSNO could react with an electron from the surface of ZnO while in the dark is possible. After the electron is removed from the ZnO surface, a hole is generated with a net positive charge. An oxidation reaction could then occur between the GS^- and the hole, yielding GS radical and subsequently glutathione disulfide (GSSG).

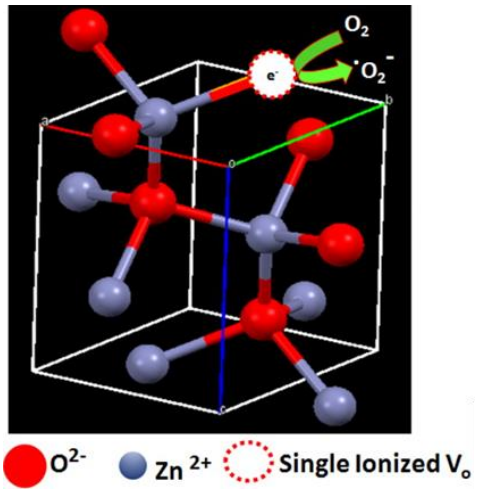

Figure 6.2. Image depicting the production of superoxide radicals via atmospheric oxygen reacting with an electron from the surface of ZnO (oxygen vacancy).[19]

One method for detecting oxygen vacancies on the surface of ZnO involves using X-ray photoelectron spectroscopy (XPS). This technique is described in detail by Zhang *et al*.[20] Briefly, analyzing the O 1s spectra of ZnO nanoparticles normally yields a signal at ~530.1 eV relating to oxygen present in the ZnO crystal lattice (O_L) and a signal at ~532.1 eV relating to surface hydroxyl groups bound to oxygen vacancies/defects (O_H).[19, 20] Then, the atomic ratio of O_L to O_H can be calculated and related to the concentration of oxygen vacancies present, where a higher atomic ratio corresponds to a higher concentration of oxygen vacancies.[19, 20] Thus, analyzing the different sized ZnO nanoparticles used in Chapter 4 (30, 50, and 200 nm in diameter) via XPS and calculating their corresponding atomic ratios between O_L and O_H may determine if the relative

concentration of oxygen vacancies relates to the rate of NO release each size of ZnO nanoparticle causes.

Another method for detecting oxygen vacancies on the surface of ZnO involves using electron paramagnetic resonance (EPR). This technique is described in detailed by the same authors Zhang *et al*.[20] Briefly, EPR has been used to observe the electron spin state and the structure on the surface of ZnO nanoparticles.[20] Specifically, ZnO nanoparticles naturally produce an EPR signal at a g-factor of ~1.9568 (g-factor is a proportionality factor used to describe the electron spin state).[20] However, an EPR signal at a g-factor of ~2.0035 corresponds to an unpaired electron trapped in an oxygen vacancy site.[20-23] A stronger signal at g-factor 2.0035 will correspond to a higher concentration of oxygen vacancies present on the surface of ZnO.[20] Analyzing the different sized ZnO nanoparticles used in Chapter 4 (30, 50, and 200 nm diameter) could indicate any difference in concentration of oxygen vacancies present and any correlations to the rate of NO release from GSNO cause by the different sized ZnO nanoparticles, may be determined.

Another experiment that could help prove or disprove the mechanism proposed in Figure 6.1 is determination of the products of the reaction between GSNO and ZnO nanoparticles. Currently, the proposed product is glutathione disulfide (GSSG). Therefore, a long term experiment could be performed where the consumptions of GSNO and the formation of GSSG are monitored via nuclear magnetic resonance (NMR) spectroscopy and high-performance liquid chromatography-mass spectrometry (HPLC-MS). Each reaction will have a known amount of GSNO and ZnO nanoparticles in a reaction vessel and be performed at room temperature (24°C), in the dark, under constant stirring via a stir bar and bubbling with N_2 gas. One reaction will be performed in the presence of D_2O for NMR experiments and the other reaction performed in purified deionized water for HPLC-MS experiments. Each reaction will be monitored for GSNO consumption and

GSSG formation daily via NMR and HPLC-MS until the full reaction is completed (no more detection of GSNO).

6.2.4 Leaching study for NO releasing insert

There is probable cause to determine if any component from inside of the NO releasing insert devices (GSNO/ZnO) described in Chapter 5 are able to leach out from the silicone tubing. After construction of a NO releasing insert is complete (GSNO/ZnO dry powder inside of a silicone tube, securely sealed at both ends using a silicone adhesive glue) the components inside of the insert should not be able to leach out of the interior of the insert when soaked in solution. A leaching study can be performed to determine if this hypothesis is true.

Preliminary data was collected for the detection of zinc in the leaching solutions using inductively coupled plasma mass spectrometry (ICP-MS). Two scenarios pictured in Figure 6.3b, were tested. The NO releasing formulation (a) inserts/caps were prepared as described in Chapter 5, Sections 5.2.3 and 5.2.9. The leaching study was performed by soaking the insert samples in a defined volume (10 mL) of purified deionized water. Purified deionized water was used because the ICP-MS could be damaged by the high salt concentration in saline solution. Control insert samples were only the silicone tubing and the glue adhesive with no GSNO or ZnO present. After 24 h of soaking, the insert samples were removed, thoroughly washed, dried using a Kimwipe, and submerged again in fresh purified deionized water (1^{st} 24 h samples in Fig. 6.3a). This process was repeated the following two days. After collection of the solutions, the concentration of zinc content in each was measured using ICP-MS. The results of this preliminary leaching study are found in Figure 6.3a.

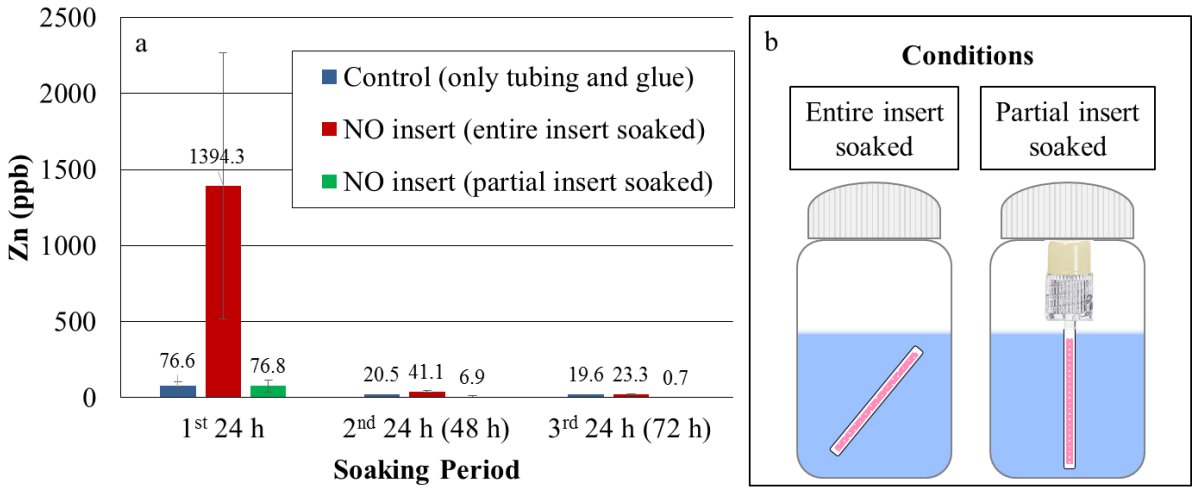

Figure 6.3. Preliminary leaching study from the NO releasing inserts using ICP-MS. (a) Concentration of Zn (ppb) detected for Control (only silicone tubing and glue, no GSNO and no ZnO present), NO insert under the condition defined as "entire insert soaked", and NO insert under the condition defined as "partial insert soaked" after 24 h soaking increments in purified deionized water for a total of 72 h. Data represents the mean ± SD (n = 3). (b) Conditions defined for the leaching test, defined as entire insert soaked or partial insert soaked.

The concentration of zinc detected for the two different soaking conditions of the NO releasing inserts and NO releasing insert caps after the first 24 h are extremely different (1394.3 ppb vs. 76.8 ppb, respectively) (Fig. 6.3a). The difference between the two soaking methods was that the end of the silicone tube that was sealed second (right after filling the silicone tube with the GSNO/ZnO powder), was directly exposed to solution when the entire NO releasing insert was soaked. In contrast, the other scenario was where this end of the silicone tubing was inside of the cap and not exposed to solution. Thus, a conclusion can be made that ZnO is able to creep out of the end of the silicone tubing that is sealed on the second end because that end of the tubing is directly exposed to the ZnO before sealing, whereas the other end of the silicone tubing is pre-sealed and dried before any exposure to ZnO (creating a more solid seal). The large error bar for the NO releasing insert that was entirely soaked, indirectly demonstrates this phenomenon because the amount of ZnO that could be close to the edge of the second sealed end could vary immensely

because the inserts are made by hand (Fig 6.3a). Overall, this data definitely proves that zinc is not leaching out from the walls of the silicone tubing of the NO releasing insert.

Further studies need to be completed to determine if GSNO or related compounds (GSH, GSSG) leach out from the silicone tubing when soaked in solution. For the detection/quantification of GSNO the same leaching study can be performed as described above and the liquid samples can be analyzed by high-performance liquid chromatography-mass spectrometry (HPLC-MS).

6.3 References

(1) Duran-Struuck, R.; Reddy, P. *Transplantation* **2008,** *85* (3), 303-308.

(2) Wolf, D.; von Lilienfeld-Toal, M.; Wolf, A. M.; Schleuning, M.; von Bergwelt-Baildon, M.; Held, S. A. E.; Brossart, P. *Blood* **2012,** *119* (1), 16-25.

(3) Ferrara, J. L. M.; Deeg, H. J. *New England Journal of Medicine* **1991,** *324* (10), 667-674.

(4) Paczesny, S.; Braun, T. M.; Levine, J. E.; Hogan, J.; Crawford, J.; Coffing, B.; Olsen, S.; Choi, S. W.; Wang, H.; Faca, V.; Pitteri, S.; Zhang, Q.; Chin, A.; Kitko, C.; Mineishi, S.; Yanik, G.; Peres, E.; Hanauer, D.; Wang, Y.; Reddy, P.; Hanash, S.; Ferrara, J. L. M. *Science Translational Medicine* **2010,** *2* (13), 13ra2.

(5) Belkaid, Y.; Segre, J. A. *Science* **2014,** *346* (6212), 954-959.

(6) Teshima, T.; Reddy, P.; Zeiser, R. *Biology of Blood and Marrow Transplantation* **2016,** *22* (1), 11-16.

(7) Lai, Y.; Di Nardo, A.; Nakatsuji, T.; Leichtle, A.; Yang, Y.; Cogen, A. L.; Wu, Z.-R.; Hooper, L. V.; Schmidt, R. R.; von Aulock, S.; Radek, K. A.; Huang, C.-M.; Ryan, A. F.; Gallo, R. L. *Nature Medicine* **2009,** *15* (12), 1377-1382.

(8) Naik, S.; Bouladoux, N.; Wilhelm, C.; Molloy, M. J.; Salcedo, R.; Kastenmuller, W.; Deming, C.; Quinones, M.; Koo, L.; Conlan, S.; Spencer, S.; Hall, J. A.; Dzutsev, A.; Kong, H.; Campbell, D. J.; Trinchieri, G.; Segre, J. A.; Belkaid, Y. *Science* **2012,** *337* (6098), 1115-1119.

(9) Kong, H. H.; Oh, J.; Deming, C.; Conlan, S.; Grice, E. A.; Beatson, M. A.; Nomicos, E.; Polley, E. C.; Komarow, H. D.; Murray, P. R.; Turner, M. L.; Segre, J. A. *Genome Res.* **2012,** *22* (5), 850-859.

(10) Silva, S.; Guedes, A.; Gontijo, B.; Ramos, A.; Carmo, L.; Farias, L.; Nicoli, J. *Journal of the European Academy of Dermatology and Venereology* **2006,** *20* (9), 1114-1120.

(11) Yu, C.; Fitzpatrick, A.; Cong, D.; Yao, C.; Yoo, J.; Turnbull, A.; Schwarze, J.; Norval, M.; Howie, S. E. M.; Weller, R. B.; Astier, A. L. *Journal of Allergy and Clinical Immunology* **2017,** *140* (5), 1441-1444.e6.

(12) Rosselli, M.; Keller, R. J.; Dubey, R. K. *Hum. Reprod. Update* **1998,** *4* (1), 3-24.

(13) Wo, Y.; Brisbois, E. J.; Bartlett, R. H.; Meyerhoff, M. E. *Biomater. Sci.* **2016,** *4* (8), 1161-1183.

(14) Loscalzo, J.; Welch, G. *Prog. Cardiovasc. Dis.* **1995,** *38* (2), 87-104.

(15) Hetrick, E. M.; Shin, J. H.; Stasko, N. A.; Johnson, C. B.; Wespe, D. A.; Holmuhamedov, E.; Schoenfisch, M. H. *ACS Nano* **2008,** *2* (2), 235-246.

(16) Barraud, N.; Hassett, D. J.; Hwang, S.-H.; Rice, S. A.; Kjelleberg, S.; Webb, J. S. *J Bacteriol* **2006,** *188* (21), 7344-7353.

(17) Xu, L.-C.; Wo, Y.; Meyerhoff, M. E.; Siedlecki, C. A. *Acta Biomater.* **2017,** *51*, 53-65.

(18) Wo, Y.; Li, Z.; Brisbois, E. J.; Colletta, A.; Wu, J.; Major, T. C.; Xi, C.; Bartlett, R. H.; Matzger, A. J.; Meyerhoff, M. E. *ACS Appl. Mater. Interfaces* **2015,** *7* (40), 22218-22227.

(19) Lakshmi Prasanna, V.; Vijayaraghavan, R. *Langmuir* **2015,** *31* (33), 9155-9162.

(20) Zhang, Q.; Xu, M.; You, B.; Zhang, Q.; Yuan, H.; Ostrikov, K. K. *Appl. Sci.* **2018,** *8* (3), 353.

(21) Ischenko, V.; Polarz, S.; Grote, D.; Stavarache, V.; Fink, K.; Driess, M. *Advanced Functional Materials* **2005,** *15* (12), 1945-1954.

(22) Zhuang, J.; Weng, S.; Dai, W.; Liu, P.; Liu, Q. *The Journal of Physical Chemistry C* **2012,** *116* (48), 25354-25361.

(23) Liu, H.; Ma, H. T.; Li, X. Z.; Li, W. Z.; Wu, M.; Bao, X. H. *Chemosphere* **2003,** *50* (1), 39-46.